TESIS DE LA UNIVERSIDAD DE ZARAGOZA

2013

124

Raquel Herrero Latorre

Valor diagnóstico y pronóstico de la evaluación de la capa de fibras nerviosas de la retina en la esclerosis múltiple

Departamento

Cirugía, Ginecología y Obstetricia

Director/es

Polo Llorens, Vicente
Frezzotti, Paolo
García Martín, Elena

ISSN 2254-7606

Prensas de la Universidad Universidad Zaragoza

Universidad Zaragoza
1542

Tesis Doctoral

VALOR DIAGNÓSTICO Y PRONÓSTICO DE LA EVALUACIÓN DE LA CAPA DE FIBRAS NERVIOSAS DE LA RETINA EN LA ESCLEROSIS MÚLTIPLE

Autor

Raquel Herrero Latorre

Director/es

Polo Llorens, Vicente
Frezzotti, Paolo
García Martín, Elena

UNIVERSIDAD DE ZARAGOZA

Cirugía, Ginecología y Obstetricia

VALOR DIAGNÓSTICO Y PRONÓSTICO DE LA EVALUACIÓN DE LA CAPA DE FIBRAS NERVIOSAS DE LA RETINA EN LA ESCLEROSIS MÚLTIPLE

Tesis doctoral

Raquel Herrero Latorre

Universidad de Zaragoza

Facultad de Medicina

Departamento de Cirugía, Obstetricia y Ginecología

Servicio de Oftalmología

Trabajo de investigación presentado por la Licenciada en

Medicina y Cirugía

Raquel Herrero Latorre

Para optar al grado de doctora

Dra. Elena García Martín
Servicio de Oftalmología
Hospital Universitario Miguel Servet
Zaragoza

Dr.Paolo Frezzotti
U.O.C. Oftalmologia
Azienda Ospedaliera Universitaria Senesa
Siena
Italia

Dr. Vicente Polo Llorens
Servicio de Oftalmología
Hospital Universitario Miguel Servet
Zaragoza

La modalidad de presentación de la presente tesis doctoral es por compendio de publicaciones.

A continuación se detallan los cuatro artículos previamente publicados que constituyen el cuerpo de la tesis:

1. Herrero R, Garcia-Martin E, Almarcegui C, Ara JR, Rodriguez-Mena R, Martin J, Satue M, Dolz I, Fernandez J, Pablo LE. Progressive degeneration of the retinal nerve fiber layer in patients with multiple sclerosis. Invest Ophthalmol Vis Sci. 2012;53(13):8344-9. ISSN: 0146-0404. PMID: 23154461
2. Garcia-Martin E, Pablo LE, Herrero R, Satue M, Polo V, Larrosa JM, Martin J, Fernandez J. Diagnostic ability of a linear discriminant function for Spectral domain optical coherence tomography in multiple sclerosis patients. Ophthalmology 2012;119(8):1705-11. ISSN: 0161-6420. PMID: 22480742.
3. Garcia-Martin E, Calvo B, Malvè M, Herrero R, Fuertes I, Ferreras A, Larrosa JM, Polo V, Pablo LE. Three-dimensional geometries representing the retinal nerve fiber layer in multiple sclerosis, optic neuritis, and healthy eyes. Ophthalmic Research 2013 (en prensa). ISSN: 0030-3747
4. García-Martín E, Herrero R, Bambo MP, Ara JR, Martin J, Polo V, Larrosa JM, Garcia-Feijoo J, Pablo LE. Artificial neural network techniques to improve the ability of optical coherence tomography to detect optic neuritis. Seminars of Opthalmology 2013 (en prensa). ISSN: 0882-0538

Dª. ELENA GARCIA MARTIN, Doctora en Medicina y Cirugía, facultativo especialista en Oftalmología del Hospital Universitario Miguel Servet, y profesora asociada de la Universidad de Zaragoza.

Certifica:

Que el trabajo de investigación titulado *"*Valor diagnóstico y pronóstico de la evaluación de la capa de fibras nerviosas de la retina en la esclerosis múltiple*"* que presenta RAQUEL HERRERO LATORRE, Licenciada en Medicina y Cirugía, para optar al GRADO DE DOCTOR, fue realizado bajo mi dirección y reúne las condiciones necesarias para su defensa como tesis por compendio de publicaciones.

Y para que conste a los efectos oportunos, firmo el presente en Zaragoza, a 27 de abril de 2013.

Fdo. Dra. Elena García Martín

D. VICENTE POLO LLORENS, Doctor en Medicina y Cirugía, facultativo especialista en Oftalmología del Hospital Universitario Miguel Servet, y profesor titular de la Universidad de Zaragoza.

Certifica:

Que el trabajo de investigación titulado *"*Valor diagnóstico y pronóstico de la evaluación de la capa de fibras nerviosas de la retina en la esclerosis múltiple*"* que presenta RAQUEL HERRERO LATORRE, Licenciada en Medicina y Cirugía, para optar al GRADO DE DOCTOR, fue realizado bajo mi dirección y reúne las condiciones necesarias para su defensa como tesis por compendio de publicaciones.

Y para que conste a los efectos oportunos, firmo el presente en Zaragoza, a 27 de abril de 2013.

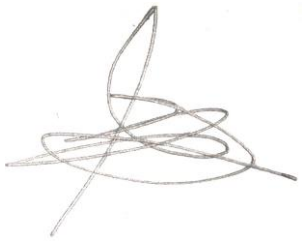

Fdo. Dr. Vicente Polo Llorens

D. PAOLO FREZZOTTI, Doctor en Medicina y Cirugía, facultativo especialista en Oftalmología de la Azienda Ospedaliera Universitaria Senesa, Siena (Italia).

Certifica:

Que el trabajo de investigación titulado *"*Valor diagnóstico y pronóstico de la evaluación de la capa de fibras nerviosas de la retina en la esclerosis múltiple*"* que presenta RAQUEL HERRERO LATORRE, Licenciada en Medicina y Cirugía, para optar al GRADO DE DOCTOR, fue realizado bajo mi dirección y reúne las condiciones necesarias para su defensa como tesis por compendio de publicaciones.

Y para que conste a los efectos oportunos, firmo el presente en Zaragoza, a 23 de Mayo de 2013.

ÍNDICE

ABREVIATURAS

AV: Agudeza visual

EM: Esclerosis múltiple

OCT: Tomografía óptica de coherencia

CV: Campo visual

PIO: Presión intraocular

DM: Desviación media

PEV: Potenciales evocados visuales

CFNR: Capa de fibras nerviosas de la retina

AUC: Área bajo la curva ROC

ROC: Receiver operating characteristic

INTRODUCCIÓN GENERAL

El tema principal de las cuatro publicaciones internacionales que componen esta tesis doctoral se centra en el estudio de la capa de fibras nerviosas de la retina en pacientes con esclerosis múltiple como método para mejorar y acelerar el proceso diagnóstico así como el seguimiento y la monitorización de esta enfermedad.

La esclerosis múltiple (EM) es una compleja enfermedad neurodegenerativa que se caracteriza por lesiones axonales en el sistema nervioso central que conducen a déficits neurológicos progresivos.

Clásicamente se ha considerado una enfermedad desmielinizante en la que la mielina que recubre los nervios es destruida por procesos de inflamación y cicatrización; sin embargo en los últimos años se ha demostrado que se asocian otros procesos de daño axonal[1,2].

Existen evidencias de que el daño axonal aparece desde fases precoces de la enfermedad, sin relación con episodios inflamatorios o autoinmunes contra la mielina, y de que esta degeneración axonal está directamente relacionada con la discapacidad funcional permanente[1,2]. Estudios previos han demostrado que el deterioro axonal de los pacientes con EM puede ser observado y cuantificado a nivel de la capa de fibras nerviosas de la retina (CFNR) mediante técnicas de análisis digital de la imagen[3-8].

Algunos autores han sugerido que la evaluación de la CFNR podría ser incluso más útil que la resonancia magnética para medir la atrofia neuronal[9] y un número creciente de neurólogos utiliza la evaluación de la CFNR para monitorizar la progresión de la enfermedad[10,11].

La retina es una parte del sistema nervioso central de fácil acceso para el examen clínico y la evaluación de la CFNR. La CFNR se compone fundamentalmente de axones no mielinizados de las células ganglionares de la retina; por lo que las

mediciones de su espesor aportan una valoración relativamente directa de las fibras nerviosas y por lo tanto del daño axonal.

La aplicación de las técnicas de análisis digital de imagen en oftalmología, como la tomografía de coherencia óptica (OCT), ha supuesto la aparición y desarrollo de parámetros que aportan una medición cuantitativa, objetiva y reproducible de la CFNR. Estos instrumentos han permitido observar alteraciones en la CFNR de pacientes con EM, incluso sin el antecedente de episodios clínicos de neuritis óptica, lo que sugiere la existencia de un daño axonal no asociado a inflamación en esta patología. Numerosos autores han sugerido la utilidad del estudio de la CFNR como marcador biológico del daño axonal en la EM[12-17], y se ha observado que el estudio del espesor de la CFNR con OCT puede ser un método útil para monitorizar la progresión de la EM EM[6,7].

La OCT nos permite obtener imágenes de muy alta resolución de cortes transversales de la retina y del disco óptico basados en patrones de interferometría de baja coherencia producidos por la luz reflejada en los tejidos retinianos. La reciente introducción de nuevas tecnologías en la OCT, como la OCT de alta resolución en tres dimensiones (3D) usando el dominio Fourier, nos proporciona una mayor resolución si la comparamos con la clásica OCT de dominio tiempo[17-19].

Existen muchas compañías en el mercado que comercializan dispositivos OCT de dominio Fourier. Todas ellas nos permiten medir el espesor macular y de la CFNR. Actualmente no existen directrices claras sobre si uno, varios, o todos los parámetros de la CFNR proporcionados por la OCT pueden ser utilizados para establecer el diagnóstico y evaluar la progresión de la EM. Varios estudios han demostrado que el espesor medio de la CFNR es el mejor parámetro diagnóstico en diferentes patologías, como el glaucoma y la EM[9-11,20-22], así como el parámetro más sensible para detectar progresión[7]. Sin embargo, estudios más recientes indican que el diagnóstico precoz de la EM mejora con la combinación de varios parámetros y que cada parámetro puede

realizar una contribución diferente para distinguir entre sujetos sanos y pacientes con EM y para detectar el antecedente de neuritis óptica subclínica en dichos pacientes[23].

Con el objetivo de mejorar la exactitud diagnóstica de las mediciones de la OCT, algunos investigadores han analizado la implementación de algoritmos de aprendizaje de las máquinas, tales como las redes neuronales artificiales, utilizando las mediciones de la CFNR. Estudios realizados por el Departamento de Ingeniería Electrónica e Informática de la Universidad de Miami han demostrado la viabilidad de los métodos de redes neuronales artificiales para distinguir entre los sujetos control y los pacientes con EM usando el Potencial Evocado Cognitivo P300[24-26]. El modelo de red neuronal, sin embargo, aún no había sido utilizado hasta ahora para evaluar la capacidad diagnóstica de la OCT en ojos con neuritis óptica. Pablo y colaboradores[27] usaron la combinación de parámetros de la CFNR para mejorar la capacidad diagnóstica de la OCT en la detección del glaucoma mediante una función lineal discriminante.

A continuación se incluye una breve presentación de cada trabajo y se justifica su unidad temática:

1. *Herrero R, Garcia-Martin E, Almarcegui C, Ara JR, Rodriguez-Mena R, Martin J, Satue M, Dolz I, Fernandez J, Pablo LE. Progressive degeneration of the retinal nerve fiber layer in patients with multiple sclerosis. Invest Ophthalmol Vis Sci. 2012;53(13):8344-9. ISSN: 0146-0404. PMID: 23154461*

Este trabajo, se trata de un estudio longitudinal prospectivo con un periodo de seguimiento de 3 años en el que se incluyeron un total de 94 pacientes con EM y 50 sujetos sanos. El objetivo del estudio consistió en evaluar los cambios que se producían a nivel de la CFNR en este periodo de seguimiento y cuantificar las diferencias entre sujetos sanos y pacientes con EM, así como analizar las diferencias

entre pacientes que habían recibido tratamiento modificador de la enfermedad y aquellos que no habían recibido ningún tratamiento.

De esta manera, cuantificamos los cambios en la CFNR durante tres años para analizar la capacidad de la evaluación de la CFNR como biomarcador de neurodegeneración y discapacidad en pacientes con EM, y comparar si existen diferencias en la degeneración axonal que se produce entre los pacientes tratados y los no tratados.

Numerosos estudios han demostrado que el adelgazamiento de la CFNR se produce no sólo en los ojos que han sufrido un episodio previo de neuritis óptica, sino también en los pacientes que no han presentado ninguna manifestación ocular previa[11,15,28]. Las mediciones del espesor de la CFNR proporcionadas por las técnicas de análisis digital de imagen como la OCT pueden ser utilizadas como marcador de pérdida axonal en EM[9,29,30]. En nuestros resultados observamos un claro descenso estadísticamente significativo en los espesores medio, superior, inferior y temporal de la CFNR, así como un descenso del volumen macular obtenidos mediante la OCT en el grupo de pacientes con EM a los tres años de seguimiento. Pocos autores han estudiado el efecto de los tratamientos de la EM en la degeneración de la CFNR. Garcia-Martin y colaboradores[31] concluyen que el tratamiento puede ser un factor protector contra la pérdida de la CFNR asociada a la progresión de la enfermedad. En el presente estudio, observamos que los pacientes no tratados presentaron una mayor pérdida del espesor en todos los cuadrantes de la CFNR salvo en el cuadrante nasal a los tres años de seguimiento, siendo estadísticamente significativa en el espesor medio y superior. De esta forma, nuestros resultados demostraron que el tratamiento reduce la tasa de pérdida de la CFNR, aunque no encontramos diferencias entre los distintos tipos de tratamiento.

2. *Garcia-Martin E, Pablo LE, Herrero R, Satue M, Polo V, Larrosa JM, Martin J, Fernandez J. Diagnostic ability of a linear discriminant function for Spectral domain optical coherence tomography in multiple sclerosis patients. Ophthalmology 2012;119(8):1705-11. ISSN: 0161-6420. PMID: 22480742.*

Este trabajo es un estudio transversal y prospectivo llevado a cabo con 115 sujetos sanos y 115 pacientes afectos de EM del área sanitaria del Hospital Universitario Miguel Servet de Zaragoza que fueron reclutados por un oftalmólogo y un neurólogo según los criterios de inclusión detallados en el artículo. Todos los pacientes con EM presentaban el fenotipo remitente-recurrente de enfermedad y el diagnóstico se había llevado a cabo basándose en los criterios clínicos y de neuroimagen proporcionados por la resonancia magnética. El objetivo del estudio fue calcular y validar una función lineal discriminante para la OCT de Dominio Spectral que mejore la habilidad diagnóstica empleando únicamente los espesores de la CFNR en pacientes con EM. Ésta prueba proporciona una manera rápida, objetiva, reproducible y no invasiva de evaluar la CFNR. Actualmente no hay guías claras sobre si uno, varios o todos los parámetros de la CFNR proporcionados mediante la OCT pueden contribuir al diagnóstico y evaluación de la progresión de la EM. En la práctica clínica es importante realizar un diagnóstico precoz de esta patología para poder iniciar el tratamiento con las terapias modificadoras de la enfermedad de forma temprana, puesto que de ello depende su efectividad. Este estudio proporciona una fórmula para ayudar a discriminar entre sujetos sanos y pacientes con EM, de forma que se pueda mejorar el diagnóstico precoz en fases tempranas de la enfermedad o en ciertas circunstancias que hacen difícil decidir la presencia o no de EM basándose sólo en otros criterios como la resonancia magnética o los signos clínicos.

3. Garcia-Martin E, Calvo B, Malvè M, Herrero R, Fuertes I, Ferreras A, Larrosa JM, Polo V, Pablo LE. Three-dimensional geometries representing the retinal nerve fiber layer in multiple sclerosis, optic neuritis, and healthy eyes. Ophthalmic Research 2013 (en prensa). ISSN: 0030-3747.

En este estudio transversal y prospectivo se incluyeron un total de 110 sujetos sanos y 130 pacientes con EM, todos ellos de fenotipo clínico remitente-recurrente. El objetivo de este estudio fue utilizar la geometría tridimensional para representar e interpretar la distribución del daño axonal que se produce en la morfología de la CFNR en pacientes con EM. Debido a que la evaluación del nervio óptico se considera un biomarcador de daño axonal en la EM, resulta importante determinar qué sectores o áreas de la CFNR se van a encontrar más afectadas tras sufrir un episodio de neuritis óptica. Algunos estudios han encontrado que el espesor de la CFNR está relacionado con parámetros cerebrales, así como con la atrofia de la sustancia blanca y gris en la EM[29,32,33]. Aunque un episodio de neuritis óptica, daña principalmente el nervio óptico, también podría interferir en esta relación interrumpiendo la asociación con la sustancia gris[32]. Dörr y colaboradores[30] demostraron que la fracción dañada del parénquima cerebral refleja la gravedad de la EM, mientras que el espesor de la CFNR podría ser un parámetro más específico en el seguimiento longitudinal del daño axonal. En relación a los mecanismos por los que la EM produce el daño axonal se han propuesto varios, como cambios en la ultraestructura de las células ganglionares, astrocitos y células endoteliales. Los tejidos y las células pueden sufrir una deformación por varios mecanismos, ya sea por extensión, compresión, desmielinización o atrofia, aunque no son independientes unos de otros. La respuesta de los tejidos y células depende del tipo de deformación, así como de la magnitud y del tiempo que recibe los estímulos, del tipo de tejidos y células y su estado biológico[34,35,36]. Por tanto, es importante determinar qué deformaciones se encuentran a nivel de los tejidos de la CFNR en los

pacientes con EM con o sin daño oftalmológico. En este estudio, analizamos la deformación de la CFNR causada por la neurodegeneración progresiva que sufren los pacientes con EM y por los episodios de neuritis óptica que frecuentemente padecen estos pacientes. En esta publicación internacional se describe el daño de la cabeza del nervio óptico mediante una representación geométrica en tres dimensiones. En cuanto a nuestros resultados, el análisis basado en las 768 mediciones obtenidas mediante la OCT Spectralis mostró un mayor descenso de todos los parámetros en los ojos con antecedentes de neuritis óptica comparados con los ojos de pacientes sin historia de neuritis óptica y ojos sanos. En la representación de la morfología de la CFNR usando el modelo en tres dimensiones en los pacientes con EM con y sin previo episodio de neuritis óptica encontramos un mayor daño en el área temporal.

4. García-Martín E, Herrero R, Bambo MP, Ara JR, Martin J, Polo V, Larrosa JM, Garcia-Feijoo J, Pablo LE. Artificial neural network techniques to improve the ability of optical coherence tomography to detect optic neuritis. Seminars of Opthalmology 2013 (en prensa). ISSN: 0882-0538.

Se trata de un estudio transversal y prospectivo en el que se incluyeron 108 sujetos sanos y 122 pacientes con EM que fueron reclutados por un oftalmólogo y un neurólogo dentro del área sanitaria del Hospital Universitario Miguel Servet de Zaragoza. El objetivo del estudio fue analizar la habilidad de la OCT de dominio Fourier Spectralis para detectar EM y el antecedente de neuritis óptica usando la tecnología de las redes neuronales artificiales. Se determinó de esta forma, si una combinación selectiva de parámetros de la CFNR podría optimizar o acelerar el diagnóstico de la EM y ayudar a detectar el antecedente de episodios de inflamación subclínica en el nervio óptico.

La inflamación del nervio óptico puede cursar de forma subclínica y pasar inadvertida, por lo que es importante determinar si la OCT de dominio Fourier puede

ser capaz de detectar episodios previos de neuritis óptica en pacientes con EM. Con el objetivo de mejorar la capacidad diagnóstica de los parámetros proporcionados mediante la OCT Spectralis y determinar qué combinación selectiva de las mediciones de la CFNR logra optimizar el diagnóstico de EM y la presencia de antecedente de neuritis óptica subclínica, hemos diseñado un modelo estadístico de red neuronal artificial. En nuestros resultados obtuvimos una sensibilidad de este sistema de red neuronal para detectar EM usando la OCT Spectralis del 89,3%, una especificidad del 87,6% y una precisión diagnóstica del 88,5%. Todos estos parámetros fueron mejores que usando los espesores estándar de la CFNR proporcionados por el equipo. La precisión diagnóstica para detectar ojos de EM con antecedente de neuritis óptica fue buena, pero la sensibilidad y especificidad (84,5% y 83,2%, respectivamente) fueron inferiores que para diferenciar entre sanos y enfermos de EM.

TRABAJOS PUBLICADOS

Eye Movements, Strabismus, Amblyopia, and Neuro-Ophthalmology

Progressive Degeneration of the Retinal Nerve Fiber Layer in Patients with Multiple Sclerosis

Raquel Herrero,[1,2] *Elena Garcia-Martin,*[1,2] *Carmen Almarcegui,*[2,3] *Jose R. Ara,*[2,3] *Diego Rodriguez-Mena,*[2,3] *Jesus Martin,*[2,3] *Sofia Otin,*[1] *Maria Satue,*[1,2] *Luis E. Pablo,*[1,2] *and Francisco J. Fernandez*[1,2]

Purpose. To quantify changes in the retinal nerve fiber layer (RNFL) of patients with multiple sclerosis (MS) over 3 years and to evaluate whether treatment protects against RNFL degeneration.

Methods. Ninety-four MS patients and 50 healthy subjects were followed-up over 3 years. All subjects underwent a complete ophthalmic examination, which included assessment of visual acuity (Snellen chart), color vision (Ishihara pseudoisochromatic plates), visual field examination, optical coherence tomography (OCT), and visual evoked potentials (VEPs). All patients were reevaluated at 12, 24, and 36 months to quantify changes in the RNFL.

Results. Changes were detected in RNFL thickness at the 36-month follow-up. Significant decreases ($P < 0.05$, *t*-test) were observed in the mean, superior, inferior, and temporal RNFL thicknesses, and macular volume provided by OCT, and in the P100 latency of VEP of the MS group, but only in the mean and inferior RNFL thicknesses of the healthy control group. Greater changes in the superior and inferior RNFL thicknesses during follow-up were detected in the MS group. Differences between treatments were not detected, but untreated patients had higher degeneration in the mean and superior RNFL thicknesses during the follow-up ($P = 0.040$ and $P = 0.19$, respectively).

Conclusions. Progressive axonal loss can be detected in the optic nerve fiber layer of MS patients. Analysis of the RNFL by OCT can be useful for evaluating MS progression and efficacy of treatment as a neuroprotective factor against axonal degeneration. (*Invest Ophthalmol Vis Sci.* 2012;53:8344–8349) DOI:10.1167/iovs.12-10362

Multiple sclerosis (MS) is a neurodegenerative disease characterized by axonal injury in the central nervous system (CNS), leading to progressive neurologic deficits. Evidence indicates that axonal damage occurs already in the early stages of the disease, not related to inflammatory or autoimmune episodes against myelin, and axonal degeneration is directly related to permanent functional disability.[1,2] Axonal damage in patients with MS can be detected and quantified at the level of the retinal nerve fiber layer (RNFL) using ocular imaging technologies, such as optical coherence tomography (OCT).[3–8]

The retina is a part of the CNS that is easily accessible to clinical examination. The RNFL comprises mainly nonmyelinated axons of retinal ganglion cells, so RNFL thickness measurements provide a relatively direct assessment of the axons and axonal damage.

Technologies for digital image analysis in ophthalmology, such as OCT, include the development of parameters to provide quantitative, objective, and reproducible RNFL measurements. Some studies have demonstrated RNFL loss in eyes of MS patients without optic neuritis antecedent.[3–7]

Numerous investigators have suggested the importance of examining RNFL thickness with OCT as a biologic marker of axonal damage in patients with MS,[9–14] and as a useful method for monitoring MS progression.[6,7] Some authors have even suggested that OCT could substitute for magnetic resonance imaging as a method for monitoring the disease.[8,14,15] Long-term follow-up studies are needed, however, to evaluate this hypothesis.

Fourier-domain optical coherence tomography (FD-OCT) uses a spectrometer consisting of transmission grating and an air-spaced focusing lens. In FD-OCT, depth information is acquired by analysis of the interference patterns in a spectrum of mixed reflected lights.[16] To achieve ultrahigh resolution images, time-domain (TD) OCT requires a longer acquisition time, but FD-OCT obtains 2- to 3-mm axial resolution images without a remarkable increase in the acquisition time.[17]

The signal-to-noise ratio can be further reduced with the pulsed illumination that is used by FD-OCT instead of the continuous wave illumination used in TD-OCT. The pulsed illumination reduces the detrimental effects of sample motion during scanning, so fewer artifacts and clearer images are acquired.[18]

Some investigators have used high-definition OCT to evaluate MS patients in cross-sectional studies,[19] but very few longitudinal studies using FD-OCT[20,21] have been published. These studies did not incorporate an exhaustive neuro-ophthalmologic examination of changes in visual evoked potentials (VEPs) over time. The purpose of this study was to evaluate structural and functional changes of the RNFL and correlations between these RNFL changes and disease progression or severity over a period of 3 years.

Methods

We performed a prospective longitudinal study with a duration of 3 years. In all, 188 eyes of 94 MS patients and 50 healthy subjects were evaluated at baseline, and at 12, 24, and 36 months. The study was

From the [1]Ophthalmology Department and [3]Neurology Department, Miguel Servet University Hospital, Zaragoza, Spain; and the [2]Aragones Institute of Health Science, Zaragoza, Spain.

Supported in part by Instituto de Salud Carlos III Grant PI11/01553.

Submitted for publication June 8, 2012; revised August 16 and October 2, 2012; accepted October 3, 2012.

Disclosure: **R. Herrero**, None; **E. Garcia-Martin**, None; **C. Almarcegui**, None; **J.R. Ara**, None; **D. Rodriguez-Mena**, None; **J. Martin**, None; **S. Otin**, None; **M. Satue**, None; **L.E. Pablo**, None; **F.J. Fernandez**, None

Corresponding author: Raquel Herrero, C/Padre Arrupe, Consultas Externas de Oftalmología, 50009 Zaragoza, Spain; raquelherrero84@yahoo.es.

Investigative Ophthalmology & Visual Science, December 2012, Vol. 53, No. 13

approved by the hospital ethics committee and all patients signed an informed consent form detailing the purpose of this study and the tests included in the exploratory protocol, as well as the ability to stop participating in the study at any time they desired.

The study inclusion criteria were: confirmed diagnosis of MS by a neurologist based on the Poser criteria,[22] visual acuity ≥ 0.1 with the Snellen scale, and applanation intraocular pressure < 20 mm Hg. Patients with active MS outbreaks (of any neurologic deficit, not only optic neuritis) in the 6 months preceding enrollment in the study or during follow-up were excluded from the study. The reason for the study was to evaluate axonal damage secondary to the progression of MS reflecting chronic MS neurodegeneration, and acute losses that appear in times of outbreaks were not included. Patients with refractive errors > 5 diopters (D) of equivalent spherical or 3 D of astigmatism were also excluded from the study.

All subjects underwent a complete ophthalmic examination that included assessment of best-corrected visual acuity (BCVA; Snellen chart), color vision (Ishihara pseudoisochromatic plates), ocular motility, pupillary reflexes, anterior segment exam, applanation intraocular pressure (Goldmann), papillary morphology with fundoscopic exam, visual field examination, OCT, and VEP. Each eye was considered separately. All subjects were reevaluated at 12, 24, and 36 months to quantify the changes in the RNFL and assess correlations with other associated factors, such as functional disability progression measured using the EDSS (Expanded Disability Status Scale).

The neurologic variables assessed were MS phenotype (relapsing-remitting, primary progressive, and secondary progressive), disease duration, EDSS, and EDSS Fvi (visual system subset of the EDSS). Age and sex were included as covariates in the analyses. Visual acuity was measured with Snellen charts, monocular, and with a viewing distance of 6 meters. Visual field examination was performed using a Humphrey field analyzer (Carl Zeiss Meditec, Dublin, CA) using the SITA Standard 30-2 program and mean deviation was evaluated. The fundoscopy study was based on observation of the papilla morphology (normal, diffuse, or sectorial atrophy or edema) with a 78-D lens. Optical coherence tomography with a spectral-domain (SD) OCT system (Cirrus OCT 3000; Carl Zeiss Meditec) used the following protocols for retinal imaging: fast RNFL thickness (3.4-mm circular scans) and fast macula. Parameters evaluated were mean thickness, RNFL thicknesses of the four quadrants, and macular volume. VEP analysis was performed using commercial software that facilitates the acquisition and analysis of auditory, visual, and somatosensory evoked potentials (Neuronic Sense Witness System 4.0 device; IC Neuronic S.L.; Zaragoza, Spain). Silver chloride–plated disk electrodes were placed on the scalp at the occipital (Oz, active electrode) and frontal (Fz, reference electrode) areas. The frequency of the stimulation pattern was 2 Hz. Mean luminance was 93.5 candelas/m^2, with a contrast of 99%. The latency and amplitude of the positive fundamental component (P100) were analyzed.[23]

All variables were registered in a database created with a commercial database application program (FileMaker Pro 8.5; FileMaker, Inc., Santa Clara, CA). Two statistical analyses were performed: first, an observational cross-sectional study using baseline measurements, and then a longitudinal study. In the cross-sectional analysis, the independent variables were MS phenotype and immunomodulatory therapy, and the dependent variables were the parameters provided by the different techniques included in the study protocol. Modifier variables were age, sex, and intraocular pressure. All subjects were revaluated after 12, 24, and 36 months from baseline, and the longitudinal analysis was performed.

Statistical analysis was performed using commercial predictive analytics software (SPSS, version 19.0; SPSS, Inc., Chicago, IL). The normality of the sample distribution was confirmed using the Kolmogorov-Smirnov test. Values of $P < 0.05$ were considered statistically significant. Results of each variable in subsequent visits were compared for both groups (MS and healthy controls) by ANOVA, to detect differences in RNFL associated with disease progression. Pearson's correlation test was used to correlate changes in structural (OCT) and functional (visual field, BCVA, chromatic vision, and VEP) variables, and to correlate measurements registered during the study on the disability status of the MS patients (EDSS). Correlation analysis was used to determine the Pearson correlation coefficient (r) and the statistical significance of the association (P). The Pearson correlation coefficient (r) can range between +1 and −1: a value of 0 indicates that there is no association between the two variables. A value > 0 indicates a positive association, that is, as the value of one variable increases so does the value of the other variable. A value < 0 indicates a negative association, that is, as the value of one variable increases the value of the other variable decreases.

Finally, patients were divided into two groups: patients with treatment for MS and patients without treatment. Patients treated with mitoxantrone were excluded to minimize bias. A statistical comparison between the groups was performed to analyze whether treatment is a protective factor against RNFL degeneration in patients with MS.

Results

The MS group included 64 females and 30 males with a female/male ratio of 3:2. The control group included 17 females and 33 males (ratio of 3:2). Age and sex in the MS and control groups were not significantly different ($P = 0.568$ and 0.394, respectively). Eighty-six patients (92.6%) belonged to the relapsing–remitting MS group, 6 patients (6.4%) to the secondary progressive group, and 1 patient (1.1%) to the

Table 1. Functional and Structural Measurements Obtained at Baseline and Annual Examinations in Patients with Multiple Sclerosis (at 1, 2, and 3 Years of Follow-Up)

	Baseline	1 Year	2 Years	3 Years	Annual Change	*P*
BCVA	0.91 (0.24)	0.94 (0.21)	0.92 (0.11)	0.90 (0.34)	−0.003	**0.034**
Ishihara test	18.06 (3.04)	17.93 (3.22)	18.12 (3.76)	18.08 (3.23)	0.03	0.278
Visual field, MD (dB)	−3.08 (2.44)	−3.01 (3.23)	−3.62 (2.14)	−3.87 (2.76)	−0.42	0.689
OCT mean thickness	89.43 (10.65)	86.95 (11.28)	84.50 (10.62)	81.03 (10.65)	−3.67	**0.004**
OCT superior thickness	115.78 (15.03)	114.26 (16.23)	109.45 (14.79)	105.01 (13.45)	−4.98	**0.005**
OCT nasal thickness	69.06 (17.47)	68.12 (17.08)	67.57 (16.16)	66.99 (15.89)	−1.12	0.061
OCT inferior thickness	113.67 (14.56)	109.30 (16.34)	105.30 (19.22)	101.12 (15.59)	−4.88	**0.008**
OCT temporal thickness	59.61 (13.45)	56.57 (18.97)	55.91 (15.63)	52.78 (15.11)	−3.61	**0.019**
OCT macular volume	6.57 (0.43)	6.43 (0.23)	6.42 (0.39)	6.43 (0.34)	−0.18	**0.031**
VEP amplitude, mV	11.09 (2.99)	11.05 (5.77)	11.12 (5.27)	10.99 (4.57)	−0.04	0.443
VEP latency, ms	124.59 (11.32)	118.45 (6.45)	116.17 (5.54)	114.16 (7.31)	0.40	**0.039**

Results reported as mean and SD in parentheses; mean of annual change in each parameter over the 3-year follow-up and significance level (ANOVA) comparing changes between visits in longitudinal analysis. Significant measurements are indicated in bold font ($P < 0.05$). RNFL thickness is measured in micrometers (μm), and macular volume is measured in mm^3.

TABLE 2. Functional and Structural Measurements Obtained in the Healthy Control Group at Baseline and Annual Examinations (at 1, 2, and 3 Years of Follow-Up)

	Baseline	1 Year	2 Years	3 Years	Annual Change	P
BCVA	0.95 (0.14)	0.95 (0.18)	0.95 (0.17)	0.95 (0.16)	<−0.001	0.876
Ishihara test	19.65 (1.34)	19.64 (1.78)	19.66 (1.66)	19.63 (1.82)	−0.001	0.573
Visual field, MD (dB)	−0.77 (2.10)	−0.78 (1.98)	−0.75 (1.61)	−0.75 (1.55)	−0.008	0.770
OCT mean thickness	95.97 (11.60)	94.72 (11.82)	93.02 (10.62)	91.13 (10.65)	−0.152	**0.045**
OCT superior thickness	117.95 (15.61)	116.34 (15.71)	115.45 (14.39)	115.04 (13.45)	−0.079	0.245
OCT nasal thickness	72.53 (9.59)	72.27 (10.02)	72.00 (10.34)	71.66 (11.70)	−0.022	0.156
OCT inferior thickness	126.25 (13.34)	125.87 (13.24)	124.03 (14.29)	123.19 (13.33)	−0.180	**0.032**
OCT temporal thickness	68.53 (11.90)	67.96 (11.39)	67.56 (15.03)	67.25 (15.11)	−0.042	0.441
OCT macular volume	7.11 (0.34)	7.10 (0.28)	7.11 (0.21)	7.10 (0.20)	−0.005	0.398
VEP amplitude, mV	14.55 (2.53)	14.56 (2.77)	14.54 (3.34)	14.54 (3.67)	<−0.001	0.689
VEP latency, ms	100.32 (5.92)	100.11 (4.65)	100.43 (5.01)	110.41 (6.88)	0.003	0.220

Results are reported as mean and SD in parentheses; mean of annual change in each parameter over the 3-year follow-up and significance level (ANOVA) comparing changes between visits in longitudinal analysis. Significant measurements are indicated in bold font ($P < 0.05$). RNFL thickness is measured in micrometers (μm), and macular volume is measured in mm^3.

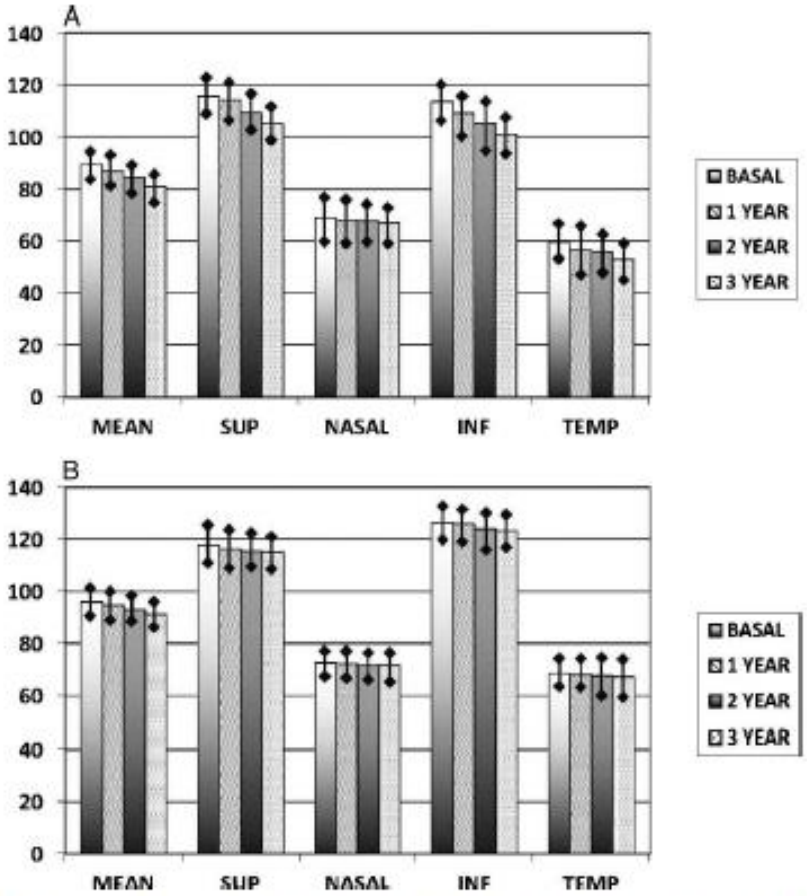

FIGURE 1. (A) Mean RNFL thickness measured by OCT in patients with multiple sclerosis at baseline examination and the revisions made in the first, second, and third years. Thickness of the RNFL is measured in micrometers (μm). (B) Mean RNFL thickness measured by OCT in healthy controls at baseline examination and the revisions made in the first, second, and third years. SUP, superior; INF, inferior; TEMP, temporal.

TABLE 3. Differences in Mean Change in Each Variable during the 3-Year Follow-Up for Two Groups: Treated and Untreated Patients

	Change at 3 Years in Untreated Patients	Change at 3 Years in Treated Patients	P
Functional variables			
BCVA (Snellen)	−0.003 (0.001)	−0.002 (0.001)	0.257
Ishihara test	0.02 (0.002)	0.04 (0.001)	0.487
Visual field MD (dB)	−0.22 (0.10)	−0.49 (0.07)	0.312
EDSS	0.10 (0.01)	−0.10 (0.01)	**0.034**
EDSS Pvi	0.03 (0.002)	−0.01 (0.001)	0.457
RNFL thickness (OCT)			
Mean, μm	−3.67 (0.72)	−3.39 (0.66)	**0.040**
Superior, μm	−4.98 (0.54)	−3.97 (0.72)	**0.019**
Nasal, μm	−1.12 (0.52)	−1.21 (0.38)	0.298
Inferior, μm	−4.88 (0.91)	−4.61 (0.80)	0.389
Temporal, μm	−3.61 (0.83)	−3.60 (0.91)	0.053
Macular volume, mm^3	−0.18 (0.02)	−0.15 (0.02)	0.076
VEP			
Latency, ms	0.05 (0.01)	0.05 (0.01)	0.770
Amplitude, mV	−0.41 (0.01)	−0.37 (0.01)	0.523

Differences in mean change of each parameter during the 3-year follow-up and SD in parentheses, for the two groups: treated and untreated. Significance difference in change between treated and untreated groups based on Student's *t*-test.

primary progressive group. Antecedents of diplopia were present in 56 patients (29.8%) and neuritis in 45 patients (23.9%). The mean EDSS score at baseline was 2.5 (range: 0–8).

With respect to the percentage of patients assigned to each treatment group, the largest group comprised subjects who received no treatment (36%). Among treated patients, the largest group received beta interferon 1b (Betaferon; Bayer HealthCare, Leverkusen, Germany) (21.3%), followed by beta interferon 1a (Rebif; EMD Serono, Inc., Rockland, MA [16.0%] or Avonex; Biogen Idec International GmbH, Zug, Switzerland [12.8%]), glatiramer acetate (Copaxone; Teva Pharmaceutical Industries Ltd., Petach Tikva, Israel) (11.7%), and mitoxantrone (Mitoxantrona; Beijing Mesochem Technology Co., Ltd., Beijing, China) (2.0%).

Results of functional and structural parameters evaluated and significant differences between the baseline and 3-year examinations are shown in Tables 1 and 2. In MS patients, we detected a significant loss in BCVA; mean, superior, inferior, temporal RNFL thicknesses, and macular volume obtained with OCT; and a significant delay in the P100 wave latency in VEP (Table 1 and Fig. 1A). In healthy subjects, we observed a significant loss only in the mean and inferior RNFL thicknesses (annual changes of −0.152 and −0.180 μm, respectively; $P = 0.045$ and 0.032; Table 2 and Fig. 1B).

In the MS group, annual mean RNFL thickness measured by OCT showed a clear decrease over 3 years (Fig. 1A). The parameters with the most changes between baseline and the 3-year follow-up in MS patients were the superior and inferior RNFL thicknesses, with a decrease in annual mean thickness of 4.98 ($P = 0.015$) and 4.88 μm, respectively ($P < 0.001$).

Correlation analysis was performed to determine the association between the changes registered in parameters during the 3-year follow-up. The changes in structural variables during the follow-up provided by OCT were not significantly correlated with the changes in the functional variables during these 3 years (BCVA, chromatic vision, VEP, EDSS, and EDSS Pvi); however, there was a moderate positive correlation between the change registered during the 3-year follow-up in the mean deviation of the visual field and changes in mean ($r = 0.407$, $P = 0.034$) and temporal ($r = 0.521$, $P = 0.029$) RNFL thicknesses during the 3 years of the longitudinal study.

Changes in the functional and structural parameters over the 3-year follow-up were compared between treated and nontreated patients. Untreated patients showed a higher loss of thickness over the 3-year follow-up in all RNFL parameters (except in the nasal quadrant), but statistical differences were detected only in the mean and superior RNFL thicknesses (Table 3, Fig. 2).

Discussion

In the present study, we quantified changes in the RNFL over a 3-year period to analyze the ability of RNFL evaluation to be used as a biomarker of neurodegeneration and disability in patients with MS, and to compare axonal degeneration

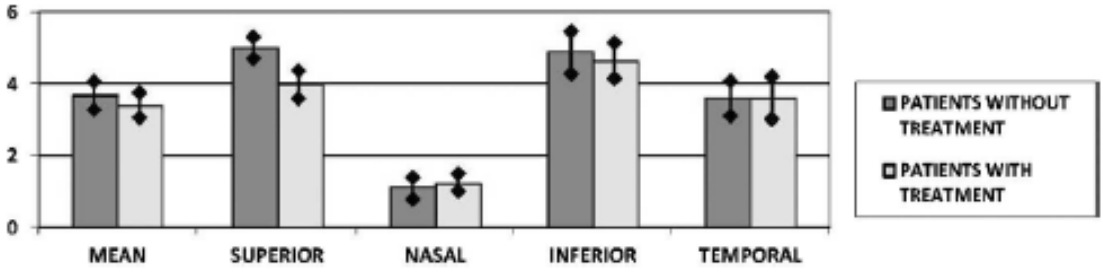

FIGURE 2. Mean decrease in RNFL thickness (measured in μm) over the 3-year follow-up in treated and nontreated groups.

between treated and untreated patients. Numerous studies have demonstrated RNFL thinning not only in eyes with a previous episode of optic neuritis, but also in patients with MS who have never had an acute clinical episode of optic neuritis.[12,24,25] Measurements of RNFL thickness provided by digital imaging devices such as OCT have been suggested to be useful as an indirect marker of brain atrophy in MS.[15,26,27] In addition to RNFL thickness, OCT can also measure macular volume. The macula is composed of ganglion cell bodies, so macular volume may be a useful measurement of axonal loss (based on RNFL thickness) associated with neuronal degeneration.[28]

The new SD-OCT has advantages over previous TD instruments. SD-OCT provided axial resolutions of approximately 5 to 7 μm (compared with Stratus TD-OCT at 10 μm),[29] and the measurements provided by SD devices (such as Cirrus OCT) have better intraobserver and interobserver reproducibility.[8] In addition, several studies suggest that SD technology detects more retinal and RNFL conditions than conventional TD technology.[30,31]

We analyzed each eye separately because each eye can be affected differentially, especially in patients who present with unilateral episodes of optic neuritis. In addition, the OCT devices interpret the three-dimensional profile of the RNFL thickness in each eye and compare it separately with the normative base. Finally, a macular volume reduction in MS patients has been correlated with neuronal necrosis, demyelination, and axonal damage. The loss of ganglion cells also leads to a reduction of the macular volume (independently in each eye).[32–40] Some authors, however, consider the inclusion of only one eye of each patient adequate for statistical analysis because RNFL measurements correlate significantly between the two eyes.

The P100 wave latency of VEP is a parameter with high diagnostic ability in MS.[41,42] The P100 latency is delayed after an optic neuritis episode and this delay is maintained for years.[43] We observed an increase in the latency over the 3-year follow-up period due to the loss of visual pathway function in patients with MS disease progression. Nonreduction of VEP amplitude despite the reduction of the OCT RNFL can be caused by the remaining macular volume. Eighty percent of the VEP amplitude depends on the macula response and, therefore, does not involve the RNFL of the arcuate area. We also observed a nonsignificant increase in the P100 latency in the control group, which may be due to the variability of the device. Our findings reveal that a reduction in the mean or temporal RNFL thickness is associated with a decrease in the mean deviation of the visual field.

Only a few authors have examined the effects of MS treatments on RNFL degeneration. Garcia-Martin et al.[44] concluded that treatment might be a protective factor against RNFL loss associated with disease progression. In the present study, we observed that the treatment for MS has a protective effect on the loss of RNFL thickness, but there were no differences between different types of treatments. MS is a chronic degenerative disease in which axonal loss occurs slowly and gradually in the absence of active inflammatory outbreaks, so a 3-year follow-up is a short time to detect small RNFL modifications in a population such as ours, which included only stable patients who had no acute relapsing MS episodes. Longer studies with a larger sample are needed to assess whether any of the currently approved treatments for MS have a significant protective effect on axonal loss detected by RNFL analysis.

Based on other studies, 6 months is the time required for measurements made with digital image analysis techniques to record retrograde degeneration after an inflammatory episode in the optic nerve.[32,33] In the present study, patients with optic neuritis in the 6 months preceding the study were excluded, so all subjects were considered to have stable MS. If patients with active acute relapsing MS episodes had been included, higher differences between treatments may have been detected. The reason for excluding patients with acute relapsing MS episodes was to assess only axonal damage secondary to the progression of MS disease. The RNFL changes registered in our study were caused only by MS-related chronic neurodegeneration, not by acute heavy axonal loss that occurs in acute relapsing MS episodes.

In conclusion, analysis of RNFL measured by OCT has good capability for detecting axonal damage in MS patients, and can be used to evaluate disease progression and effectiveness of the various therapies currently in use.

References

1. Palace J. Inflammation versus neurodegeneration: consequences for treatment. *J Neurol Sci*. 2007;259:46–49.
2. Hauser SL, Oksenberg JR. The neurobiology of multiple sclerosis: genes, inflammation, and neurodegeneration. *Neuron*. 2006;52:61–76.
3. Khanifar AA, Parlitsis GJ, Ehrlich JR, et al. Retinal nerve fiber layer evaluation in multiple sclerosis with spectral domain optical coherence tomography. *Clin Ophthalmol*. 2010;4:1007–1013.
4. Sergott RC. Optical coherence tomography: measuring in-vivo axonal survival and neuroprotection in multiple sclerosis and optic neuritis. *Curr Opin Ophthalmol*. 2005;16:346–350.
5. Zaveri MS, Conger A, Salter A, et al. Retinal imaging by laser polarimetry and optical coherence tomography evidence of axonal degeneration in multiple sclerosis. *Arch Neurol*. 2008;65:924–928.
6. Gundogan FC, Demirkaya S, Sobaci G. Is optical coherence tomography really a new biomarker candidate in multiple sclerosis? A structural and functional evaluation. *Invest Ophthalmol Vis Sci*. 2007;48:5773–5781.
7. Garcia-Martin E, Pueyo V, Martin J, et al. Progressive changes in the retinal nerve fiber layer in patients with multiple sclerosis. *Eur J Ophthalmol*. 2010;20:167–173.
8. Garcia-Martin E, Pueyo V, Pinilla I, Ara JR, Martin J, Fernandez J. Fourier-domain OCT in multiple sclerosis patients: reproducibility and ability to detect retinal nerve fiber layer atrophy. *Invest Ophthalmol Vis Sci*. 2011;52:4124–4131.
9. Henderson AP, Trip SA, Schlottmann PG, et al. A preliminary longitudinal study of the retinal nerve fiber layer in progressive multiple sclerosis. *J Neurol*. 2010;257:1083–1091.
10. Ratchford JN, Quigg ME, Conger A, et al. Optical coherence tomography helps differentiate neuromyelitis optica and MS optic neuropathies. *Neurology*. 2009;73:302–308.
11. Syc SB, Warner CV, Hiremath GS, et al. Reproducibility of high-resolution optical coherence tomography in multiple sclerosis. *Mult Scler*. 2010;16:829–839.
12. Pueyo V, Martin J, Fernandez J, et al. Axonal loss in the retinal nerve fiber layer in patients with multiple sclerosis. *Mult Scler*. 2008;14:609–614.
13. Pueyo V, Polo V, Larrosa JM, Mayoral F, Ferreras A, Honrubia FM. Reproducibility of optic nerve head and retinal nerve fiber layer thickness measurements using optical coherence tomography. *Arch Soc Esp Oftalmol*. 2006;81:205–211.
14. Garcia-Martin E, Pueyo V, Ara JR, et al. Effect of optic neuritis on progressive axonal damage in multiple sclerosis patients. *Mult Scler*. 2011;17:850–857.
15. Frohman EM, Dwyer MG, Frohman T, et al. Relationship of optic nerve and brain conventional and non-conventional MRI measures and retinal nerve fiber layer thickness, as assessed by OCT and GDx: a pilot study. *J Neurol Sci*. 2009;282:96–105.

16. Yi K, Mujat M, Park BH, et al. Spectral domain optical coherence tomography for quantitative evaluation of drusen and associated structural changes in non-neovascular age-related macular degeneration. *Br J Ophthalmol*. 2009;93:176–181.
17. Wojtkowski M, Srinivasan V, Fujimoto JG, et al. Three-dimensional retinal imaging with high-speed ultrahigh-resolution optical coherence tomography. *Ophthalmology*. 2005; 112:1734–1746.
18. You JW, Chen TC, Mujat M, Park BH, De Boer JF. Pulsed illumination spectral-domain optical coherence tomography for human retinal imaging. *Opt Express*. 2006;14:6739–6748.
19. Fjeldstad C, Bemben M, Pardo G. Reduced retinal nerve fiber layer and macular thickness in patients with multiple sclerosis with no history of optic neuritis identified by the use of spectral domain high-definition optical coherence tomography. *J Clin Neurosci*. 2011;18:1469–1472.
20. Garcia-Martin E, Pueyo V, Almarcegui C, et al. Risk factors for progressive axonal degeneration of the retinal nerve fibre layer in multiple sclerosis patients. *Br J Ophthalmol*. 2011;95: 1577–1582.
21. Serbecic N, Aboul-Enein F, Beutelspacher SC, et al. High resolution spectral domain optical coherence tomography (SD-OCT) in multiple sclerosis: the first follow up study over two years. *PLoS One*. 2011;6:e19843.
22. Beer S, Rösler KM, Hess CW. Diagnostic value of paraclinical tests in multiple sclerosis: relative sensitivities and specificities for reclassification according to the Poser committee criteria. *J Neurol Neurosurg Psychiatry*. 1995;59:152–199.
23. Almarcegui C, Dolz I, Pueyo V, et al. Correlation between functional and structural assessments of the optic nerve and retina in multiple sclerosis patients. *Neurophysiol Clin*. 2010; 40:129–135.
24. Parikh RS, Parikh SR, Sekhar GC, Prabakaran S, Babu JG, Thomas R. Normal age-related decay of retinal nerve fiber layer thickness. *Ophthalmology*. 2007;114:921–926.
25. Talman LS, Bisker ER, Sackel DJ, et al. Longitudinal study of vision and retinal nerve fiber layer thickness in multiple sclerosis. *Ann Neurol*. 2010;67:749–760.
26. Dörr J, Wernecke KD, Bock M, et al. Association of retinal and macular damage with brain atrophy in multiple sclerosis. *PLoS One*. 2011;6:e18132.
27. Gordon-Lipkin E, Chodkowski B, Reich DS, et al. Retinal nerve fiber layer is associated with brain atrophy in multiple sclerosis. *Neurology*. 2007;69:1603–1609.
28. Burkholder BM, Osborne B, Loguidice MJ, et al. Macular volume determined by optical coherence tomography as a measure of neuronal loss in multiple sclerosis. *Arch Neurol*. 2009;66:1366–1372.
29. Chen TC, Zeng A, Sun W, Mujat M, de Boer JF. Spectral domain optical coherence tomography and glaucoma. *Int Ophthalmol Clin*. 2008;48:29–45.
30. Garcia-Martin E, Pinilla I, Sancho E, et al. Optical coherence tomography in retinitis pigmentosa: reproducibility and capacity to detect macular and retinal nerve fiber layer thickness alterations. *Retina*. 2012;32:1581–1591.
31. Costa-Cunha LV, Cunha LP, Malta RF, Monteiro ML. Comparison of Fourier-domain and time-domain optical coherence tomography in the detection of band atrophy of the optic nerve. *Am J Ophthalmol*. 2009;147:56–63.
32. Costello F, Coupland S, Hodge W, et al. Quantifying axonal loss after optic neuritis with optical coherence tomography. *Ann Neurol*. 2006;59:963–969.
33. Noval S, Contreras I, Rebolleda G, Muñoz-Negrete FJ. Optical coherence tomography versus automated perimetry for follow-up of optic neuritis. *Acta Ophthalmol Scand*. 2006; 84:790–794.
34. Klistorner A, Arvind H, Garrick R, et al. Interrelationship of optical coherence tomography and multifocal visual-evoked potentials after optic neuritis. *Invest Ophthalmol Vis Sci*. 2010;51:2770–2777.
35. Gordon-Lipkin E, Chodkowski B, Reich DS, et al. Retinal nerve fiber layer is associated with brain atrophy in multiple sclerosis. *Neurology*. 2007;69:1603–1609.
36. Fisher JB, Jacobs DA, Markowitz CE, et al. Relation of visual function to retinal nerve fiber layer thickness in multiple sclerosis. *Ophthalmology*. 2006;113:324–332.
37. Grazioli E, Zivadinov R, Weinstock-Guttman B, et al. Retinal nerve fiber layer thickness is associated with brain MRI outcomes in multiple sclerosis. *J Neurol Sci*. 2008;268:12–17.
38. Iester M, Cioli F, Uccelli A, et al. Retinal nerve fibre layer measurements and optic nerve head analysis in multiple sclerosis patients. *Eye*. 2009;23:407–412.
39. Trip SA, Schlottmann PG, Jones SJ, et al. Retinal nerve fiber layer axonal loss and visual dysfunction in optic neuritis. *Ann Neurol*. 2005;58:383–391.
40. Zaveri MS, Conger A, Salter A, et al. Retinal imaging by laser polarimetry and optical coherence tomography evidence of axonal degeneration in multiple sclerosis. *Arch Neurol*. 2008; 65:924–928.
41. Balnytė R, Ulozienė I, Rastenytė D, Vaitkus A, Malcienė L, Laučkaitė K. Diagnostic value of conventional visual evoked potentials applied to patients with multiple sclerosis. *Medicina (Kaunas, Lithuania)*. 2011;47:263–269.
42. You Y, Klistorner A, Thie J, Graham SL. Latency delay of visual evoked potential is a real measurement of demyelination in a rat model of optic neuritis. *Invest Ophthalmol Vis Sci*. 2011; 52:6911–6918.
43. Halliday AM. Visual evoked potentials in demyelinating disease. *Adv Neurol*. 1981;31:201–215.
44. García-Martín E, Pueyo V, Fernández J, et al. Effect of treatment in loss of retinal nerve fibre layer in multiple sclerosis patients. *Arch Soc Esp Oftalmol*. 2010;85:209–214.

Diagnostic Ability of a Linear Discriminant Function for Spectral-Domain Optical Coherence Tomography in Patients with Multiple Sclerosis

Elena Garcia-Martin, PhD,[1,2] Luis E. Pablo, PhD,[1,2] Raquel Herrero, MD,[1,2] Maria Satue, MD,[1] Vicente Polo, PhD,[1,2] Jose M. Larrosa, PhD,[1,2] Jesus Martin, PhD,[2,3] Javier Fernandez, PhD[1,2]

Purpose: To calculate and validate a linear discriminant function (LDF) for spectral-domain optical coherence tomography (OCT) to improve the diagnostic ability of retinal nerve fiber layer (RNFL) thickness parameters for the detection of multiple sclerosis (MS).

Design: Observational cross-sectional study.

Participants: Patients with multiple sclerosis (n = 115) and age-matched healthy subjects (n = 115) were enrolled in the study.

Methods: The Spectralis OCT system (Heidelberg Engineering, Heidelberg, Germany) was used to obtain the circumpapillary RNFL thickness in both eyes of each participant.

Main Outcome Measures: A validating set including 60% of the study subjects (69 healthy individuals and 69 patients with MS) was used to test the performance of the LDF in an independent population. Receiver operating characteristic (ROC) curves were plotted and compared with the RNFL parameters measured using OCT. Sensitivity and specificity were used to evaluate diagnostic performance.

Results: The optimized function was 4.965 − 0.40 × (mean thickness 15–30 degrees) − 0.17 × (mean thickness 300–315 degrees) + 2.743 − 0.032 × (mean thickness 105–120 degrees) − 0.031 × (mean thickness 120–135 degrees) − 0.018 × (mean thickness 225–240 degrees). The largest area under the ROC curve was 0.834 for our LDF in the validating population. At 95% fixed specificity, the LDF yielded the highest sensitivity values.

Conclusions: Measurements of RNFL thickness obtained with Spectralis OCT had good ability to differentiate between healthy individuals and individuals with MS. On the basis of the area under the ROC curve, the LDF performed better than any single parameter.

Financial Disclosure(s): The author(s) have no proprietary or commercial interest in any materials discussed in this article. *Ophthalmology 2012;119:1705–1711*

Axonal loss is detected in patients with multiple sclerosis (MS) and is the main cause of disability in this neurodegenerative disease. Several studies report a correlation between axonal loss in the optic nerve of patients with MS and the extent of functional disability.[1–3]

Ganglion cell loss can be detected by ocular imaging technologies, such as optical coherence tomography (OCT) and scanning laser polarimetry, providing noninvasive, rapid, objective, and reproducible methods for evaluating the retinal nerve fiber layer (RNFL). Optical coherence tomography allows for cross-sectional imaging of the retina and the optic disc based on interference patterns produced by low coherence light reflected from retinal tissues.

Improvements in OCT technology were recently introduced, including 3-dimensional high-resolution OCT, which uses Fourier-domain detection to provide increased resolution in relation to classic time-domain OCT, such as the Stratus instrument (Carl Zeiss Meditec, Dublin, CA).[4–6] Many imaging companies market Fourier-domain OCT machines, including RTVue (Optovue, Fremont, CA), Spectralis (Heidelberg Engineering Inc, Heidelberg, Germany), SOCT Copernicus (Optopol Technology, Zawiercie, Poland), Cirrus HD-OCT (Carl Zeiss Meditec), and 3D OCT-1000 (Topcon, Paramus, NJ). All of these devices can be used to measure macular and RNFL thickness.

There are currently no clear guidelines on whether one, several, or all of the RNFL parameters provided by OCT can be used to establish the diagnosis and evaluate the progression of MS. On the basis of the area under the receiver operating characteristic curve (ROC), overall RNFL average thickness is the best diagnostic parameter in different pathologies, such as glaucoma and MS,[6,7] and the most sensitive parameter to detect MS progression.[8] However, optimal MS detection likely requires the use of a combination of several parameters. Pablo et al[9] used combinations of RNFL parameters to evaluate the detection of perimetric glaucoma and to calculate and validate a linear discriminant function (LDF) for the Stratus OCT.

ISSN 0161-6420/12/$–see front matter
doi:10.1016/j.ophtha.2012.01.046

On the basis of the area under the ROC curve (AUC), their LDF performed better than any single parameter in the ability to differentiate between healthy and glaucomatous eyes.[9]

The aim of the present study was to analyze whether a selective combination of Spectralis RNFL parameters could further optimize MS diagnosis. The design of the study followed the 25 items of the guidelines suggested by the Standards for Reporting of Diagnostic Accuracy initiative to increase the quality of reporting diagnostic accuracy studies.[10] To the best of our knowledge, this is the first study to assess the diagnostic ability of an LDF designed for the Spectralis OCT, based exclusively on RNFL parameters, and to assess an LDF for MS disease. The strength of this study lies in the validation of the LDF using an independent sample.[11]

Materials and Methods

The design of the study followed the Declaration of Helsinki Principles. The study protocol was approved by the Clinical Research Ethics Committee of Aragon (Zaragoza, Spain), and informed written consent was obtained from all participants.

Subjects and Measurement Protocol

Required inclusion criteria were as follows: best-corrected visual acuity of ≥20/40, refractive error within ±5.00 diopters equivalent sphere and ±2.00 diopters astigmatism, transparent ocular media (nuclear color/opalescence, cortical or posterior subcapsular lens opacity <1), according to the Lens Opacities Classification System III system.[12] Exclusion criteria included previous intraocular surgery, diabetes, or other diseases affecting the visual field or neurologic system, and current use of medications that could affect visual function.

From April 2010 to June 2011, 2 independent samples of 115 consecutive healthy individuals and 115 patients with MS were prospectively recruited from 2 clinics (1 ophthalmologist and 1 neurologist) in the area of our hospital. The diagnosis of MS was based on standard clinical and neuroimaging criteria provided by magnetic resonance imaging.[13] Related medical records were carefully reviewed, including disease duration, the Expanded Disability Status Scale (EDSS), disease-modifying treatments, acute MS attacks, and the presence of prior episodes of optic neuritis as reported by the treating neurologist and the patient. At a routine 6-month clinical visit, the EDSS was scored by a neurologist with experience in MS. Subjects referred for refraction who underwent routine examination without abnormal ocular findings were recruited as normal eye controls. One sample was randomly selected for developing the LDF (teaching set) and the other sample for checking the performance of the LDF (validating set). The validating set was randomly selected from different MS and healthy populations to test the performance of the LDF in an independent population.

Nine patients with MS did not complete all of the required tests and were therefore excluded from further analysis. A total of 211 eyes of subjects of white European origin were included in the statistical analysis. One eye from each subject was randomly chosen for the study, unless only 1 eye met the inclusion criteria.

All participants underwent a full ophthalmologic examination, including clinical history, visual acuity, biomicroscopy of the anterior segment using a slit lamp, Goldmann applanation tonometry, and ophthalmoscopy of the posterior segment. At least 1 reliable standard automated perimetry test per eye was performed using a Humphrey Field analyzer, model 750i (Zeiss Humphrey Systems, Dublin, CA), with the SITA Standard 30–2 strategy. If fixation losses were greater than 15% and false-positive or false-negative rates were greater than 20%, the test was repeated.[14] The subjects completed the perimetry tests before any clinical examination or structural test. Each perimetry test was performed on different days to avoid a fatigue effect.

The OCT tests were performed to obtain measurements of the peripapillary RNFL using the Spectralis OCT device. With this instrument, RNFL thickness was measured around the disc with 16 averaged consecutive circular B-scans (diameter of 3.5 mm, 768 A-scans); an online tracking system was used to compensate for eye movement. All scans were performed by the same experienced operator. Between scan acquisitions, there was a time delay and subject position and focus were randomly disrupted, meaning that alignment parameters had to be newly adjusted at the start of each image acquisition.[3] No manual correction was applied to the OCT output. An internal fixation target was used because it is reported to have the highest reproducibility.[15] The quality of the scans was assessed before the analysis and poor-quality scans were rejected. The Spectralis OCT uses a blue quality bar in the image to indicate signal strength. The quality score range is 0 (poor quality) to 40 (excellent quality). Only images scored more than 25 were analyzed. Eight images with artifacts, missing parts, or showing seemingly distorted anatomy were excluded, and these scans were repeated.[16]

Image acquisitions using circular peripapillary Spectralis OCT scans (RNFL protocol) were performed using *TruTrack* eye-tracking technology that recognizes, locks onto, and follows the patient's retina during scanning and automatically places follow-up scans to ensure accurate monitoring of disease progression. The Spectralis OCT system simultaneously captures infrared fundus and SD-OCT images at 40 000 A-scans per second. A real-time eye tracking system measures eye movements and provides feedback to the scanning mechanism to stabilize the retinal position of the B-scan. This system thus enables sweep averaging at each B-scan location to reduce speckle noise. The mean number of scans to produce each circular B-scan was 9.[3] The RNFL Spectralis protocol generates a map showing the average thickness and 6 sector thicknesses (superonasal, nasal, inferonasal, inferotemporal, temporal, and superotemporal in the clockwise direction for the right eye and counterclockwise for the left eye). The Spectralis device also generates a database with RNFL thickness measurements at all 768 points registered during circular peripapillary scan acquisition. Spectralis software version 3.2 was used.

Statistical Analysis

All statistical analyses were calculated using SPSS (version 19.0; SPSS Inc, Chicago, IL) and MedCalc (version 9.6.4.0; MedCalc Software, Mariakerke, Belgium) statistical software. The teaching set was used for binary logistic regression analysis, a regression analysis that is used when the dependent variable is dichotomous (healthy or diseased) and the independent variables are of any type. The dependent variable was MS diagnosis (yes or no), and the predictive variables were the 768 RNFL thickness measurements, the average thickness, and 6 sector thicknesses (superonasal, nasal, inferonasal, inferotemporal, temporal, and superotemporal) measured with the Spectralis OCT.

For a logistic regression, the predicted dependent variable is a function of the probability that a particular subject will be in one of the categories (e.g., the probability that 1 subject has MS, given his/her set of scores on the predictor variables). The relative importance of each independent variable was assessed by stepwise

binary logistic regression analysis using the forward Wald method. The Wald w2-statistic tests the unique contribution of each predictor in the context of the other predictors (holding constant the other predictors), eliminating any overlap between predictors.

Thus, the parameters with higher sensitivity/specificity values do not necessarily have to be the selected variables in the logistic regression method. The stepwise probability test determined the criteria by which variables were entered into and removed from the model. The LDF was a score calculated by taking the weighted sum of the predictor variables. The significant OCT parameters were combined to generate a new variable (the LDF) in such a way that the measurable differences between healthy and MS eyes were maximized. The validating set was used to test and compare the diagnostic accuracy of our LDF with other RNFL parameters of the Spectralis OCT. The ROC curves were plotted for all of the parameters and compared with the proposed LDF.

Differences between the ROC curves were tested to compare the AUCs using the Hanley–McNeil method.[17] The cutoff points were calculated with MedCalc software as the points with the best sensitivity–specificity balance. Sensitivities at 85% and 95% (15% and 5% false-positive rate, respectively) fixed specificities, and positive and negative likelihood ratios (LRs) were also calculated.

Results

A total of 115 eyes from 115 patients with relapsing-remitting MS were examined. A previous acute optic neuritis attack was reported for 35 eyes (30%), whereas 80 eyes (70%) were studied from patients with no history of optic neuritis. The duration of the MS ranged from 6 months to 40 years with a median of 9.3 years since diagnosis. The ages of patients ranged from 20 to 62 years with a mean of 41.2 years (Table 1). The ratio of women to men was 2:1 (76 female, 39 male). Mean intraocular pressure was 14.3 mmHg. Mean EDSS was 2.5. Forty-five of the patients (39%) received no specific treatment for MS, whereas 60 patients (51%) were treated with interferon beta and 11 patients (10%) received natalizumab.

All RNFL parameters were more affected in patients with MS than in healthy controls (Table 1). We found significant differences between groups in relation to structural (RNFL thickness measurements provided by the Spectralis OCT) and functional parameters (best-corrected visual acuity, standard automated perimetry mean deviation) examined in the ophthalmologic evaluation.

The validating set comprised 69 healthy eyes and 69 MS eyes, not included in the teaching set. The mean age of the normal group was 41.6±10.7 years, and the mean age of the MS group was 41.4±10.9 years. Sex and age did not differ significantly between the groups in either sample (Table 1).

A stepwise procedure was used to identify the RNFL parameter of the Spectralis OCT that accounted for the greatest amount of error, which was then included in the model. The next best variable was then identified and included, and so on.

All 768 A-scans provided by the Spectralis OCT to measure RNFL thickness were included in statistical analysis to calculate 3 LDFs: superior LDF, inferior LDF, and definitive LDF. In the superior LDF, the mean RNFL thickness between 15 and 30 degrees around the disc was selected at the first iteration, and mean RNFL thickness between 300 and 315 degrees was selected at the second iteration. To calculate inferior LDF, the mean RNFL thickness between 90 and 105 degrees, 105 and 120 degrees, 120 and 135 degrees, 180 and 195 degrees, and 225 and 240 degrees were selected at the subsequent iterations. By using this procedure, our definitive LDF was defined as follows: 4.965 − 0.40 × (mean thickness 15–30 degrees) − 0.17 × (mean thickness 300–315 degrees) + 2.743 − 0.032

Table 1. Clinical Characteristics and Retinal Nerve Fiber Layer Measurements of Both Populations Included in the Study

	Teaching Set					Validating Set				
	Healthy Subjects (n = 115)		*Patients with MS (n = 115)*			*Healthy Subjects (n = 69)*		*Patients with MS (n = 69)*		
	Mean (Range)	*SD*	*Mean (Range)*	*SD*	*P**	*Mean (Range)*	*SD*	*Mean (Range)*	*SD*	*P**
Age (yrs)	41.1 (20–62)	10.8	41.2 (20–62)	9.9	0.765	41.6 (20–61)	10.9	41.4 (21–62)	10.9	0.651
BCVA (Snellen)	1 (0.8–1)	0.1	0.8 (0.3–1)	0.2	**0.003**	1 (0.8–1)	0.1	0.8 (0.4–1)	0.2	**0.004**
IOP (mm Hg)	14.5 (11–20)	2.4	14.3 (10–19)	2.2	0.800	14.4 (11–19)	2.2	14.3 (10–19)	2.1	0.771
MD of SAP	1.1 (−3.5–4.0)	2.1	−0.9 (−18.1–2.1)	3.1	**0.011**	1.1 (−3.4–4.0)	2.2	−1.1 (−18.1–1.2)	3.4	**0.021**
Average thickness (μm)	109.5 (37–152)	8.2	100.3 (78–127)	9.4	**<0.001**	108.2 (40–150)	8.5	98.9 (80–119)	9.7	**0.001**
Temporal-superior thickness (μm)	137.2 (38–166)	10.2	136.5 (63–178)	19.9	0.123	138.0 (41–166)	10.1	135.3 (70–178)	18.5	0.145
Temporal thickness (μm)	78.9 (25–130)	8.5	72.6 (51–114)	12.4	**<0.001**	78.5 (29–128)	9.1	70.7 (53–114)	11.1	**<0.001**
Temporal-inferior thickness (μm)	154.8 (58–173)	12.4	150.3 (68–224)	20.2	**0.009**	153.4 (58–169)	11.4	150.4 (68–158)	20.5	**0.002**
Nasal-inferior thickness (μm)	135.5 (17–208)	16.5	112.3 (56–256)	26.7	**0.025**	135.2 (17–208)	17.2	112.2 (56–209)	26.0	**0.001**
Nasal thickness (μm)	93.9 (40–129)	12.3	72.9 (36–108)	15.0	0.215	93.7 (42–129)	13.1	72.8 (39–108)	15.4	0.415
Nasal-superior thickness (μm)	112.9 (18–202)	17.8	112.1 (27–175)	21.6	0.085	113.0 (39–189)	19.2	111.5 (31–170)	21.1	0.145
LDF	4.2 (−0.8–7.2)	1.2	2.2 (−4.4–5.7)	1.8	**<0.001**	4.3 (0.5–7.1)	1.5	2.1 (−4.2–5.7)	1.9	**<0.001**
MS duration (yrs)	—	—	9.3 (2–40)	0.9	—	—	—	9.4 (4–40)	0.8	—
EDSS score	—	—	2.5 (0–8)	0.3	—	—	—	2.4 (0–7.5)	0.2	—
Gender (female : male)	76 : 39	—	76 : 39	—	0.598	47 : 22	—	47 : 22	—	0.623

BCVA = best-corrected visual acuity; EDSS = Expanded Disability Status Scale; IOP = basal intraocular pressure; LDF = linear discriminant function; MD = mean deviation; MS = multiple sclerosis; SAP = standard automated perimetry; SD = standard deviation.
*Significant difference ($P<0.05$) in Student t test between normal and MS groups for each population. Bold values represents statistical significant differences ($P<0.05$).

Table 2. In the Validating Set, Areas Under the Receiver Operating Characteristic Curves, Best Sensitivity–Specificity Balance, and Likelihood Ratios of Retinal Nerve Fiber Layer Parameters of Optical Coherence Tomography to Discriminate between Normal Subjects and Patients with Multiple Sclerosis

OCT Parameters	AUC	95% CI	AUC P Value	Cutoff Point	Sensitivity (%)	Specificity (%)	+LR	−LR	Sensitivity Specificity 85%	Sensitivity Specificity 95%
LDF	0.806	0.748–0.856	<0.001	>3.14	83.02	68.70	2.62	0.25	60.4	31.3
LDF sup	0.748	0.686–0.804	<0.001	≤−43.41	71.7	68.7	2.29	0.41	44.3	23.6
LDF inf	0.732	0.668–0.789	<0.001	≤5.84	61.3	71.3	2.17	0.53	42.5	31.1
Average thickness	0.641	0.574–0.704	<0.001	≤87	39.6	96.5	11.3	0.63	49.1	39.6
Temporal-sup thickness	0.635	0.567–0.699	<0.001	≤113	35.9	93.0	5.12	0.69	38.8	30.1
Temporal thickness	0.735	0.671–0.792	<0.001	≤142	73.3	72.8	2.70	0.40	46.0	26.7
Temporal-inf thickness	0.639	0.603–0.729	<0.001	≤60	47.6	84.2	3.02	0.62	47.7	34.3
Nasal-inf thickness	0.542	0.474–0.609	0.281	≤86	34.9	89.5	3.32	0.73	19.9	35.6
Nasal thickness	0.519	0.451–0.587	0.619	≤67	40.6	74.6	1.59	0.80	17.9	5.7
Nasal-sup thickness	0.633	0.607–0.724	<0.001	≤108	72.1	60.5	1.83	0.46	41.3	20.2

AUC = area under the receiver operating characteristic curve; CI = confidence interval; inf = inferior; LDF = linear discriminant function; +LR = positive likelihood ratio; −LR = negative likelihood ratio; OCT = optical coherence tomography; sup = superior.
The cutoff points were calculated using the MedCalc software as the points with the best sensitivity–specificity balance. Sensitivities at 85% and 95% fixed specificities are shown.

× (mean thickness 105–120 degrees) − 0.031 × (mean thickness 120–135 degrees) − 0.018 × (mean thickness from 225–240 degrees).

In the teaching set, the highest sensitivity–specificity balance was observed for our LDF (84–71; cutoff point: >3.14) and temporal thickness (74–73; cutoff point: ≤142). The AUC was 0.834 (95% confidence interval [CI], 0.752–0.865) for the LDF. The largest AUCs for the provided OCT parameters were 0.698 (95% CI, 0.631–0.758) for the average thickness and 0.732 (95% CI, 0.669–0.794) for the temporal quadrant thickness. The differences between the AUCs of the LDF were significantly different from those of the average thickness ($P = 0.006$) and the temporal sector thickness ($P = 0.036$).

In the validating set (Table 2), the average thickness, temporal quadrant thickness, and LDFs had the best sensitivity–specificity pairs. The average and temporal superior thicknesses had the highest positive LRs (11.29 and 5.12, respectively), and the LDF had the lowest negative LRs (0.25). The greatest AUCs (Table 2; Fig 1) were 0.806 (95% CI, 0.748–0.856) for the LDF, 0.641 (95% CI, 0.574–0.704) for average thickness, and 0.735 (95% CI, 0.674–0.792) for temporal thickness. Compared with the OCT-provided parameters (Table 3), the LDF had the largest AUC, except for temporal thickness ($P = 0.158$) and temporal-inferior thickness ($P = 0.324$).

Logistic regression analysis was repeated to compare sensitivity and specificity in severely affected patients with MS (group performed by patients with EDSS score ≥4.0) and slightly or moderately affected patients with MS (patients with EDSS score ≤3.5). The LDF had better diagnostic accuracy for the LDF in the group with an EDSS ≥4 (Fig 2).

Discussion

Previous studies have reported the sensitivity and specificity of OCT for discriminating between healthy and MS eyes.[18,19] In addition, some studies have attempted to increase the diagnostic ability of OCT for some pathologies using learning classifiers,[9,20,21] yet the sensitivity and specificity of OCT to diagnose MS have not improved. We were unable to find published studies aimed at calculating an LDF solely on the basis of RNFL parameters measured with OCT in patients with MS. The diagnosis of MS was made by a neurologist according to standard clinical and neuroimaging criteria,[13] and OCT measurements were not used to classify healthy patients and patients with MS.

Our LDF yielded the highest sensitivities at high specificities compared with any single RNFL parameter determined using OCT. Depending on the pre-test probability, positive or negative LRs indicate the extent to which a factor (i.e., probability of disease) will increase or decrease, respectively. An LR value close to 1 indicates insignificant effects, whereas LR values >10 or <0.1 often indicate higher post-test odds of the disease. The LDF had the lowest negative LR; thus, normal results were associated with a

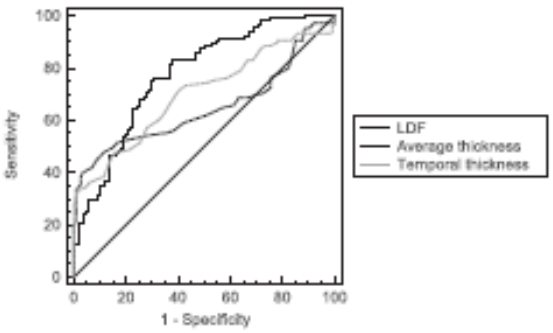

Figure 1. Receiver operating characteristic curves of the linear discriminant function (LDF), average thickness, and temporal thickness between healthy eyes and multiple sclerosis (MS) eyes in the validating set. These parameters exhibited the largest AUCs: 0.806 (95% CI, 0.748–0.856), 0.641 (95% CI, 0.574–0.704), and 0.735 (95% CI, 0.674–0.792), respectively. The LDF differed significantly from average thickness but not from temporal thickness. AUC = area under the receiver operating characteristic curve.

Table 3. In the Validating Set, Differences between the Areas Under the Receiver Operating Characteristic Curves (Hanley–McNeil method) for Linear Discriminant Function (Mean, Superior, and Inferior) and Standard Parameters of Spectralis Optical Coherence Tomography*

	LDF	LDF Sup	LDF Inf	Average Thickness	TS Thickness	T Thickness	TI Thickness	NI Thickness	N Thickness	NS Thickness
LDF	—									
LDF sup	**<0.001**	—								
LDF inf	**0.048**	0.762	—							
Average thickness	**0.008**	**0.042**	0.102	—						
TS thickness	**0.002**	**0.014**	**0.036**	0.500	—					
T thickness	0.158	0.405	0.577	0.151	**0.029**	—				
TI thickness	0.324	0.768	0.993	**0.011**	**0.013**	0.491	—			
NI thickness	**<0.001**	**<0.001**	**<0.001**	**0.001**	0.077	**0.001**	**<0.001**	—		
N thickness	**<0.001**	**<0.001**	**<0.001**	**<0.001**	**0.016**	**<0.001**	**<0.001**	0.360	—	
NS thickness	**0.034**	0.259	0.439	0.265	0.148	0.863	0.498	**<0.001**	**<0.001**	—

LDF = linear discriminant function; LDF inf = linear discriminant function for OCT parameters in inferior area; LDF sup = linear discriminant function for OCT parameters in superior area; N = nasal; NI = nasal-inferior; NS = nasal-superior; T = temporal; TI = temporal-inferior; TS = temporal-superior. *Significant differences ($P<0.05$). Bold values represents statistical significant differences ($P<0.05$)

high post-test probability of disease for these variables, indicating a better ability to exclude the presence of MS. This is the strength of the LDF, which yielded a good sensitivity (83.02%). An LR value >3.14 for the LDF (cutoff point for 95% specificity) virtually rules out the chance that the patient has the disease.

Linear discriminant functions using time-domain OCT (Stratus OCT 3000, Carl Zeiss Meditec) have been designed to diagnose glaucoma,[9,22] but to the best of our knowledge, RNFL measurements in MS have not been reported. In addition, we analyzed measurements provided by Fourier-domain OCT. Studies developing logistic regression analysis with digital imaging parameters have been published using only Stratus OCT,[21,23] scanning laser polarimetry,[24] or confocal scanning laser ophthalmoscope,[25] but not Fourier-domain OCT devices.

The formula of the LDF proposed in this study is based only on RNFL thicknesses and yielded a good sensitivity–specificity balance in the validation sample for MS diagnosis. Other proposed diagnostic tests are based on several parameters or protocols that potentially introduce an additional source of variability, increase the time required to perform the test, extend the time needed to interpret the results, increase the cost per examination, and frequently require invasive methods.[13,25]

More severe disease status is associated with increased sensitivity; therefore, our LDF might have better diagnostic accuracy in populations of patients with more advanced MS. We performed a statistical analysis to compare sensitivity and specificity for the LDF in patients with EDSS scores >4 or <4 and found better diagnostic accuracy in subjects with severe functional deficits (EDSS ≥4). Nevertheless, the sensitivity–

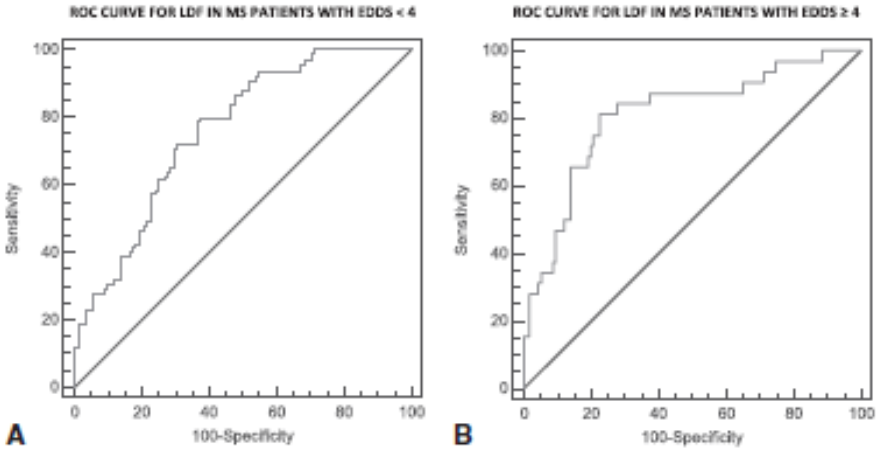

Figure 2. Representation of area under the receiver operating characteristic curve (AUCs) of the linear discriminant function (LDF) in severely affected patients with multiple sclerosis (MS) (Expanded Disability Status Scale [EDSS] score ≥4.0) and (**A**) slightly or moderately affected patients with MS (EDSS score <4.0). (**B**) Patients with higher disability had better sensitivity (AUC 0.811; 95% CI, 0.738–0.870) than patients with EDSS <4 (AUC 0.761; 95% CI, 0.693–0.819). ROC = receiver operating characteristic.

specificity balance of the LDF and other OCT parameters was somewhat lower in the validating set. However, the validating set comprised patients with MS with milder disease states, which may explain the lower diagnostic ability of the Spectralis OCT in this population. The age, sex, ethnic characteristics, and MS severity of the validation sample were similar to those of the teaching set, and this may have biased the findings toward our LDF when compared with other OCT parameters in the second population. In our study, the results in the validating set confirmed those obtained in the teaching set.

The quality of the data obtained by the imaging devices is influenced by media opacity, retinal pigment epithelium status, instrument variability, and positioning and centering of the images. In our study, we selected only good-quality scans, but in clinical practice this is not always possible. These limitations must be taken into account when interpreting the OCT and LDF results.

Conclusions

Although we were unable to find other combinations of RNFL parameters with better diagnostic ability, other statistical analyses could provide alternative formulas that would increase the diagnostic performance of the Spectralis OCT. The AUC of the proposed LDF was not significantly different from the temporal and the temporal inferior sector thicknesses, but the sensitivity values were higher for the LDF at a high fixed specificity. Also, the lowest negative LR was found for the LDF, and these characteristics give the LDF an advantage for classifying healthy subjects as normal subjects. This is a key point when clinicians must discriminate between normal subjects and patients with MS with an early diagnosis or a nondefinitive MS diagnosis. Thus, further studies with this LDF and other discriminant functions are needed to determine the ability of learning classifiers at early stages of the disease or in certain circumstances, such as recognizing MS when it is difficult to decide on the basis of other parameters (e.g., magnetic resonance imaging and clinical findings) or to decide whether changes should be made to any disease-modifying treatment for MS. Linear classifiers are additional tools and should be used in combination with the other parameters and clinical explorations. A review of MS diagnostic criteria including some OCT parameters may improve the sensitivity–specificity balance in diagnostic performance.

References

1. Fisher JB, Jacobs DA, Markowitz CE, et al. Relation of visual function to retinal nerve fiber layer thickness in multiple sclerosis. Ophthalmology 2006;113:324–32.
2. Gordon-Lipkin E, Chodkowski B, Reich DS, et al. Retinal nerve fiber layer is associated with brain atrophy in multiple sclerosis. Neurology 2007;69:1603–9.
3. Garcia-Martin E, Pueyo V, Pinilla I, et al. Fourier-domain OCT in multiple sclerosis patients: reproducibility and ability to detect retinal nerve fiber layer atrophy. Invest Ophthalmol Vis Sci 2011;52:4124–31.
4. Wojtkowski M, Srinivasan V, Fujimoto JG, et al. Three-dimensional retinal imaging with high-speed ultrahigh-resolution optical coherence tomography. Ophthalmology 2005;112:1734–46.
5. Garcia-Martin E, Pueyo V, Almarcegui C, et al. Risk factors for progressive axonal degeneration of the retinal nerve fibre layer in multiple sclerosis patients. Br J Ophthalmol 2011;95:1577–82.
6. Garcia-Martin E, Pueyo V, Ara JR, et al. Effect of optic neuritis on progressive axonal damage in multiple sclerosis patients. Mult Scler 2011;17:830–7.
7. Burgansky-Eliash Z, Wollstein G, Chu T, et al. Optical coherence tomography machine learning classifiers for glaucoma detection: a preliminary study. Invest Ophthalmol Vis Sci 2005;46:4147–52.
8. Garcia-Martin E, Pueyo V, Martin J, et al. Progressive changes in the retinal nerve fiber layer in patients with multiple sclerosis. Eur J Ophthalmol 2010;20:167–73.
9. Pablo LE, Ferreras A, Pajarín AB, Fogagnolo P. Diagnostic ability of a linear discriminant function for optic nerve head parameters measured with optical coherence tomography for perimetric glaucoma. Eye (Lond) 2010;24:1051–7.
10. Bossuyt PM, Reitsma JB, Bruns DE, et al. The STARD statement for reporting studies of diagnostic accuracy: explanation and elaboration. Clin Chem 2003;49:7–18.
11. Bleeker SE, Moll HA, Steyerberg EW, et al. External validation is necessary in prediction research: a clinical example. J Clin Epidemiol 2003;56:826–32.
12. Chylack LT Jr, Wolfe JK, Singer DM, et al, Longitudinal Study of Cataract Study Group. The Lens Opacities Classification System III. Arch Ophthalmol 1993;111:831–6.
13. Frohman EM, Dwyer MG, Frohman T, et al. Relationship of optic nerve and brain conventional and non-conventional MRI measures and retinal nerve fiber layer thickness, as assessed by OCT and GDx: a pilot study. J Neurol Sci 2009;282:96–105.
14. Heijl A, Lindgren A, Lindgren G. Test-retest variability in glaucomatous visual fields. Am J Ophthalmol 1989;108:130–5.
15. Schuman JS, Pedut-Kloizman T, Hertzmark E, et al. Reproducibility of nerve fiber layer thickness measurements using optical coherence tomography. Ophthalmology 1996;103:1889–98.
16. Wu Z, Huang J, Dustin L, Sadda SR. Signal strength is an important determinant of accuracy of nerve fiber layer thickness measurement by optical coherence tomography. J Glaucoma 2009;18:213–6.
17. Hanley JA, McNeil BJ. A method of comparing the areas under receiver operating characteristic curves derived from the same cases. Radiology 1983;148:839–43.
18. Frohman E, Costello F, Zivadinov R, et al. Optical coherence tomography in multiple sclerosis. Lancet Neurol 2006;5:853–63.
19. Costello F, Hodge W, Pan YI, et al. Using retinal architecture to help characterize multiple sclerosis patients. Can J Ophthalmol 2010;45:520–6.
20. Lu AT, Wang M, Varma R, et al, Advanced Imaging for Glaucoma Study Group. Combining nerve fiber layer parameters to optimize glaucoma diagnosis with optical coherence tomography. Ophthalmology 2008;115:1352–7.
21. Chen HY, Huang ML, Hung PT. Logistic regression analysis of glaucoma diagnosis using Stratus optical coherence tomography. Optom Vis Sci 2006;83:527–34.
22. Ferreras A, Pablo LE, Pajarín AB, et al. Logistic regression analysis for early glaucoma diagnosis using optical coherence tomography. Arch Ophthalmol 2008;126:465–70.
23. Chen HY, Huang ML. Discrimination between normal and glaucomatous eyes using Stratus optical coherence tomogra-

phy in Taiwan Chinese subjects. Graefes Arch Clin Exp Ophthalmol 2005;243:894–902.
24. Ferreras A, Pablo LE, Pajarín AB, et al. Scanning laser polarimetry: logistic regression analysis for perimetric glaucoma diagnosis. Eye (Lond) 2009;23:593–600.
25. Medeiros FA, Zangwill LM, Bowd C, Weinreb RN. Comparison of the GDx VCC scanning laser polarimeter, HRT II confocal scanning laser ophthalmoscope, and Stratus OCT optical coherence tomograph for the detection of glaucoma. Arch Ophthalmol 2004;122:827–37.

Footnotes and Financial Disclosures

Originally received: November 28, 2011.
Final revision: January 7, 2012.
Accepted: January 24, 2012.
Available online: April 4, 2012. Manuscript no. 2011-1704.

[1] Ophthalmology Department, Miguel Servet University Hospital, Zaragoza, Spain.

[2] Aragones Institute of Health Sciences, Zaragoza, Spain.

[3] Neurology Department, Miguel Servet University Hospital, Zaragoza, Spain.

Financial Disclosure(s):
The author(s) have no proprietary or commercial interest in any materials discussed in this article.

Correspondence:
Elena Garcia-Martin, PhD, C/Padre Arrupe, Consultas Externas de Oftalmologia, 50009, Zaragoza, Spain. E-mail: egmvivax@yahoo.com.

Original Paper

Ophthalmic Research

Ophthalmic Res
DOI: 10.1159/000350413

Received: September 26, 2012
Accepted after revision: January 24, 2013
Published online: ■■■

Three-Dimensional Geometries Representing the Retinal Nerve Fiber Layer in Multiple Sclerosis, Optic Neuritis, and Healthy Eyes

Elena Garcia-Martin[a, b] Begoña Calvo[c, d] Mauro Malvè[c, d] Raquel Herrero[a, b] Isabel Fuertes[a] Antonio Ferreras[a, b] Jose M. Larrosa[a, b] Vicente Polo[a, b] Luis E. Pablo[a, b]

[a]Ophthalmology Department, Miguel Servet University Hospital, [b]Aragón Institute of Health Sciences, [c]Aragón Institute of Engineering Research (I3A), University of Zaragoza, and [d]Centro de Investigación Biomédica en Red en Bioingeniería, Biomateriales y Nanomedicina, Zaragoza, Spain

Key Words
Multiple sclerosis · Optical coherence tomography · Retinal nerve fiber layer · Optic neuritis · Three-dimensional geometry

Abstract
Background: To represent and interpret the three-dimensional (3D) geometry and the distribution of the axonal damage to the retinal nerve fiber layer (RNFL) in patients with multiple sclerosis (MS) compared with healthy subjects. To analyze alterations in RNFL morphology in eyes of MS patients with or without previous episodes of optic neuritis (ON). ***Methods:*** MS patients (n = 122) and age-matched healthy subjects (n = 108) were enrolled. The Spectralis optical coherence tomography system was used to determine the circumpapillary RNFL thickness. The 768 RNFL thickness measurements were used to evaluate thickness measurements in patients with or without antecedent ON and to design a 3D reconstruction of the RNFL thickness representing the mechanobiologic tissue response to neurodegeneration caused by MS and ON episodes. ***Results:*** RNFL thickness was decreased in MS patients, and was higher in the MS group with previous ON. Statistical analysis and 3D RNFL reconstruction revealed greater damage to the ganglionar cells in the superonasal RNFL area (101.77 μm in MS vs. 125.47 μm in healthy subjects) and in the inferotemporal RNFL (119.05 μm in MS eyes and 149.26 μm in healthy eyes). ***Conclusions:*** The 3D representation of RNFL thickness based on measurements allows physicians to better observe damage in the temporal areas, especially in patients with previous ON.

Introduction

Loss of retinal ganglion cells can be detected using ocular imaging technologies such as optical coherence tomography (OCT) and scanning laser polarimetry, that provide noninvasive, objective, and reproducible methods for evaluating the retinal nerve fiber layer (RNFL) [1]. OCT allows for cross-sectional imaging of the retina and optic disk based on interference patterns produced by low-coherence light reflected from retinal tissues. Recently introduced improvements in OCT technology, including three-dimensional (3D) high-resolution OCT using Fourier domain detection, provide increased resolution compared to classic time domain OCT, such as the Stratus instrument [2–6].

KARGER

E-Mail karger@karger.com
www.karger.com/ore

0030–3747/13/0000–0000$38.00/0

Elena Garcia-Martin
C/Padre Arrupe
Consultas Externas de Oftalmología
ES–50009 Zaragoza (Spain)
E-Mail egmvivas@yahoo.com

Multiple sclerosis (MS) is an autoimmune-mediated disease of the central nervous system with a multifactorial pathogenesis. Some recent models support the presence of three related mechanisms – inflammation, demyelination, and neurodegeneration – taking place in MS, as Garcia-Martin et al. described [4]. Several studies report a correlation between axonal loss in the optic nerve of MS patients and the extent of functional disability [7–9], but the risk factors for increased axonal degeneration remain unclear. RNFL atrophy has been demonstrated in MS patients [10–12], with axonal loss being greater in patients who reported a previous episode of optic neuritis (ON) [7, 12, 13]. Given that optic nerve evaluation is used as an axonal damage biomarker in MS patients, it is important to determine which sectors or RNFL areas are preferentially affected by ON. To this extent, if ON attacks cause a higher reduction in specific areas of the RNFL, this information may modify the interpretation of measurements made to quantify axonal degeneration associated with MS. Frohman et al. [14] suggested that RNFL evaluation could be more useful than magnetic resonance imaging (MRI) for measuring neuronal atrophy, and a growing number of neurologists such as Lamirel et al., [15] and Talman et al. [10] use RNFL evaluation for monitoring disease progression in MS patients. Some studies have reported that RNFL thickness is linked to whole-brain as well as white and gray matter atrophy [8, 16, 17], although an ON episode, which further damages the optic nerve and especially disrupts the association with gray matter, may interfere with this relation [16]. Dörr et al. [18] demonstrated that the brain parenchymal fraction reflects MS severity, while RNFL thickness might be a better parameter for monitoring axonal damage longitudinally.

Several mechanisms have been proposed by which axonal loss caused by MS disease could lead to tissue degeneration and ultrastructural changes of the retinal ganglionar cells, astrocytes, and endothelial cells [19, 20], and are supported by evidence based on the effects of ON on the RNFL [4, 21–23].

Cells and tissues can deform in various ways, such as extension, compression, demyelination, atrophy, or shearing, although these modes of alteration are not independent of each another. The mechanobiologic response of tissues [24, 25] and cells [26–28] depends on the mode of deformation, as well as the magnitude and temporal profile of the stimulus, and the type of tissue or cell and its biologic state. It is therefore of interest to determine which deformations are found in RNFL tissues of patients with MS with or without ophthalmologic damage.

Sigal et al. [29], Bellezza et al. [30] and Burgoyne et al. [31] have reported that regions of the RNFL are differentially damaged in eyes with glaucoma. Burgoyne et al. [31] proposed a conceptual framework for understanding the optic nerve head as a biomechanical structure, using basic principles of biomechanical engineering to propose a central role for intraocular pressure-related stress and strain in the physiology of optic nerve aging and the pathophysiology of glaucomatous damage [31].

Here, we analyzed the deformation of the RNFL caused by the progressive neurodegeneration in patients with MS and by the ON episodes that frequently affect these patients [29–31]. The aim of the present study is to describe the 3D geometries of the optic nerve head [32] in patients with MS. RNFL damage was observed in different areas in MS patients who reported ON episodes in the context of MS disease.

Materials and Methods

Experimental measurements of the biomechanical environment of the optic nerve and RNFL are extremely challenging. We therefore used engineering techniques that allow for simulation of the RNFL biomechanics while accounting for the geometric complexity of the relevant tissue regions [33, 34].

The design of the study followed the Declaration of Helsinki principles. The study protocol was approved by the Clinical Research Ethics Committee of Aragon (Zaragoza, Spain), and informed written consent was obtained from all participants.

Subjects and Measurement Protocol

The inclusion criteria were as follows: best corrected visual acuity of 20/40 or better, refractive error within ±5.00 dpt equivalent sphere and ±2.00 dpt astigmatism, and transparent ocular media (nuclear color/opalescence, cortical or posterior subcapsular lens opacity <1) according to the Lens Opacities Classification System III [35]. Exclusion criteria included previous intraocular surgery, diabetes, or other diseases affecting the visual field or neurologic system, and current use of medications that could affect visual function.

Two independent samples of 110 consecutive healthy individuals and 130 relapsing-remitting MS patients were prospectively recruited from two clinics (one ophthalmologist and one neurologist) under the area of influence of our hospital. The MS clinical and neuroimaging criteria used in this study are based on the 2010 revisions of the McDonald criteria, which include demonstration of dissemination of lesions in space and time, and exclusion of alternative diagnoses [36]. Related medical records were carefully reviewed, including disease duration, the Expanded Disability Status Scale [37], disease-modifying treatments, acute MS attacks, and the presence of prior episodes of ON as reported by the treating neurologist and patient. At the time of a routine 6-month ophthalmologic exploration, the Expanded Disability Status Scale was scored by a neurologist with experience in MS. Subjects referred for routine ophthalmologic revision that underwent routine ex-

Table 1. Comparison of structural measurements provided by Spectralis OCT in MS and healthy subjects

Sector	Central position	Healthy subjects (n =108)		MS patients (n =122)		p
		mean	SD	mean	SD	
Temporal	0°	72.64	12.04	60.80	15.38	<0.001
Superior temporal	67.5°	136.28	19.17	123.17	25.58	<0.001
Inferior temporal	112.5°	149.26	20.14	129.43	26.33	<0.001
Nasal	180.0°	72.23	12.72	72.14	16.43	<0.235
Superior nasal	247.5°	125.47	15.84	98.72	21.00	<0.001
Inferior nasal	292.5°	109.89	26.27	105.99	30.26	<0.001

The last column shows the p values of the comparison between both groups. $p < 0.05$ was considered to be statistically significant. The 768 points registered during circular peripapillary scan acquisition were grouped to obtain 6 uniformly divided sectors that were used in the statistical analysis.

amination without abnormal ocular findings were recruited as normal eye controls. Eight MS patients and 2 healthy subjects did not complete all of the required tests and were therefore excluded from further analysis. A total of 230 eyes of white European origin (108 healthy individuals and 122 MS patients) were included in the statistical analysis. One eye from each subject was randomly chosen for the study.

All participants underwent a full ophthalmologic examination: clinical history, visual acuity, biomicroscopy of the anterior segment using a slit lamp, Goldmann applanation tonometry, and ophthalmoscopy of the posterior segment. OCT tests were performed to obtain measurements of the peripapillary RNFL using the Spectralis device. With this instrument, RNFL thickness was measured around the disk with 16 averaged consecutive circular B-scans (diameter 3.5 mm, 768 A-scans); an online tracking system was used to compensate for eye movement. All scans were performed by the same experienced operator. Manual correction was not applied to the OCT output. An internal fixation target was used because it has previously been shown to give the highest reproducibility, as Schuman et al. demonstrated [38]. The quality of the scans was assessed prior to the analysis and poor quality scans were rejected. The Spectralis OCT uses a blue quality bar in the image to indicate the signal strength. The quality score ranges from 0 (poor quality) to 40 (excellent quality). Only images with a score higher than 25 were analyzed. Eight images with artifacts, missing parts, or seemingly distorted anatomy were excluded and these scans were repeated [39].

Image acquisitions using the circular peripapillary Spectralis OCT scans (RNFL protocol) were performed with the TruTrak eye-tracking technology that recognizes, locks onto, and follows the patient's retina during scanning, and automatically performs follow-up scans to ensure accurate monitoring of disease progression. The Spectralis OCT system simultaneously captures infrared fundus and spectral domain OCT images at 40,000 A-scans per second. A real-time eye-tracking system measures eye movements and provides feedback to the scanning mechanism to stabilize the retinal position of the B-scan. This system thus enables sweep averaging at each B-scan location to reduce speckle noise [40]. The RNFL Spectralis protocol generates a map of the mean thickness and 6 sector thicknesses (superonasal, nasal, inferonasal, inferotemporal, temporal, and superotemporal in the clockwise direction for the right eye and counterclockwise for the left eye). The Spectralis device also generates a database with RNFL thickness measurements for all 768 points registered during circular peripapillary scan acquisition. The Spectralis software version used was 5.4b.

A geometric model of the optic nerve was created from RNFL measurements using Autodesk Invertor (version 11.0, Barcelona, Spain).

Statistical Analysis

Statistical analyses was performed using IBM SPSS (version 18.0; SPSS Inc., Chicago, Ill., USA). The dependent variable was MS diagnosis (yes or no) and the predictive variables were the 768 RNFL thickness measurements, mean RNFL thickness, and 6 sector thicknesses measured with the Spectralis OCT. OCT tests were performed to obtain thickness measurements from 6 uniformly divided locations around the peripapillary RNFL (table 1). Comparison of structural measurements provided by Spectralis OCT in healthy eyes, eyes of MS patients with previous ON (ON MS eyes) and eyes of MS patients without previous ON (non-ON MS eyes) was performed (ANOVA test) (table 2).

The RNFL thicknesses are reported in a 3D model that represents an approximation of the human eye. The model was constructed using computer-aided design software (SolidWorks Inc., Dassault, SolidWorks Corp., France). The 3D model appears as a perfect sphere divided into 6 sectors (superonasal, nasal, inferonasal, inferotemporal, temporal, and superotemporal, respectively, as defined before). In this way, it is possible to obtain a clear overview of the different RNFL thicknesses in healthy and MS eyes with and without previous ON.

Results

One hundred and twenty-two MS patients and 108 age-matched healthy subjects were examined. In the MS group, a previous acute ON attack was reported for 37

Table 2. Comparison of structural measurements provided by Spectralis OCT in healthy eyes, eyes of MS patients with previous ON (ON MS eyes) and eyes of MS patients without previous ON (Non-ON MS eyes)

Sector	Central position	Healthy eyes (n = 108)		Non-ON MS eyes (n = 85)		ON MS eyes (n = 37)		p value (ANOVA)
		mean	SD	mean	SD	mean	SD	
Temporal	0°	72.64	12.04	65.65	14.98	55.80	16.08	0.349
Superior temporal	67.5°	136.28	19.17	132.44	20.11	114.62	29.68	<0.001
Inferior temporal	112.5°	149.26	20.14	139.61	23.77	119.05	29.72	0.724
Nasal	180.0°	72.13	12.72	76.63	15.58	67.50	16.52	0.288
Superior nasal	247.5°	125.47	15.84	101.77	18.36	95.84	22.31	0.276
Inferior nasal	292.5°	109.89	26.27	111.77	32.07	95.70	29.81	0.479

The last column of the table shows the comparison between the three groups (ANOVA). $p < 0.05$ was considered to be statistically significant. The 768 points registered during circular peripapillary scan acquisition were grouped to obtain 6 uniformly divided sectors that were used in the statistical analysis.

Table 3. Clinical characteristics and RNFL average thickness of both populations included (MS patients and healthy subjects) in the study

	Healthy subjects (n =108)		MS patients (n = 122)		p value
	mean (range)	SD	mean (range)	SD	
Age, years	41.8 (19–66)	9.8	41.9 (19–66)	9.7	0.425
IOP, mm Hg	14.4 (11–20)	2.0	14.3 (10–20)	2.2	0.129
BCVA, Snellen	1 (0.8–1)	0.2	0.7 (0.4–1)	0.3	0.008
MD of SAP	0.8 (–3.2 to 3.8)	1.9	–1.2 (–20.3 to 2.1)	2.9	0.047
Mean thickness, µm	99.4 (78–145)	8.8	96.5 (37–148)	13.6	<0.001
MS duration, years	–	–	9.1 (0.5–41)	1.0	–
EDSS score, median	–	–	2.01 (0–8)	0.3	–

BCVA = Best corrected visual acuity; IOP = basal intraocular pressure; MD = mean deviation; SAP = standard automated perimetry; EDSS = Expanded Disability Status Scale. $p < 0.05$ was considered to be statistically significant. (Student's t test between normal and MS groups for each population).

eyes (30.3%), while 85 eyes (69.7%) had no history of ON. The duration of MS, patient age and gender distribution are represented in table 3. Forty-seven patients (38.5%) received no specific treatment for MS, whereas 61 patients (50%) were treated with interferon-β and 14 patients (11.5%) received natalizumab. Median and range for the Expanded Disability Status Scale were 2.01 and 0–8, respectively (table 3).

Age and intraocular pressure did not differ significantly between the groups (MS and healthy subjects) in either sample ($p = 0.425$ and 0.129, respectively; table 3). The proportion of women and men was 2:1 in both groups.

Two analyses were performed: the first evaluated the differences between healthy subjects and MS patients (including eyes with previous ON and eyes without previous ON). The second analysis compared three groups: healthy eyes, MS eyes with previous ON, and MS eyes without previous ON.

Comparison of Healthy and MS Eyes

All RNFL parameters except nasal quadrant area were significantly different between MS patients and the healthy controls. Structural (RNFL thickness measurements provided by Spectralis OCT) and functional parameters (best corrected visual acuity, mean deviation of standard automated perimetry) measured in the ophthalmologic evaluation were significantly different between MS patients and healthy controls (tables 1, 3).

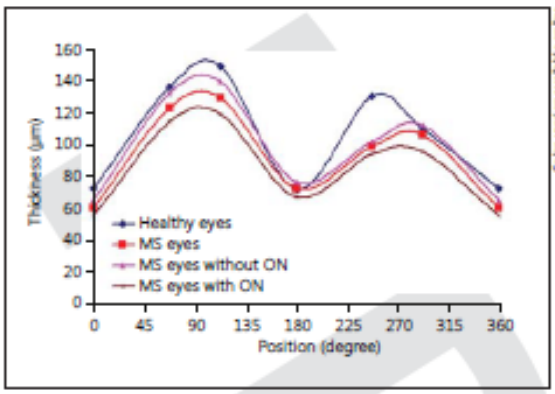

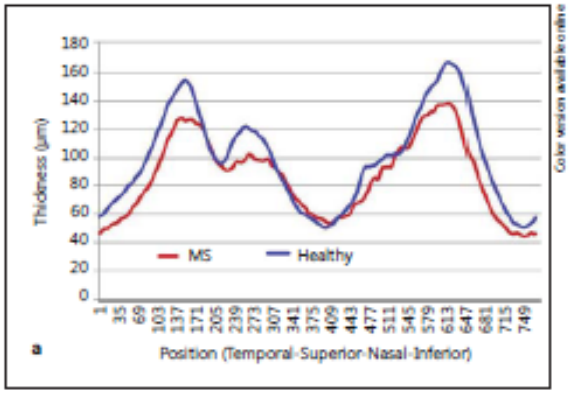

Fig. 1. Representation of the RNFL thickness map in the different study groups: healthy individuals, all MS patients, and patients with and without previous ON episodes. The figure shows higher damage in MS eyes with previous optic nerve inflammation. The nasal superior region (270°) had the highest absolute difference between patients and healthy controls, and the nasal region (180°) had the smallest difference.

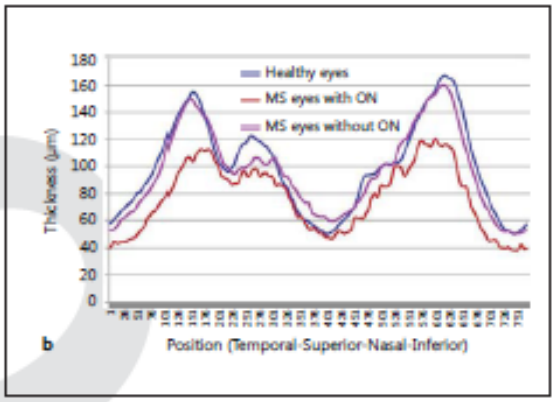

Fig. 2. Graph representing the thickness map of RNFL measurements provided by the Spectralis OCT. **a** The 768 A-scans performed by this device are shown stratified as healthy and MS eyes. **b** The 768 A-scans are stratified by healthy, MS eyes with previous ON and MS eyes without previous ON.

All 768 A-scans provided by the Spectralis OCT for measuring RNFL thickness were included in the statistical analysis. The 768 points registered during circular peripapillary scan acquisition were grouped to obtain 6 uniformly divided regions (each region representing the mean of 60°) that were significantly decreased in MS eyes compared with healthy eyes (table 1; fig. 1). The most damage was found in the superonasal area (125.5 vs. 98.7 µm, $p < 0.001$) and the smallest difference was observed in the nasal area (72.2 vs. 72.1 µm, $p = 0.235$). Statistical analysis based on the total of the 768 A-scans revealed similar results, with MS eyes having decreased RNFL thickness compared to the healthy eyes (fig. 2a).

The 3D geometries representing the RNFL in MS patients showed a greater amount of damage in the temporal areas (fig. 3). In this figure, the mean of the color used to represent the thickness of each sector is clarified in the legend. The thickness of colored areas in the figure represents proportionally the average thickness for this sector in the studied population.

Comparison of Healthy Eyes, and MS Eyes with and without Previous ON

Statistical analysis of the 6 uniformly divided locations was repeated to compare three groups: healthy eyes, MS eyes with previous ON, and MS eyes without previous ON. The MS eyes with previous ON had a greater decrease in the RNFL thickness compared with the other two groups. The MS eyes without previous ON had significantly decreased in RNFL superotemporal thickness compared to healthy eyes (ANOVA, $p < 0.05$; table 2). Analysis of these three groups based on all of the 768 A-scans showed that eyes with previous ON had a greater decrease in all measurements compared to the eyes of patients without a history of ON (fig. 2b).

Representation of the RNFL morphology using the 3D model in MS patients with and without previous ON showed more damage in the temporal areas (fig. 4). In this figure, the mean of the color used to represent the thick-

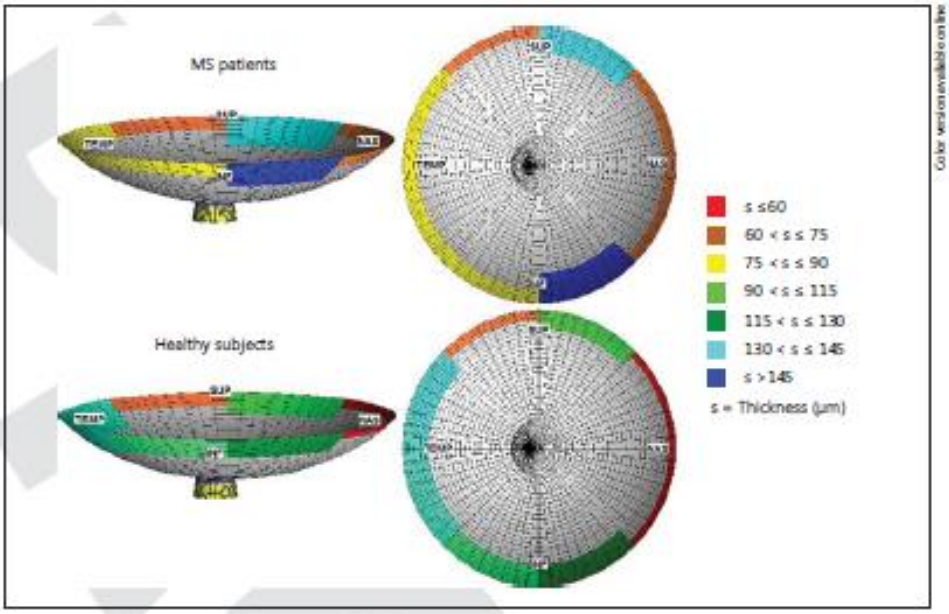

Fig. 3. Representation of 3D geometry of RNFL in MS patients and healthy controls included in the study. The thickness of each colored area represents the average thickness of this sector in the population of the study. The nasal areas are shown on the right side, and temporal areas are on the left side. Trend information is color-coded according to the RNFL mean thickness in each sector (as the legend of the figure represents) using Autodesk Invertor (version 11.0, Barcelona, Spain).

ness of each sector is clarified in the legend. The thickness of colored areas in the figure represents proportionally the average thickness for this sector in the studied population.

Discussion

In the present study, we combined the data of 230 eyes to characterize the effects of MS on RNFL morphology, describing the 3D geometries of the optic nerve and the RNFL deformation caused by progressive neurodegeneration in patients with MS and by ON episodes. The 3D representation of RNFL thickness based on measurements provided by the Spectralis OCT allows physicians to better observe optic nerve damage.

In MS, diffuse brain parenchymal damage following focal inflammation is increasingly recognized from the very onset of the disease, and, although not detectable by conventional imaging techniques, may present a major cause of permanent neurologic disability [41]. Subtle tissue alterations, such as stiffness and internal friction, significantly influence biomechanical properties that, in organs more accessible than the brain, are traditionally assessed by manual palpation during clinical exam. The RNFL is a part of the central nervous system that can be imaged using digital imaging technologies such as OCT. Our current knowledge of RNFL elasticity and its biomechanical damage in neurodegenerative diseases, however, is very limited.

The principles of mechanics can be applied to explore biologic problems by evaluating the mechanics of hard and soft tissues, biofluid mechanics, and cellular mechanics. Modeling the optic nerve as a biomechanical structure generates a group of testable hypotheses regarding the central mechanisms of optic nerve damage [31] and provides a logical framework for classifying the principal components of the susceptibility of an individual RNFL to MS and previous ON episodes.

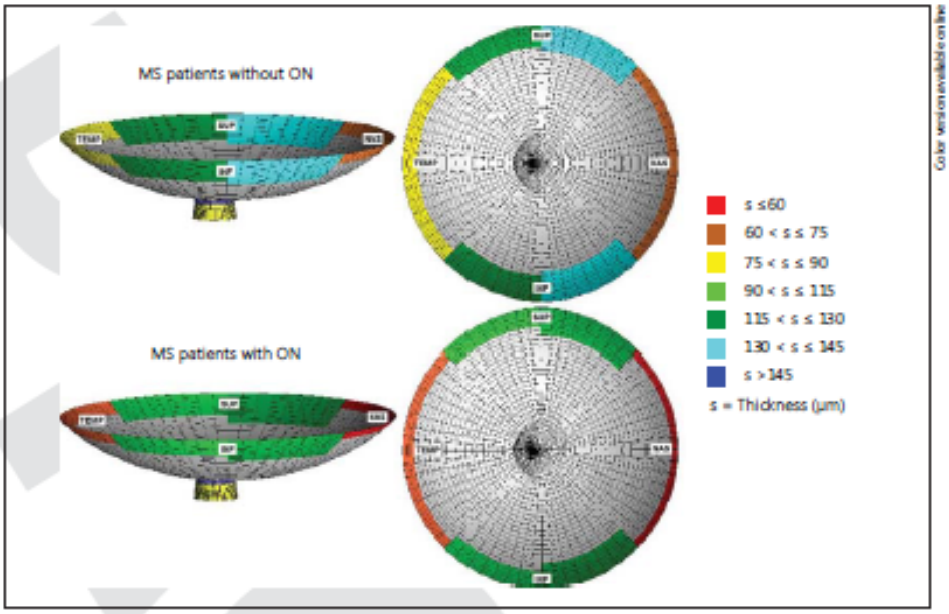

Fig. 4. Representation of 3D geometry of RNFL in two groups of eyes: the first group comprised eyes without previous ON and the second group comprised eyes with previous ON. The nasal areas are shown on the right side, and the temporal areas are on the left side. Trend information is color-coded according to the RNFL mean thickness in each sector (as the legend of the figure represents) using Autodesk Invertor (version 11.0, Barcelona, Spain).

This study may be an introduction to the analysis of biomechanical damage of the optic nerve in MS disease, because the 3D reconstruction of RNFL thickness allows us to obtain a model of areas with early atrophy in patients with MS and in patients with previous ON. Future research should consider numerically modeling RNFL atrophy in MS subjects. Further variations of the conditions (type of MS, treatment, etc.) could also be evaluated.

We evaluated changes in the morphology of the RNFL caused by MS and ON episodes, by observing alterations in RNFL structure-geometry. Spectral domain OCT may represent a novel in vivo marker of neuroinflammatory and neurodegenerative pathology affecting the RNFL, which will be useful for diagnosis and follow-up in diseases such as MS, Alzheimer's disease, or Parkinson's disease [42].

The 3D reconstruction of RNFL damage in patients with MS and in eyes with previous ON allows us to understand the mechanobiologic response of retinal tissues affected by this pathology and the mode of axonal loss in ganglionar cells. The 3D model provides information about which RNFL areas are more affected, which may help us to understand the biomechanical effects of MS on the optic nerve. These findings may be useful to help neuro-ophthalmologists to distinguish between eyes with previous ON episodes and eyes without this antecedent. The diagnosis of ON attacks in MS patients is very important since these episodes are included as one of the diagnostic criteria for MS (ON attack or objective clinical lesion) [43].

The nasal area showed no significant differences between healthy and MS eyes, but this area is the most variable in OCT analysis, as described in our previous report [7]. In that study, we evaluated the reproducibility in 222 eyes of 222 subjects (100 MS eyes and 122 healthy eyes) and found higher variability in the nasal areas of both groups using different Fourier domain OCT devices (Cirrus and Spectralis) [7].

Blumenthal et al. [43] and Schuman et al. [38] have reported similar results in their evaluations of glaucoma

and healthy eyes, and the most accepted theory is that it is difficult to calculate the RNFL thickness in the nasal area using the current measurement algorithm [9, 12], although Knighton and Qian [44] suggested that this problem is due to the angle of incidence of the illuminating beam, which makes the RNFL image on the nasal side dimmer.

Some authors report that temporal areas suffer higher atrophy in MS patients, especially those with previous ON episodes [4, 45, 46]. RNFL thickness in the temporal quadrant is considered a sensitive parameter to detect ON antecedents or optic nerve damage in MS patients [45]. Our findings also demonstrate greater effects in temporal areas in RNFL analysis.

RNFL thickness is increasingly being used as a biomarker of MS. Some authors have reported that the diagnostic ability of OCT in MS is high, and even superior to that of MRI [47]. These authors suggest that OCT should be considered another diagnostic criterion for MS, neurodegenerative and neuroinflammatory diseases such as neuromyelitis optica or Susac syndrome, and that different neurodegenerative diseases cause distinct RNFL sectorial loss [48–51]. Although OCT seems to be sensitive for the detection of RNFL damage, many investigators do not consider it a very specific diagnostic test for neurodegenerative diseases to distinguish between MS and healthy subjects [47]. For the detection of ON, evoked potentials have a sensitivity of 81%, while the sensitivity of OCT is 60% [52].

New Fourier domain technology in OCT provides 3D high-resolution images of each eye and thickness maps similar to those shown in figure 1, but these devices do not allow for analysis of several eyes or for the integration of several scans at the same thickness or morphology representation.

The goal of the present study was to combine the information of 230 eyes to describe the effects of MS and ON on RNFL morphology. Longitudinal studies to analyze progressive biomechanical deformation of the RNFL in MS patients may enhance our knowledge of the etiopathogenic processes of this neurodegenerative disease, and clarify how optic nerve inflammatory episodes affect RNFL morphology and function.

The diagnostic criteria for MS are based on MRI assessment combined with clinical and other paraclinical methods [14], and an ON episode may clarify or speed diagnosis in some patients. The ability of OCT to distinguish patients with MS from healthy subjects might be especially useful in cases reporting subclinical or doubtful ON. Despite the improved diagnostic efficiency using MRI, patients commonly wait months, even years, for a definite diagnosis because the symptoms and signs may not always fall within the parameters of the McDonald criteria. Investigators continue to search for a definitive test for MS, because evidence of both multiple attacks and central nervous system lesions must be found before a definite diagnosis can be made. In addition, a rapid diagnosis is considered critical to take advantage of new disease-modifying drugs, but accuracy is also imperative. New diagnostic tools are currently being developed and may someday make the diagnosis of this complex disease less challenging. In the meantime, Fourier domain OCT may be useful for improving and accelerating the diagnosis.

This study provides a 3D representation of RNFL thickness based on measurements provided by the Spectralis OCT. These 3D models represent areas with more or less damage in the optic nerve caused by MS and ON episodes. We observed that temporal areas, especially in patients with previous ON, showed more atrophy than other RNFL areas [4, 9, 10]. The Spectralis OCT may be a useful diagnostic tool for improving and accelerating the diagnosis of MS.

Acknowledgment

This study was supported in part by the Instituto de Salud Carlos III grant FIS PI11/01553 (E.G.-M., R.H., ■■■, J.M.-L., L.E.P.).

Disclosure Statement

No conflicting relationship exists for any author.

References

1 Trip SA, Schlottmann PG, Jones SJ, Trip SA, Schlottmann PG, Jones SJ, Kallis C, Altmann DR, Garway-Heath DF, Thompson AJ, Plant GT, Miller DH: Scanning laser polarimetry quantification of retinal nerve fiber layer thinning following optic neuritis. J Neuroophthalmol 2010;30:235–242.

2 Wojtkowski M, Srinivasan V, Fujimoto JG, Ko T, Schuman JS, Kowalczyk A, Duker JS: Three-dimensional retinal imaging with high-speed ultrahigh-resolution optical coherence tomography. Ophthalmology 2005; 112:1734–1746.

3 Garcia-Martin E, Pueyo V, Almarcegui C, Martin J, Ara JR, Sancho E, Pablo LE, Dolz I, Fernandez J: Risk factors for progressive axonal degeneration of the retinal nerve fibre layer in multiple sclerosis patients. Br J Ophthalmol 2011;95:1577–1582.

4 Garcia-Martin E, Pueyo V, Ara JR, Almarcegui C, Martin J, Pablo L, Dolz I, Sancho E, Fernandez FJ: Effect of optic neuritis on progressive axonal damage in multiple sclerosis patients. Mult Scler 2011;17:830–837.

5 Warner CV, Syc SB, Stankiewicz AM, Hiremath G, Farrell SK, Crainiceanu CM, Conger A, Frohman TC, Bisker ER, Balcer LJ, Frohman EM, Calabresi PA, Saidha S: The impact of utilizing different optical coherence tomography devices for clinical purposes and in multiple sclerosis trials. PLoS One 2011;6:e22947.

6 Bock M, Brandt AU, Dörr J, Pfueller CF, Ohlraun S, Zipp F, Paul F: Time domain and spectral domain optical coherence tomography in multiple sclerosis: a comparative cross-sectional study. Mult Scler 2010;16:893–896.

7 Fisher JB, Jacobs DA, Markowitz CE, Galetta SL, Volpe NJ, Nano-Schiavi ML, Baier ML, Frohman EM, Winslow H, Frohman TC, Calabresi PA, Maguire MG, Cutter GR, Balcer LJ: Relation of visual function to retinal nerve fiber layer thickness in multiple sclerosis. Ophthalmology 2006;113:324–332.

8 Gordon-Lipkin E, Chodkowski B, Reich DS, Smith SA, Pulicken M, Balcer LJ, Frohman EM, Cutter G, Calabresi PA: Retinal nerve fiber layer is associated with brain atrophy in multiple sclerosis. Neurology 2007;69:1603–1609.

9 Garcia-Martin E, Pueyo V, Pinilla I, Ara JR, Martin J, Fernandez J: Fourier-domain OCT in multiple sclerosis patients: reproducibility and ability to detect retinal nerve fiber layer atrophy. Invest Ophthalmol Vis Sci 2011;52:4124–4131.

10 Talman LS, Bisker ER, Sackel DJ, Long DA Jr, Galetta KM, Ratchford JN, Lile DJ, Farrell SK, Loguidice MJ, Remington G, Conger A, Frohman TC, Jacobs DA, Markowitz CE, Cutter GR, Ying GS, Dai Y, Maguire MG, Galetta SL, Frohman EM, Calabresi PA, Balcer LJ: Longitudinal study of vision and retinal nerve fiber layer thickness in multiple sclerosis. Ann Neurol 2010;67:749–760.

11 Herrero R, Garcia-Martin E, Almarcegui C, Ara JR, Rodriguez-Mena D, Martin J, Otin S, Satue M, Pablo LE, Fernandez FJ: Progressive degeneration of the retinal nerve fiber layer in patients with multiple sclerosis. Invest Ophthalmol Vis Sci 2012;53:8344–8349.

12 Garcia-Martin E, Pueyo V, Martin J, Almarcegui C, Ara JR, Dolz I, Honrubia FM, Fernandez FJ: Progressive changes in the retinal nerve fiber layer in patients with multiple sclerosis. Eur J Ophthalmol 2010;20:167–173.

13 Kallenbach K, Frederiksen J: Optical coherence tomography in optic neuritis and multiple sclerosis: a review. Eur J Neurol 2007;14:841–849.

14 Frohman EM, Dwyer MG, Frohman T, Cox JL, Salter A, Greenberg BM, Hussein S, Conger A, Calabresi P, Balcer LJ, Zivadinov R: Relationship of optic nerve and brain conventional and non-conventional MRI measures and retinal nerve fiber layer thickness, as assessed by OCT and GDx: a pilot study. J Neurol Sci 2009;282:96–105.

15 Lamirel C, Newman NJ, Biousse V: Optical coherence tomography (OCT) in optic neuritis and multiple sclerosis. Rev Neurol (Paris) 2010;166:978–986.

16 Zimmermann H, Freing A, Kaufhold F, Gaede G, Bohn E, Bock M, Oberwahrenbrock T, Young KL, Dörr J, Wuerfel JT, Schippling S, Paul F, Brandt AU: Optic neuritis interferes with optical coherence tomography and magnetic resonance imaging correlations. Mult Scler 2013;19:443–450.

17 Siger M, Dziegielewski K, Jasek L, Bieniek M, Nicpan A, Nawrocki J, Selmaj K: Optical coherence tomography in multiple sclerosis: thickness of the retinal nerve fiber layer as a potential measure of axonal loss and brain atrophy. J Neurol 2008;255:1555–1560.

18 Dörr J, Wernecke KD, Bock M, Gaede G, Wuerfel JT, Pfueller CF, Bellmann-Strobl J, Freing A, Brandt AU, Friedemann P: Association of retinal and macular damage with brain atrophy in multiple sclerosis. PLoS One 2011;6:e18132.

19 Trapp BD, Peterson J, Ransohoff RM, Rudick R, Mörk S, Bö L: Axonal transection in the lesions of multiple sclerosis. N Engl J Med 1998;338:278–285.

20 Zeis T, Graumann U, Reynolds R, Schaeren-Wiemers N: Normal-appearing white matter in multiple sclerosis is in a subtle balance between inflammation and neuroprotection. Brain 2008;131:288–303.

21 Henderson AP, Altmann DR, Trip SA, Miszkiel KA, Schlottmann PG, Jones SJ, Garway-Heath DF, Plant GT, Miller DH: Early factors associated with axonal loss after optic neuritis. Ann Neurol 2011;70:955–963.

22 Costello F, Hodge W, Pan YI: Exploring the association between retinal nerve fiber layer thickness and initial magnetic resonance imaging findings in patients with acute optic neuritis. Mult Scler Int 2011; 2011:289785.

23 Hein K, Gadjanski I, Kretzschmar B, Lange K, Diem R, Sättler MB, Bähr M: An optical coherence tomography study on degeneration of retinal nerve fiber layer in rats with autoimmune optic neuritis. Invest Ophthalmol Vis Sci 2012;53:157–163.

24 Bain AC, Meaney DF: Tissue-level thresholds for axonal damage in an experimental model of central nervous system white matter injury. J Biomech Eng 2000;122:615–622.

25 Edwards ME, Wang SS, Good TA: Role of viscoelastic properties of differentiated SH-SY5Y human neuroblastoma cells in cyclic shear stress injury. Biotechnol Prog 2001;17:760–767.

26 LaPlaca MC, Cullen DK, McLoughlin JJ, Cargill RS: High rate shear strain of three-dimensional neural cell cultures: a new in vitro traumatic brain injury model. J Biomech 2005;38:1093–1105.

27 Pedersen JA, Swartz MA: Mechanobiology in the third dimension. Ann Biomed Eng 2005;33:1469–1490.

28 Wang JH, Thampatty BP: An introductory review of cell mechanobiology. Biomech Model Mechanobiol 2006;5:1–16.

29 Sigal IA, Flanagan JG, Tertinegg I, Ethier CR: Finite element modeling of optic nerve head biomechanics. Invest Ophthalmol Vis Sci 2004;45:4378–4387.

30 Bellezza AJ, Hart RT, Burgoyne CF: The optic nerve head as a biomechanical structure: initial finite element modeling. Invest Ophthalmol Vis Sci 2000;41:2991–3000.

31 Burgoyne CF, Downs JC, Bellezza AJ, Suh JK, Hart RT: The optic nerve head as a biomechanical structure: a new paradigm for understanding the role of IOP-related stress and strain in the pathophysiology of glaucomatous optic nerve head damage. Prog Retin Eye Res 2005;24:39–73.

32 Kaufhold F, Kadas EM, Schmidt C, Kunte H, Hoffmann J, Zimmermann H, Oberwahrenbrock T, Harms L, Polthier K, Brandt AU, Paul F: Optic nerve head quantification in idiopathic intracranial hypertension by spectral domain OCT. PLoS One 2012;7:e36965.

33 Meakin JR, Shrive NG, Frank CB, Hart DA: Finite element analysis of the meniscus: the influence of geometry and material properties on its behaviour. Knee 2003;10:33–41.

34 Viceconti M, Pancanti A, Varini E, Traina F, Cristofolini L: On the biomechanical stability of cementless straight conical hip stems. Proc Inst Mech Eng 2006;220:473–480.

35 Chylack LT Jr, Wolfe JK, Singer DM, Leske MC, Bullimore MA, Bailey IL, Friend J, McCarthy D, Wu SY: The Lens Opacities Classification System III. The Longitudinal Study of Cataract Study Group. Arch Ophthalmol 1993;111:831–836.

36 Polman CH, Reingold SC, Banwell B, Clanet M, Cohen JA, Filippi M, Fujihara K, Havrdova E, Hutchinson M, Kappos L, Lublin FD, Montalban X, O'Connor P, Sandberg-Wollheim M, Thompson AJ, Waubant E, Weinshenker B, Wolinsky JS: Diagnostic criteria for multiple sclerosis: 2010 revisions to the McDonald criteria. Ann Neurol 2011;69:292–302.

37 Kurtzke JF: Rating neurologic impairment in multiple sclerosis: an expanded disability status scale (EDSS). Neurology 1983;33:1444–1452.

38 Schuman JS, Pedut-Kloizman T, Hertzmark E, Hee MR, Wilkins JR, Coker JG, Puliafito CA, Fujimoto JG, Swanson EA: Reproducibility of nerve fiber layer thickness measurements using optical coherence tomography. Ophthalmology 1996;103:1889–1898.

39 Wu Z, Huang J, Dustin L, Sadda SR: Signal strength is an important determinant of accuracy of nerve fiber layer thickness measurement by optical coherence tomography. J Glaucoma 2009;18:213–216.

40 Garcia-Martin E, Pinilla I, Idoipe M, Fuertes I, Pueyo V: Intra and interoperator reproducibility of retinal nerve fibre and macular thickness measurements using Cirrus Fourier-domain OCT. Acta Ophthalmol 2011;89:e23–e29.

41 Wuerfel J, Paul F, Beierbach B, Hamhaber U, Klatt D, Papazoglou S, Zipp F, Martus P, Braun J, Sack I: MR-elastography reveals degradation of tissue integrity in multiple sclerosis. Neuroimage 2010;49:2520–2525.
42 Albrecht P, Müller AK, Südmeyer M, Ferrea S, Ringelstein M, Cohn E, Aktas O, Dietlein T, Lappas A, Foerster A, Hartung HP, Schnitzler A, Methner A: Optical coherence tomography in parkinsonian syndromes. PLoS One 2012;7:e34891.
43 Blumenthal EZ, Williams JM, Weinreb RN, Girkin CA, Berry CC, Zangwill LM: Reproducibility of nerve fiber layer thickness measurements by use of optical coherence tomography. Ophthalmology 2000;107:2278–2282.
44 Knighton RW, Qian C: An optical model of the human retinal nerve fiber layer: implications of directional reflectance for variability of clinical measurements. J Glaucoma 2000;9:56–62.
45 Petzold A, de Boer JF, Schippling S, Vermersch P, Kardon R, Green A, Calabresi PA, Polman C: Optical coherence tomography in multiple sclerosis: a systematic review and meta-analysis. Lancet Neurol 2010;9:921–932.
46 Bock M, Brandt AU, Dörr J, Kraft H, Weinges-Evers N, Gaede G, Pfueller CF, Herges K, Radbruch H, Ohlraun S, Bellmann-Strobl J, Kuchenbecker J, Zipp F, Paul F: Patterns of retinal nerve fiber layer loss in multiple sclerosis patients with or without optic neuritis and glaucoma patients. Clin Neurol Neurosurg 2010;112:647–652.
47 Garcia-Martin E, Pablo LE, Herrero R, Satue M, Polo V, Larrosa JM, Martin J, Fernandez J: Diagnostic ability of a linear discriminant function for spectral-domain optical coherence tomography in multiple sclerosis patients. Ophthalmology 2012;119:1705–1711.
48 Naismith RT, Tutlam NT, Xu J, Klawiter EC, Shepherd J, Trinkaus K, Song SK, Cross AH: Optical coherence tomography differs in neuromyelitis optica compared with multiple sclerosis. Neurology 2009;72:1077–1082.
49 Ratchford JN, Quigg ME, Conger A, Frohman T, Frohman E, Balcer LJ, Calabresi PA, Kerr DA: Optical coherence tomography helps differentiate neuromyelitis optica and MS optic neuropathies. Neurology 2009;73:302–308.
50 Brandt AU, Zimmermann H, Kaufhold F, Promesberger J, Schippling S, Finis D, Aktas O, Geis C, Ringelstein M, Ringelstein EB, Hartung HP, Paul F, Kleffner I, Dörr J: Patterns of retinal damage facilitate differential diagnosis between Susac syndrome and MS. PLoS One 2012;7:e38741.
51 De Seze J, Blanc F, Jeanjean L, Zéphir H, Labauge P, Bouyon M, Ballonzoli L, Castelnovo G, Fleury M, Defoort S, Vermersch P, Speeg C: Optical coherence tomography in neuromyelitis optica. Arch Neurol 2008;65:920–923.
52 Naismith RT, Tutlam NT, Xu J, Shepherd JB, Klawiter EC, Song SK, Cross AH: Optical coherence tomography is less sensitive than visual evoked potentials in optic neuritis. Neurology 2009;73:46–52.

Seminars in Ophthalmology

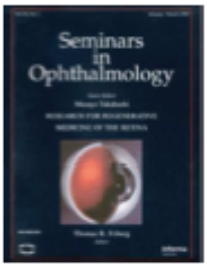

Artificial neural network techniques to improve the ability of optical coherence tomography to detect optic neuritis.

Journal:	*Seminars In Ophthalmology*
Manuscript ID:	Draft
Manuscript Type:	Original Article
Date Submitted by the Author:	n/a
Complete List of Authors:	Garcia-Martin, Elena; Miguel Servet University Hospital, Ophthalmology; Aragones Institute Of Health Sciences, Research Herrero, Raquel; Miguel Servet University Hospital, Ophthalmology Bambo, Maria; Miguel Servet University Hospital, Ophthalmology Ara, Jose; Miguel Servet University Hospital, Neurology Martin, Jesus; Miguel Servet University Hospital, Neurology Polo, Vicente; Miguel Servet University Hospital, Neurology Larrosa, Jose; Miguel Servet University Hospital, Ophthalmology Garcia-Feijoo, Julian; San Carlos Clinico University Hospital, Ophthalmology Pablo, Luis; Miguel Servet University Hospital, Ophthalmology
Keywords:	Multiple sclerosis, Optical coherence tomography, Optic neuritis, Retinal nerve fiber layer, Sensitivity

TITLE: Artificial neural network techniques to improve the ability of optical coherence tomography to detect optic neuritis.

AUTHORS: Elena Garcia-Martin PhD[1,2], Raquel Herrero MD[1,2], Maria P. Bambo MD[1], Jose R. Ara PhD[2,3], Jesus Martin PhD[2,3], Vicente Polo PhD[1,2], Jose M. Larrosa PhD[1,2], Julian Garcia-Feijoo PhD[4]; Luis E. Pablo PhD[1,2].

AFFILIATIONS:

1 Ophthalmology Department, Miguel Servet University Hospital, Zaragoza (Spain)

2 Aragones Institute of Health Sciences, Zaragoza (Spain)

3 Neurology Department, Miguel Servet University Hospital, Zaragoza (Spain)

4 Ophthalmology Department, Clinico San Carlos University Hospital, Madrid (Spain)

AUTHOR FOR CORRESPONDENCE:

Elena Garcia-Martin

C/ Padre Arrupe, Consultas Externas de Oftalmologia. 50009- Zaragoza (Spain)

Email: egmvivax@yahoo.com Telephone number: 0034.976.76.55.00

RUNNIG TITLE: Spectral OCT to identify optic neuritis in MS

The authors have no proprietary interest. Financial Support: None.

No conflicting relationship exists for any author.

KEYWORDS: Multiple sclerosis; Optical coherence tomography; Optic neuritis; Retinal nerve fiber layer; Sensitivity.

Abstract

Purpose: To analyze the ability of Spectralis optical coherence tomography (OCT) to detect multiple sclerosis (MS) and to distinguish MS eyes with antecedent optic neuritis (ON). To analyze the capability of artificial neural network (ANN) techniques to improve the diagnostic precision.

Methods: MS patients and controls were enrolled (n=217). The OCT was used to determine the 768 retinal nerve fiber layer thickness. Sensitivity and specificity were evaluated to test the ability of OCT to discriminate between MS and healthy eyes; and between MS with and without antecedent ON using ANN.

Results: Using ANN technique multilayer perceptrons, OCT could detect MS with a sensitivity of 89.3%, a specificity of 87.6%, and a diagnostic precision of 88.5%. Compared with the OCT-provided parameters, the ANN had a better sensitivity-specificity balance.

Conclusions: ANN technique improves the capability of Spectralis OCT to detect MS disease and to distinguish MS eyes with or without antecedent ON.

Introduction

Ganglion cell loss can be detected using ocular imaging technologies such as optical coherence tomography (OCT) and scanning laser polarimetry, which allow for non-invasive, rapid, objective, and reproducible evaluation of the retinal nerve fiber layer (RNFL). OCT provides cross-sectional images of the retina and optic disc based on interference patterns produced by low coherence light reflected from retinal tissues. Recent improvements in OCT technology provide increased resolution, such as three-dimensional high-resolution OCT, which uses Fourier-domain detection (1-3). These new devices, such the Spectralis (Heidelberg Engineering Inc, Heidelberg, Germany), have a spectrometer composed of transmission grating and an air-spaced focusing lens. These devices obtain 2 to 3-μm axial resolution high-quality images with an increased acquisition speed (4).

Multiple sclerosis (MS) is an autoimmune-mediated disease of the central nervous system with a multifactorial pathogenesis. Axonal loss is considered to be the main cause of disability in this neurodegenerative disease. RNFL atrophy has been demonstrated in MS patients, with axonal loss being greater in patients who reported antecedent optic neuritis (ON) (5,6). Because optic nerve inflammation is considered an MS biomarker, it is important to determine if Spectralis OCT can detect previous optic nerve inflammation episodes. ON attacks lead to a reduction in the RNFL thickness, and may thus alter the measurements provided by OCT devices. Some authors have suggested that RNFL evaluation could be more useful than magnetic resonance imaging to measure neuronal atrophy (7), and a growing number of neurologists use RNFL evaluation to monitor disease progression in MS patients (8,9). Several studies have demonstrated that overall mean RNFL thickness is the best diagnostic parameter in different pathologies such as glaucoma and MS (3,10) and that it is the most sensitive parameter to detect MS progression (5). The

results of the most recent studies, however, indicate that optimal MS detection might best be achieved by a combination of several parameters and that each measurement may make a different contribution to distinguish between healthy and MS subjects, and to detect antecedent subclinical ON in MS patients (11).

In an effort to improve the diagnostic accuracy of OCT measurements, previous studies have explored the implementation of machine learning algorithms, such as artificial neural networks (ANN), using RNFL measurements as input parameters (10-17). In contrast to conventional statistical techniques, such as linear discriminant analysis, these methods do not fit the data into a pre-existing set of model variables; instead, ANN nonlinearly adapts the classification decision based on the data that is presented. Provided a representative and adequately large training dataset in relation to the input parameters, this approach produces robust classifiers that are able to generalize well, even in the absence of a model of the underlying process, and are insensitive to noise and outliers in the data (18). Studies performed by the Department of Electrical and Computer Engineering of the University of Miami demonstrated the feasibility of ANN methods for distinguishing between control subjects and MS patients using the P300 cognitive evoked potential (19-21). The neural network model, however, has not yet been used to assess the diagnostic ability of OCT in eyes with ON.

In the present study, we analyzed the diagnostic precision of the Spectralis OCT to detect MS and antecedent ON using an ANN multilayer perceptron technique. The aim of the present study was to determine whether a selective combination of RNFL measurements could further optimize or accelerate MS diagnosis and help to detect antecedent subclinical inflammation episodes in the optic nerve.

Materials and methods

The design of the study followed the Declaration of Helsinki Principles. The study protocol was approved by the Clinical Research Ethics Committee of Aragon (Zaragoza, Spain), and informed written consent was obtained from all participants.

Subjects and measurement protocol

Required inclusion criteria were as follows: best corrected visual acuity of 20/40 or better, refractive error within ±5.00 diopters equivalent sphere and ±2.00 diopters astigmatism, transparent ocular media (nuclear color/opalescence, cortical or posterior subcapsular lens opacity <1) according to the Lens Opacities Classification System III (22). Exclusion criteria included previous intraocular surgery, diabetes, optic neuritis in previous 6 months, or other diseases affecting the visual field or neurologic system (including optic neuromyelitis), and current use of medications that could affect visual function.

Two independent samples of 108 consecutive healthy individuals and 122 patients with MS were prospectively recruited from two clinics (one ophthalmologist and one neurologist) under the area of influence of our hospital. The diagnosis of MS was based on standard clinical and neuroimaging criteria (7). Related medical records were carefully reviewed, including disease duration since diagnostic, the Expanded Disability Status Scale (EDSS) in the last 6 months, disease-modifying treatments, acute MS attacks, and the presence of prior episodes of ON as reported by the treating neurologist and patient. At the time of a routine 6-month clinical visit, the EDSS was scored by a neurologist with experience in MS. Subjects referred for refraction that underwent routine examination without abnormal ocular findings were recruited as normal eye controls. Six MS patients did not complete all of the required tests and were therefore excluded

from further analysis. Seven subjects with artifacts, missing parts, or showing seemingly distorted anatomy were excluded (4 patients and 3 healthy subjects) (23). A total of 217 eyes of white European origin (105 healthy individuals and 112 MS patients) were included in the statistical analysis. One eye from each subject was randomly chosen for the study, unless only one eye met the inclusion criteria.

All participants underwent a full ophthalmologic examination that included clinical history, visual acuity, biomicroscopy of the anterior segment using a slit lamp, visual field evaluation using Humphrey field analyzer (Carl-Zeiss Meditec, Dublin, CA), Goldmann applanation tonometry, and ophthalmoscopy of the posterior segment.

OCT tests were performed to obtain measurements of the peripapillary RNFL using the Spectralis device. With this instrument, RNFL thickness was measured around the disc with 16 averaged consecutive circular B-scans (diameter of 3.5 mm, 768 A-scans); an online tracking system was used to compensate for eye movement. All scans were performed by the same experienced operator. Between scan acquisitions, there was a time delay and subject position and focus were randomly disrupted, meaning that alignment parameters had to be newly adjusted at the start of each image acquisition (24). No manual correction was applied to the OCT output. An internal fixation target was used to give the highest reproducibility (25). The quality of the scans was assessed prior to the analysis and poor quality scans were rejected. The Spectralis OCT uses a blue quality bar in the image to indicate signal strength. The quality score ranges from 0 (poor quality) to 40 (excellent quality). Only images with a score greater than 25 were analyzed.

Image acquisition using circular peripapillary Spectralis OCT scans (RNFL protocol) was performed using *TruTrack* eye-tracking technology, which recognizes, locks onto, and follows

the patient's retina during scanning, and automatically places follow-up scans to ensure accurate monitoring of disease progression. The Spectralis OCT system simultaneously captures infrared fundus and SD-OCT images at 40,000 A-scans per second. A real-time eye tracking system measures eye movements and provides feedback to the scanning mechanism to stabilize the retinal position of the B-scan. This system thus enables sweep averaging at each B-scan location to reduce speckle noise. The mean number of scans to produce each circular B scan was 9 (24). The RNFL Spectralis protocol generates a map with mean thickness and six sector thicknesses (superonasal, nasal, inferonasal, inferotemporal, temporal, and superotemporal in the clockwise direction for the right eye and counterclockwise for the left eye). The Spectralis device also generates a database of RNFL thickness measurements at all 768 points registered during the circular peripapillary scan acquisition. We used the Spectralis software version 5.4b.

All 768 A-scans provided by the Spectralis OCT to measure RNFL thickness, mean, and 6 sectors thicknesses were registered and included in a database designed for this study using File Maker Pro 8.5 program (File Maker Inc., Santa Clara, CA). All statistical analyses were evaluated using IBM SPSS (version 18.0; SPSS Inc., Chicago, IL) and Rapidminer 5.1.006 Software (Rapid I GmbH, Dortmund, Germany) to perform the ANN analysis.

Eyes of MS patients were divided into two subgroups: 41 eyes with antecedent ON (36.6%) and 71 eyes without previous ON attack. The diagnosis of ON was based on clinical findings, including decreased visual acuity, visual field defects, color vision loss, relative afferent pupil defects, and a compatible fundus examination (26).

Statistical analysis: Neural Network Technique

We evaluated the performance of the ANN technique for classifying RNFL measurements by the Spectralis OCT as MS or healthy. ANN are data mining tools used fundamentally to look for patterns in training sets of data, then the procedure learns these patterns and develops the ability to classify new patterns correctly (27-32). In this study, we used a feed-forward neural network trained by a back-propagation algorithm (multi-layer perceptron [MLP]). The MLP, one of the most commonly used neural network architectures, uses a feed forward architecture and can have multiple hidden layers. The processing elements in each layer are connected to all processing elements of the preceding and following layers, but not to processing elements of the same layer. The MLP comprises an input layer (in our case OCT thickness measurements), an output layer (in our case MS or control, and ON and Non-ON), and one or more hidden layers (33).

Training of machine-learning classifiers and testing were performed with each RNFL thickness parameter separately, as well as with all 768 RNFL measurements used conjointly. To maximize the use of our collected data and avoid bias, the 10-fold cross-validation resampling method was used. Accordingly, all data were randomly divided into 10 subsets, each containing approximately the same number of healthy and MS OCT thickness measurements. Nine subsets were used for training the classifiers while the remaining subset was used for testing classification performance. In training the ANN ensemble, one of the training subsets was used for early stopping of network training to avoid over-fitting of the MLPs. Training data for the 35 MLPs were created with bagging from the remaining 8 subsets. ANN training was repeated by keeping the same test subset and changing the early stopping set until all training data were used both in training and early stopping of the ANNs, and the classification results were averaged. The

training and testing process for the ANN ensemble and the SVM were iterated, each time with a different test set, and the results were merged to produce a single output for each classifier.

By modeling the relationship of age, refraction, and measured RNFL thickness our normative database, we conducted a linear regression analysis and used the derived coefficients to calculate the corrected values of the measured RNFL thickness.

To test for significant differences in the distribution of sex between the healthy and MS groups, the chi square test was used, whereas significance testing for differences in the distributions of age, visual acuity, and refractive error was performed using the Mann-Whitney test.

Nonlinear dimensionality reduction based on manifold learning OCT A-scan data can be characterized as multidimensional, because they require multiple parameters (dimensions) to be represented. One approach to simplify the data representation is to use techniques that are able to map the data to a set containing fewer parameters (i.e., a lower dimensional space). Nonlinear dimensionality reduction techniques based on manifold learning function by constructing parameters with values that are assumed to be measurement points embedded in a specific type of topologic space (a nonlinear manifold), existing within the high-dimensional space of the complete dataset. In contrast to linear methods, such as principal component analysis, these techniques retain information on nonlinear relationships between measurement points and are able to represent nonlinear structures in the data. The local tangent space alignment algorithm that is used in this study is considered a local embedding technique, and functions by constructing an approximation for the tangent space at each data point, and aligning these tangent spaces to provide the global coordinates of the data points.

The selected number of transformed parameters that describes the A-scan data was based on estimations of the intrinsic dimensionality of the dataset.

Results

Two hundred and seventeen eyes of 112 MS patients and 105 age-matched healthy subjects were analyzed. In MS group, a previous acute ON attack was reported for 41 eyes (36.6%), while 71 eyes (63.4%) were studied from patients who had no history of ON. The duration of the MS (since diagnosis) ranged from 6 months to 41 years with a median of 9.8 years since diagnosis. The ages of patients ranged from 20 to 71 years with a mean of 38.7 ± 9.7 years. The ratio of women to men was 2:1 (75 women and 37 men). Mean intraocular pressure was 13.9 mmHg. Forty-two of the patients (37.5%) received no specific treatment for MS, whereas 50 patients (44.6%) were treated with interferon beta and 10 patients (8.9%) received natalizumab. Mean EDSS was 2.41 (Table 1).

Mean age of the healthy group was 39.0 ± 10.1 years and the ratio of women to men was 2:1 (70 women and 35 men). Age and intraocular pressure did not differ significantly between groups in either sample (p= 0.452 and 0.674, respectively; Table 1).

Different experiments were performed by changing the number of measurements included in each thickness group (Table 2). The 768 points (RNFL measurements provided by the Spectralis OCT) were divided equally of different sizes in each experiment; in all of them, an ANN based on multilayer perceptrons was used with a unique secret network whose neural number was input number +2/2. The best sensitivity-specificity balance was found in the experiment with 16 groups.

All RNFL parameters were significantly different between MS patients and healthy controls. The structural (RNFL thickness measurements provided by Spectralis OCT) and functional parameters (best corrected visual acuity, mean deviation of standard automated perimetry) registered in the ophthalmologic evaluation were significantly different between groups (Tables 1 and 3). RNFL thicknesses were significantly different between the group of MS eyes with a previous ON episode and those without previous ON (Table 3, Figure 1)

The 768 points registered during circular peripapillary scan acquisition were grouped to obtain 16 uniformly divided locations (each with 48 consecutive RNFL thickness measurements) that were included in ANN statistical analysis (Table 3). ANN performed with 16 locations identified more pathology in MS patients (Figures 1 and 2) and had the best sensitivity-specificity balance for distinguishing between MS and healthy eyes and between ON eyes and non-ON eyes of MS patients (Table 4). The sensitivity of the network was calculated as the number of true-positive results divided by the number of true-positive results plus the number of false-negative results; the specificity was calculated as the number of true-negative results divided by the number of true-negative results plus the number of false-positive results; the diagnostic precision was calculated as the number of correct diagnoses divided by the total number of test trials.

The sensitivity of the network to detect MS using the Spectralis OCT was 89.3%; the specificity was 87.6%; the diagnostic precision was 88.5% (Table 4). The sensitivity, specificity, and positive and negative likelihood ratios (LR) of Spectralis OCT were better using ANN than using standard RNFL thicknesses provided by the device (Table 4).

The diagnostic precision of the ANN to detect MS eyes with antecedent ON was good, but the sensitivity and specificity (84.5% and 83.2%, respectively) were smaller than that to diagnose MS vs healthy subjects (Table 4).

Discussion

The diagnosis of MS is made by a neurologist based on standard clinical and neuroimaging criteria (7). Although OCT parameters are currently not used as diagnostic criteria for MS, the RNFL measurements provided by OCT can be used to clarify if specific ophthalmologic symptoms were caused by a subclinical ON episode. This application of OCT may be useful to find evidence of both multiple attacks and central nervous system lesions that must be found before a doctor can make a definite MS diagnosis. A speedy diagnosis is considered critical in MS patients so that treatment with new disease-modifying therapies can be implemented in a timely manner.

The primary aim of our study was to analyze the ability of ANN classifiers to improve the diagnostic ability of measurements provided by the Spectralis OCT to distinguish between healthy persons and MS patients and to detect eyes of MS patients with previous ON.

Machine learning is a field of artificial intelligence concerned with the development of computational and statistical methods that are able to learn through a training process. ANNs comprise a group of machine learning methods used for both classification and function approximation tasks. They have been successfully used in a variety of fields, including medicine, for data mining, automated interpretation of tests, and feature extraction from large datasets.

MLPs, comprising multiple layers of artificial neurons, are a type of ANN developed from the original perceptron model (the first type of ANN, created in the 1940s).

The widespread use of MLPs is partly due to their ability to conduct nonlinear classification tasks and because of their efficient supervised learning algorithm based on back-propagation of error. Following developments in statistical learning theory, new techniques for classification and regression were introduced within the group of machine-learning algorithms.

One important aspect of trained ANNs is their ability to generalize their adaptively created decision rules on previously unseen data. The generalization error of ANNs can be decomposed into the factors of bias (i.e., a measure of the classification accuracy on the training data) and variance (i.e., a measure of the stability of the given classification solution provided by the ANN, depending on the variability of the training data). The two factors of bias and variance have an inverse relationship and there is a trade-off between these two. To decrease the generalization error of a classifier, one can combine the prediction of a number of classifiers in an ensemble structure.

The quality of the data obtained by the imaging devices is influenced by media opacity, retinal pigment epithelium status, instrument variability, and positioning and centering of the images. In our study, we selected only good quality scans, but in clinical practice this is not always possible. These limitations must be taken into account when interpreting OCT and ANN results.

The neural network performance was promising and the results of this study indicate that the ANN could correctly identify a high percentage of MS subjects. The neural network performance yielded the highest sensitivities at high specificities compared to any single RNFL parameter determined using OCT. Depending on the pre-test probability, positive or negative LRs indicate

the extent to which a factor (i.e., probability of disease) will increase or decrease, respectively. An LR value close to 1 indicates insignificant effects, whereas LR values higher than 10 or lower than 0.1 often indicate higher post-test odds of the disease. The ANN had the lowest negative LR, thus normal results were associated with a high post-test probability of disease for these variables. These characteristics give the ANN performance an advantage for classifying healthy subjects as normal subjects. This is a key point when clinicians must discriminate between normal and MS patients with early diagnosis or non-definitive MS diagnosis. Hence, further studies with this ANN performance and other analysis are needed to determine the ability of learning classifiers at early stages of the disease or in certain circumstances, such as recognizing MS when it is difficult to decide on the basis of other parameters (e.g., magnetic resonance imaging, clinical findings) or to decide changes in any disease modifying treatment of MS. Linear classifiers are additional tools and should be used in combination with other parameters and clinical explorations.

As our results showed, the ability of the Spectralis OCT to detect antecedent ON in MS patients was not as good as that to distinguish between healthy and MS subjects, but the negative LR of ANN was only 0.2, which suggest that the ANN of the Spectralis OCT has a good capability for classifying eyes without antecedent ON in MS patients. Further studies with a larger and more homogeneous groups of ON and Non-ON eyes of MS patients are needed to determine the ability of Spectralis OCT as a diagnostic tool.

Although magnetic resonance imaging has come a long way in helping to diagnose MS more efficiently, it is not uncommon to wait months, even years, for a definite diagnosis because not all patient's symptoms and signs fall within the parameters of the McDonald criteria. Investigators are continuing their search for a definitive test for MS, because evidence of both

multiple attacks (including ON episodes) and central nervous system lesions must be found before a doctor can make a definite diagnosis. For some patients, the wait can be difficult. Without a single "gold standard" diagnostic test, though, MS can still be a difficult disease to pinpoint. The importance of a good physician and adequate testing cannot be stressed enough. In addition, since new disease-modifying therapies have been introduced, a speedy diagnosis is considered critical, but accuracy is also imperative. New diagnostic tools are currently in the pipeline and may someday make the diagnosis of this complex disease less challenging. Fourier domain OCT may be useful for improving the diagnosis procedure.

Our results demonstrate that Fourier domain OCT may be useful to improve the diagnosis of MS by two methods: first, RNFL measurements provided by OCT may be used as an MS marker, and some authors have reported that RNFL thickness should be introduced as a diagnostic criterion (11); second, Fourier domain OCT can help to distinguish eyes with antecedent ON among MS eyes that have never before presented with ON inflammation. A review of MS diagnostic criteria, including RNFL measurements provided by Fourier domain OCT, may improve and accelerate the diagnosis of MS and increase the sensitivity-specificity balance.

Acknowledgment

Supported in part by the Instituto de Salud Carlos III grant PI11/01553.

References

1. Wojtkowski M, Srinivasan V, Fujimoto JG, et al. Three-dimensional retinal imaging with high-speed ultrahigh-resolution optical coherence tomography. Ophthalmology 2005; 112: 1734-46.

2. Garcia-Martin E, Pueyo V, Almarcegui C, et al. Risk factors for progressive axonal degeneration of the retinal nerve fibre layer in multiple sclerosis patients. Br J Ophthalmol. 2011; 95(11): 1577-82.

3. Garcia-Martin E, Pueyo V, Ara JR, et al. Effect of optic neuritis on progressive axonal damage in multiple sclerosis patients. Mult Scler. 2011; 17(7): 830-7.

4. Garcia-Martin E, Pinilla I, Sancho E, et al. Optical coherence tomography in retinitis pigmentosa: Reproducibility and capacity to detect macular and retinal nerve fiber layer thickness alterations. Retina 2012 [Epub ahead of print].

5. Garcia-Martin E, Pueyo V, Martin J, et al. Progressive changes in the retinal nerve fiber layer in patients with multiple sclerosis. Eur J Ophthalmol. 2010; 20(1): 167-73.

6. Kallenbach K, Sander B, Tsakiri A, et al. Neither retinal nor brain atrophy can be shown in patients with isolated unilateral optic neuritis at the time of presentation. Mult Scler. 2011; 17(1): 89-95.

7. Frohman EM, Dwyer MG, Frohman T, et al. Relationship of optic nerve and brain conventional and non-conventional MRI measures and retinal nerve fiber layer thickness, as assessed by OCT and GDx: a pilot study. J Neurol Sci. 2009; 282(1-2): 96-105.

8. Lamirel C, Newman NJ, Biousse V. Optical coherence tomography (OCT) in optic neuritis and multiple sclerosis. Rev Neurol (Paris) 2010; 166(12): 978-86.

9. Talman LS, Bisker ER, Sackel DJ, et al. Longitudinal study of vision and retinal nerve fiber layer thickness in multiple sclerosis. Ann Neurol 2010; 67: 749-60.

10. Burgansky-Eliash Z, Wollstein G, Chu T, et al. Optical coherence tomography machine learning classifiers for glaucoma detection: a preliminary study. Invest Ophthalmol Vis Sci 2005; 46: 4147-52.

11. Garcia-Martin E, Pablo LE, Herrero R, et al. Diagnostic ability of a linear discriminant function for Spectral domain optical coherence tomography in multiple sclerosis patients. Ophthalmology 2012 [Epub ahead of print].

12. Essock EA, Sinai MJ, Bowd C, Zangwill LM, Weinreb RN. Fourier analysis of optical coherence tomography and scanning laser polarimetry retinal nerve fiber layer measurements in the diagnosis of glaucoma. Arch Ophthalmol. 2003; 121(9): 1238-45.

13. Hougaard JL, Heijl A, Krogh E. The nerve fibre layer symmetry test: computerized evaluation of human retinal nerve fibre layer thickness as measured by optical coherence tomography. Acta Ophthalmol Scand. 2004; 82(4): 410-8.

14. Huang M, Chen H. Development and comparison of automated classifiers for glaucoma diagnosis using stratus optical coherence tomography. Invest Ophthalmol Vis Sci. 2005; 46: 4121-9.

15. Chen HY, Huang ML, Hung PT. Logistic regression analysis for glaucoma diagnosis using Stratus Optical Coherence Tomography. Optom Vis Sci. 2006; 83(7): 527-34.

16. Manassakorn A, Nouri-Mahdavi K, Caprioli J. Comparison of retinal nerve fiber layer thickness and optic disk algorithms with optical coherence tomography to detect glaucoma. Am J Ophthalmol. 2006; 141(1): 105-15.

17. Naithani P, Sihota R, Sony P, et al. Evaluation of optical coherence tomography and Heidelberg retinal tomography parameters in detecting early and moderate glaucoma. Invest Ophthalmol Vis Sci.2007; 48: 3138-45.

18. Bizios D, Heijl A, Hougaard JL, Bengtsson B. Machine learning classifiers for glaucoma diagnosis based on classification of retinal nerve fibre layer thickness parameters measured by Stratus OCT. Acta Ophthalmol. 2010: 88: 44-52.

19. Slater JD, Wu FY, Honig LS, Ramsay RE, Morgan R. Neural network analysis of the P300 event-related potential in multiple sclerosis. Electroencephalogr Clin Neurophysiol. 1994; 90(2): 114-22.

20. Wu FY, Slater JD, Honig LS, Ramsay RE. A neural network design for event-related potential diagnosis. Comput Biol Med. 1993; 23(3): 251-64.

21. Wu FY, Slater JD, Ramsay RE. Neural network approach in multichannel auditory event-related potential analysis. Int J Biomed Comput. 1994; 35(3): 157-68.

22. Chylack Jr LT, Wolfe JK, Singer DM, et al. Longitudinal Study of Cataract Study Group. The Lens Opacities Classification System III. Arch Ophthalmol 1993; 111: 831-6.

23. Wu Z, Huang J, Dustin L, Sadda SR. Signal strength is an important determinant of accuracy of nerve fiber layer thickness measurement by optical coherence tomography. J Glaucoma 2009; 18: 213-6.

24. Garcia-Martin E, Pueyo V, Pinilla I, Ara JR, Martin J, Fernandez J. Fourier-domain OCT in multiple sclerosis patients: reproducibility and ability to detect retinal nerve fiber layer atrophy. Invest Ophthalmol Vis Sci. 2011; 52(7): 4124-31.

25. Schuman JS, Pedut-Kloizman T, Hertzmark E, et al. Reproducibility of nerve fiber layer thickness measurements using optical coherence tomography. Ophthalmology 1996; 103: 1889-98.

26. Costello F, Coupland S, Hodge W, et al. Quantifying axonal loss after optic neuritis with optical coherence tomography. Ann Neurol 2006; 59: 963-9.

27. Goldbaum MH, Sample PA, Chan K, et al. Comparing machine learning classifiers for diagnosing glaucoma from standard automated perimetry. Invest Ophthalmol Vis Sci. 2002; 43: 162-9.

28. Rumelhart DE, Hinton G, Williams R. Learning representations of back-propagation errors. Nature. 1986; 323: 533-6.

29. Broomhead DS, Lowe D. Multivariable functional interpolation and adaptive networks. Complex Syst. 1988; 2: 321-55.

30. Bishop CM. Neural networks for pattern recognition. Oxford, UK: Clarendon Press; 1995.

31. Fernandez de Canete J, Gonzalez-Perez S, Ramos-Diaz JC. Artificial neural networks for closed loop control of in silico and ad hoc type 1 diabetes. Comput Methods Programs Biomed. 2011 [Epub ahead of print].

32. Takayama T, Ebinuma H, Tada S, et al. Prediction of effect of pegylated interferon alpha-2b plus ribavirin combination therapy in patients with chronic hepatitis C infection. PLoS One. 2011; 6(12): e27223.

33. Bowd C, Chan K, Zangwill LM, et al. Comparing neural networks and linear discriminant functions for glaucoma detection using confocal scanning laser ophthalmoscopy of the optic disc. Invest Ophthalmol Vis Sci. 2002; 43: 3444-54.

Figure legends

Figure 1: Neural network model used in the study for analysis of both groups (multiple sclerosis and healthy eyes). The figure shows the profiles of retinal nerve fiber layer (RNFL) thicknesses of all the patients, healthy in blue and pathologic in red, considering 16 groups of RNFL thicknesses.

Figure 2: The graph shows the profiles of retinal nerve fiber layer (RNFL) thicknesses of all the patients, considering 24 groups of RNFL thicknesses and eliminating continuous components. In this graph, negative and positive values are represented, thus each of the profiles have an mean height equal to zero or. The red color prevails on the blue because when creating the figure, the healthy group profile was inserted after the pathologic group profile. The average profiles of healthy and MS eyes are also represented using □ and ◊ symbols, respectively.

Table 1: Clinical characteristics and retinal nerve fiber layer measurements provided by standard parameters of Spectralis OCT in both populations.

	Healthy subjects (n:105)		MS patients (n:112)		P*
	Mean (range)	SD	Mean (range)	SD	
Age (years)	39.0 (19-70)	10.1	38.7 (20-71)	9.7	0.452
Intraocular pressure (mm Hg)	14.0 (11-19)	2.1	13.9 (10-20)	2.2	0.674
BCVA (Snellen charts)	1 (0.8-1)	0.2	0.7 (0.4-1)	0.3	*0.004*
Mean Deviation of perimetry	1.2 (-3.1-4.0)	2.1	-1.7 (-19.0-2.1)	3.2	*0.009*
Mean thickness	99.2 (77-129)	8.6	96.7 (39-180)	13.2	*<0.001*
Temporal-superior thickness	137.4 (62-205)	19.4	126.3 (40-251)	17.6	*<0.001*
Temporal thickness	75.7 (57-119)	12.9	71.1 (35-156)	16.5	*0.001*
Temporal-inferior thickness	149.5 (67-216)	19.2	145.5 (28-228)	24.8	*0.023*
Nasal-inferior thickness	110.3 (56-256)	20.4	110.2 (25-178)	21.2	*0.003*
Nasal thickness	72.9 (42-110)	15.7	72.4 (19-148)	18.0	0.345
Nasal-superior thickness	111.4 (67-180)	17.9	98.9 (45-158)	25.5	*<0.001*
MS duration (years)	-	-	9.8 (0.5-41)	0.8	-
EDSS score	-	-	2.41 (0-7.5)	0.4	-

Abbreviations: BCVA, best corrected visual acuity; EDSS, expanded disability status scale; MS, multiple sclerosis; n, number.

MS duration is calculated since definitive MS diagnosis date.

Retinal nerve fiber layer thicknesses are expressed in microns (µm).

*Significant differences ($P<0.05$) in Student's t-test between normal and MS groups for each population. Significant differences are indicated by letters in italics.

Table 2: Representation of experiments to group the 768 retinal nerve fiber layer measurements.

The 768 retinal nerve fiber layer measurements provided by Spectralis OCT were grouped equally of different sizes in several experiments. The first column represents the total number of groups. The second column shows the number of consecutive points included in each group, calculated as result of dividing the total number of points of the original database (768) by the number of groups. The third column shows the numbers of consecutive points included in each quadrant. The fourth column represents the number and proportion (in parenthesis) of correctly classified eyes (as MS or healthy eyes). The last column also represents the number and proportion (in parenthesis) of correctly classified eyes (as MS or healthy eyes), but in this case, the statistical program calculated each component of the input vector as the mean value of the input (mean of the inputs that comprise the input vector), to study whether or not the continuous component of the profile of thicknesses is discriminant (see Figure 2). In the two last columns, the best diagnostic balances are indicated by italic letters.

Number of groups	Group size	Number of points in each group	Correctly classified eyes	Correctly classified eyes (eliminating continue component)
192	4	48	186 (85.7%)	182 (83.9%)
128	6	32	183 (84.3%)	180 (82.9%)
96	8	24	181 (83.4%)	180 (82.9%)
64	12	16	182 (83.9%)	178 (82.1%)
48	16	12	181 (83.4%)	183 (84.3%)
32	24	8	182 (83.9%)	184 (84.8%)
24	32	6	184 (84.8%)	*190 (87.6%)*
16	**48**	**4**	***192 (88.5%)***	180 (82.9%)
12	64	3	178 (82.0%)	171 (78.8%)
8	96	2	177 (81.6%)	159 (73.3%)

Table 3: Retinal nerve fiber layer (RNFL) measurements in eyes of healthy subjects and multiple sclerosis (MS) patients, showing mean and standard deviation (SD).

The eyes of the MS group are divided by presence or absence of antecedent optic neuritis (ON). The 768 points registered during circular peripapillary scan acquisition were grouped to obtain 16 uniformly divided locations that were used in the statistical analysis. The third column in each MS group shows the significance (P) of the comparison with healthy eyes. A value of $p<0.05$ was considered to indicate statistical significance. Significant differences are indicated by letters in italics.

Group of Points	RNFL Points included	Healthy eyes (n:105)		Non- ON eyes of MS patients (n:71)			ON eyes of MS patients (n:41)		
		Mean	SD	Mean	SD	P	Mean	SD	P
1	1-48	73.3	11.2	56.2	20.1	*<0.001*	51.8	28.4	*<0.001*
2	49-96	80.3	10.2	66.0	21.2	*<0.001*	61.8	25.6	*<0.001*
3	97-144	115.5	14.5	102.3	20.3	*<0.001*	95.4	20.3	*<0.001*
4	145-192	144.5	20.2	110.2	18.8	*0.001*	107.5	19.7	*0.007*
5	193-240	140.2	19.3	135.9	22.2	0.362	131.4	25.6	*<0.001*
6	241-288	123.4	23.3	121.0	28.6	0.108	119.4	35.5	*<0.001*
7	289-336	105.9	20.9	100.9	27.3	*0.024*	95.7	31.2	*<0.001*
8	337-384	110.0	19.9	95.7	20.0	*<0.001*	90.5	20.6	*0.002*
9	385-432	99.8	25.4	98.1	24.6	0.329	94.5	19.8	*0.042*
10	433-480	92.3	27.7	90.2	15.5	*<0.001*	86.6	15.0	*0.006*
11	481-528	66.6	23.5	61.4	29.5	*<0.001*	59.6	25.1	*0.003*
12	529-576	57.1	14.6	54.2	30.1	*<0.001*	54.1	29.6	*0.018*
13	577-624	58.6	16.6	55.5	18.5	*<0.001*	52.3	28.4	*<0.001*
14	625-672	69.2	14.1	64.3	25.7	*0.007*	59.1	24.8	*0.045*
15	673-720	96.8	30.3	89.9	27.6	*<0.001*	73.9	26.6	*<0.001*
16	723-768	99.1	28.7	95.7	19.8	*<0.001*	90.0	18.5	*<0.001*

Abbreviations: RNFL, retinal nerve fiber layer; ON, optic neuritis; n, number of eyes; MS, multiple sclerosis; SD, standard deviation; P, signification value.

Table 4: Sensitivity, specificity, and likelihood ratios of the artificial neural network.

The table shows sensitivity, specificity, and likelihood ratios of the artificial neural network using 16 groups of measurements and retinal nerve fiber layer parameters of OCT to discriminate between normal and multiple sclerosis (MS) subjects, and between eyes of MS patients with previous optic neuritis (ON MS) and eyes without antecedent optic neuritis (Non-ON MS).

	Diagnostic ability Healthy vs MS eyes				Diagnostic ability ON MS vs Non-ON MS eyes			
OCT parameters	Sens	Spec	+LR	-LR	Sens	Spec	+LR	-LR
ANN (16 groups)	89.3	87.6	7.2	0.1	84.5	83.2	5.0	0.2
Average thickness	45.2	94.1	7.6	0.6	70.6	91.2	8.0	0.3
Temporal-Superior thickness	36.6	91.1	4.1	0.7	47.2	90.3	4.9	0.6
Temporal thickness	71.2	72.9	2.6	0.4	81.6	70.9	2.8	0.3
Temporal-Inferior thickness	47.8	83.2	2.8	0.6	58.9	87.5	4.7	0.5
Nasal-Inferior thickness	37.9	88.5	3.3	0.7	42.6	84.3	2.7	0.7
Nasal thickness	39.7	73.8	1.5	0.8	51.9	69.9	1.7	0.7
Nasal-superior thickness	70.4	60.6	1.8	0.5	75.0	57.7	1.8	0.4

Abbreviations: OCT, optical coherence tomography; ANN, artificial neural network; Sens, Sensitivity; Spec, Specificity; +LR, positive likelihood ratio; -LR, negative likelihood ratio. Sensibility and specificity are expressed in %.

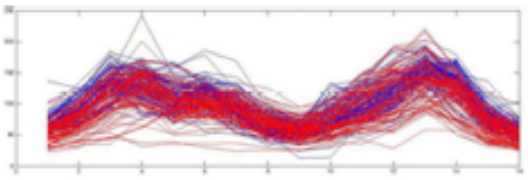

27x8mm (300 x 300 DPI)

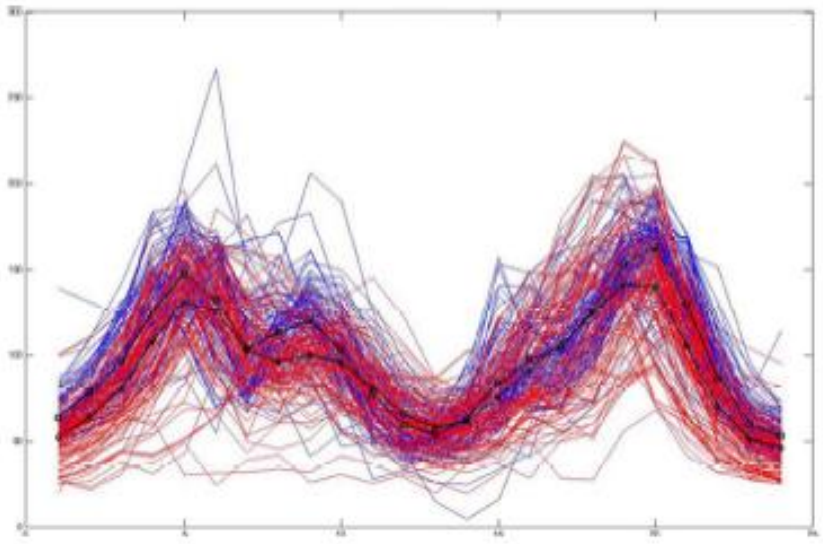

57x37mm (300 x 300 DPI)

RESUMEN DE LA TESIS DOCTORAL POR COMPENDIO DE PUBLICACIONES

1. OBJETIVOS DE LA INVESTIGACIÓN

I. Evaluar los cambios que se producen en la capa de fibras nerviosas de la retina con la evolución de la esclerosis múltiple y observar si se encuentran diferencias en función de las diferentes actitudes terapéuticas y de la progresión de la enfermedad.

II. Determinar la eficacia de las técnicas de análisis funcional y estructural del nervio óptico en la detección de daño secundario a esclerosis múltiple y el grado de correlación existente entre ellas.

III. Analizar la precisión diagnóstica de la tomografía de coherencia óptica Spectralis para detectar esclerosis múltiple y el antecedente de neuritis óptica usando la técnica estadística de redes neuronales artificiales.

IV. Describir la geometría en tres dimensiones de la cabeza del nervio óptico en pacientes con esclerosis múltiple y las zonas de la misma que se ven afectadas en mayor grado por la enfermedad y por episodios de neuritis óptica.

V. Calcular y validar una función lineal discriminante en la tomografía de coherencia óptica de dominio Fourier para mejorar la habilidad diagnóstica del espesor de la capa de fibras nerviosas de la retina en la detección de la esclerosis múltiple.

2. APORTACIONES DEL DOCTORANDO

Los artículos de la presente tesis doctoral aportan a la comunidad científica unas herramientas nuevas e inocuas para mejorar el diagnóstico y el seguimiento de esta compleja patología.

Nuestros resultados proporcionan fórmulas para ayudar a discriminar entre sujetos sanos y pacientes con EM, que conducen a mejorar el diagnóstico precoz en fases tempranas de la enfermedad o en ciertas circunstancias que hacen difícil decidir la presencia o no de EM basándose sólo en otros criterios como la resonancia magnética o los signos clínicos. Se trata de un punto clave para la práctica clínica ya que poder realizar un diagnóstico precoz de esta patología e iniciar de forma temprana el tratamiento con las terapias modificadoras de la enfermedad, resulta esencial para aumentar su efectividad.

Otra aplicación práctica muy importante para el manejo de estos pacientes que aporta el análisis de la CFNR es que puede servir como un método para evaluar la eficacia de los tratamientos en la protección de la degeneración axonal. Este aspecto resulta especialmente útil para los neurólogos a la hora de decidir sobre la conducta terapéutica a seguir, y abre una vía de investigación para el futuro donde podrían evaluarse qué tratamientos se asocian con una menor pérdida axonal.

Es importante resaltar además que el estudio de la CFNR a través de la OCT se trata de un procedimiento inocuo y no invasivo, de fácil realización tanto para el evaluador, que no requiere un entrenamiento especial, puede adquirir las imágenes con rapidez y disponer casi inmediatamente de los resultados; como para el paciente,

que se somete a una prueba rápida, sencilla de realizar y que no causa molestias durante su realización.

Finalmente, estas investigaciones aportan un enfoque multidisciplinar de los pacientes con esclerosis múltiple, basado en la colaboración entre oftalmología, neurología y neurofisiología donde la evaluación oftalmológica juega un gran papel tanto en el diagnóstico como en el seguimiento de esta enfermedad, ayudando a realizar un manejo óptimo de estos pacientes.

3. METODOLOGÍA UTILIZADA

Para la elaboración de los cuatro trabajos se ha realizado un estudio prospectivo, observacional y longitudinal que se ha llevado a cabo de modo coordinado entre los Servicios de Oftalmología, Neurología y Neurofisiología del Hospital Universitario Miguel Servet de Zaragoza desde el año 2007. El diseño del estudio siguió los principios de la Declaración de Helsinki, y el protocolo del estudio fue aprobado por el Comité Ético de Investigaciones Clínicas de Aragón.

3.1. Sujetos de estudio

Se propuso la participación en el estudio a todos los pacientes afectos de EM que fueron revisados en las consultas de Neurología de dicho hospital. Basándose en los datos de estudios previos, el número de sujetos que fue necesario incluir para poder detectar diferencias mayores o iguales a 5 μm en la CFNR asumiendo un error alpha del 5% y un error beta del 10% fue de 86. Sin embargo, con el objeto de prever

posibles pérdidas durante el seguimiento del estudio, incrementar su potencia y disponer de varias poblaciones muestrales para validar los distintos parámetros diagnósticos, se incluyeron 150 pacientes con EM. Para el correcto diseño del estudio, se realizó un muestreo estratificado según las variantes de la enfermedad (recurrente-remitente, primaria progresiva o secundaria progresiva).

Se incluyeron en el estudio 150 individuos sanos, reclutados entre el personal sanitario del Hospital Miguel Servet y familiares o amigos, que aceptaron voluntariamente participar en el estudio. La preselección de estos individuos se llevó a cabo pareándolos por edad y sexo a los pacientes con EM incluidos en el estudio.

Todos los participantes firmaron un consentimiento informado en el que se detallaba el objetivo del trabajo y las pruebas incluidas en el protocolo exploratorio, así como la posibilidad de abandonarlo en el momento en que lo deseasen.

Los criterios de inclusión fueron la confirmación del diagnóstico de EM por un neurólogo basándose en los criterios clínicos y de neuroimagen de Polman[37], agudeza visual igual o superior a 0,1 con la escala de Snellen en cada ojo, para permitir el desarrollo correcto del protocolo exploratorio, y valores de presión intraocular de aplanamiento inferiores a 20 mm Hg, para evitar incluir sujetos con glaucoma crónico que pudiera causar una reducción de la CFNR por causas ajenas a la EM. Se excluyeron del estudio aquellos pacientes que hubiesen padecido un episodio de neuritis óptica en los 6 meses previos a su inclusión en el estudio o a lo largo de su seguimiento, aquellos cuyo defecto de refracción fuese superior a 5 dioptrías de equivalente esférico o 3 dioptrías de astigmatismo, y aquellos con cirugía ocular previa, diabetes, u otras enfermedades que afectasen el campo visual o el sistema neurológico.

3.2. Protocolo exploratorio

El protocolo exploratorio constó de tres tipos de pruebas:

- Exploración oftalmológica, que incluyó la evaluación de la agudeza visual, de la visión cromática, la evaluación de la motilidad ocular, de los reflejos pupilares y del segmento anterior del ojo, así como la medición de la presión intraocular mediante tonometría de aplanación, la valoración funduscópica papilar, la exploración del campo visual y una tomografía de coherencia óptica (OCT).

- Exploración neurofisiológica, que incluyó los potenciales evocados visuales (PEV).

- Exploración neurológica que incluyó la valoración del fenotipo de EM (recidivante-remitente, primaria progresiva, y secundaria progresiva), el tiempo de evolución desde el diagnóstico, la puntuación en la escala de disfunción neurológica (EDSS), el tratamiento recibido, la presencia de brotes agudos de EM y de episodios previos de neuritis óptica.

Estas exploraciones fueron realizadas en el momento basal, al año, a los dos años y al tercer año con el objetivo de evaluar cambios en los parámetros registrados y la correlación entre dichos cambios y otros factores asociados, tales como el tratamiento aplicado o la progresión de la discapacidad funcional.

EXPLORACIÓN OFTALMOLÓGICA

La agudeza visual se midió mediante el optotipo de Snellen, de forma monocular, con la mejor corrección posible del defecto de refracción si era necesario y con el paciente a 6 metros de distancia.

Figura 1. Optotipo de Snellen clásico.

La exploración de la visión cromática con el test de Ishihara permite valorar la existencia de alteraciones en la percepción de los colores, que aparecen durante el período de estado de la neuritis óptica, generalmente en el eje rojo-verde del espectro y, con menos frecuencia, en el azul-amarillo. En los estadios finales con atrofia óptica sólo es deficiente la discriminación del rojo-verde.

La mayor parte de los pacientes presentan alteración de la visión de colores en el ojo afectado y el grado de afectación puede evidenciarse con el test de Ishihara, que a menudo es directamente proporcional al grado de pérdida visual. Sin embargo, algunos pacientes tienen una alteración de la visión cromática superior a la esperada para su afectación visual.

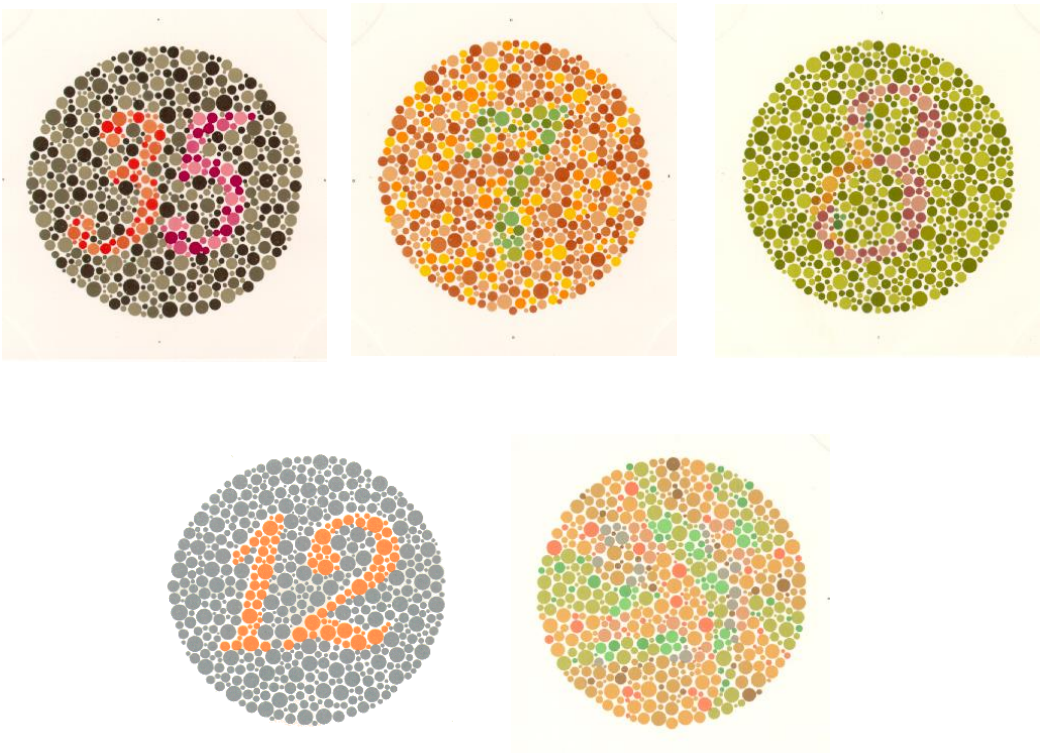

Figura 2. Ejemplos de láminas pseudoisocromáticas del test de Ishihara.

El test de Ishihara proporciona unas láminas para clasificar con precisión el defecto de visión cromática y diferenciar colores en sus diversas tonalidades. Estas láminas o mapas están dispuestas con una confusión de manchas de distintos colores. Fue ideado por el doctor Shinobu Ishihara y está disponible con diferentes números de láminas para exámenes más o menos exhaustivos. Se recomienda emplear al menos 14 láminas.

En nuestro estudio se empleó un test de Ishihara con 20 láminas seudoisocromáticas y se realizó de forma individual con cada ojo. El parámetro registrado fue el número de aciertos del paciente.

El estudio del fondo do ojo se basó en la observación del aspecto de la papila (normal, palidez difusa, palidez sectorial, o edema) con la ayuda de una lente de 78 dioptrías. La forma del nervio óptico normal es verticalmente ovalada. El anillo neuroretiniano de la papila óptica es de color rosado y está formado por axones de las células ganglionares y rodea una depresión central llamada excavación óptica que no tiene axones.

En la EM es frecuente encontrar atrofia óptica, con una papila pálida, ligeramente elevada con márgenes mal delimitados por la gliosis asociada, y una reducción del número de los pequeños vasos sanguíneos que cruzan la superficie papilar (figura 3).

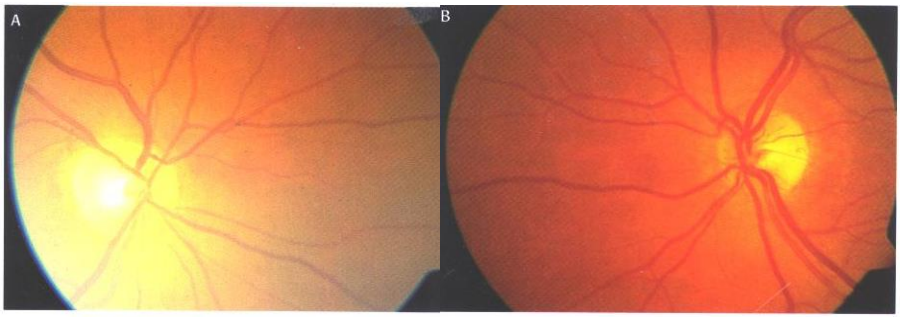

Figura 3. Atrofia por neuritis óptica asociada a EM. Se puede observar palidez temporal significativa en ambas papilas tras múltiples brotes.

El campo visual o campimetría se utiliza para cuantificar el campo de visión que presenta el paciente y es la prueba funcional más empleada en oftalmología, después de la medición de la agudeza visual.

El término de perimetría se refiere a la medida del campo visual sobre una superficie curva y ha venido a sustituir al término de campimetría en la práctica clínica.

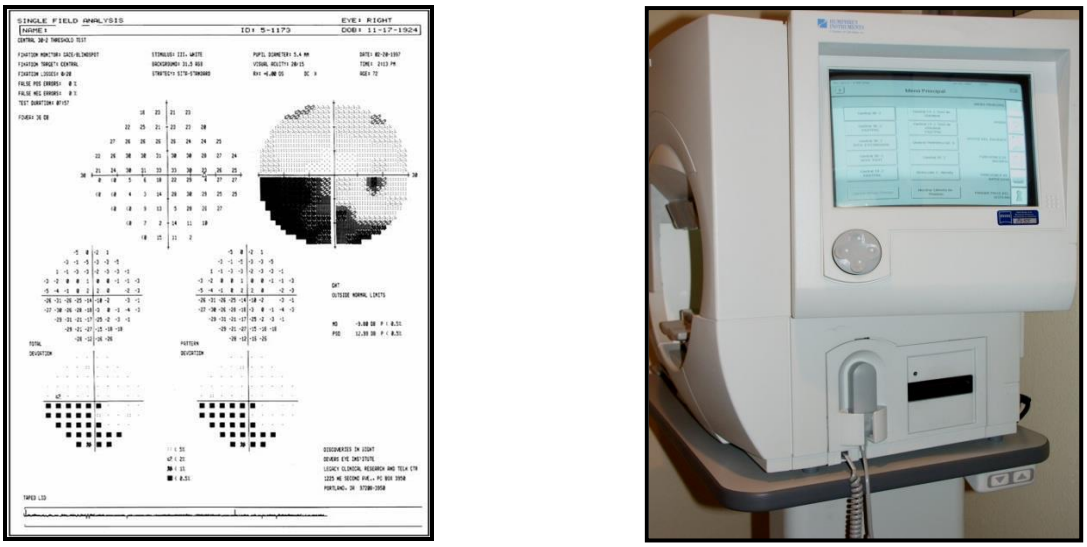

Figura 4. Campo visual (imagen de la izquierda) y Perímetro Humphrey Visual Field Analyzer (imagen de la derecha).

En el campo visual automatizado convencional los estímulos luminosos blancos se representan sobre una superficie blanca con una iluminación reproducible. La luz se presenta durante 0,2 segundos y se busca el umbral de la capacidad sensorial de cada punto incrementando y disminuyendo ligeramente la intensidad del estímulo (medida en decibelios, dB). El valor obtenido se expresa en unidades de luminancia, siendo la más utilizada el apostilb (asb). Para garantizar la fiabilidad de la exploración la fijación del paciente se controla utilizando el método de Heijil-Krakau. Una vez obtenidos los datos se representan numéricamente y mediante una escala de grises.

Las principales ventajas del campo visual automatizado estático respecto a las técnicas anteriores son su reproducibilidad, la mayor sensibilidad a los defectos leves, el hecho de que no precisa personal experto en realizarlo y la obtención de datos numéricos que nos sirven para comparar la evolución.

La reducción de la CFNR puede producir una pérdida de función visual, que generalmente pasa desapercibida en fases precoces y sólo se detecta en el campo visual cuando existe una reducción importante del número de células ganglionares. En la EM los patrones de afección más frecuentes son los defectos altitudinales (55-80%)

durante los episodios inflamatorios y la disminución difusa de la sensibilidad. También pueden observarse escotomas, defectos arcuatos, cuadrantanopsias, constricción generalizada o la combinación de éstos.

El campo visual ha demostrado una buena correlación entre la localización de los defectos perimétricos y la lesión estructural apreciable en otras pruebas diagnósticas como la fotografía de la CFNR o la polarimetría láser[38,39].

Sin embargo presenta algunas limitaciones, ya que su resultado puede verse afectado por factores que causan una reducción generalizada de la sensibilidad, como la edad, la miosis, opacidades de medios, la afaquia y las ametropías. El resultado de la prueba también puede alterarse por una ptosis o por el borde de las gafas.

Los parámetros registrados en nuestro estudio fueron la desviación media (DM) medida en decibelios y el patrón morfológico del campo visual calificado como normal, disminución difusa de la sensibilidad, escotoma arcuato superior o inferior, escotoma altitudinal superior o inferior, doble escotoma arcuato, aumento de la mancha ciega, escotoma central, centro-cecal o paracentral, escalón nasal superior, escalón nasal inferior, escalón vertical, cuatrantanopsia, triple cuadrantanopsia, hemianopsia nasal o temporal, reducción concéntrica, o focos múltiples.

La tomografía de coherencia óptica (OCT) permite estudiar cortes histológicos de la retina in vivo y analizar las estructuras de la retina posterior, entre ellas la papila óptica y la CFNR.

Figura 5.Cirrus OCT 3000 (Carl Zeiss Meditec)

El principio físico que explica su mecanismo de acción es la inferometría de baja coherencia. Una fuente emite pulsos cortos de luz hacia un espejo, donde se reflectan parcialmente hacia el ojo y hacia un espejo de referencia.

La luz que llega hasta el ojo se refleja y vuelve hacia un detector, comparándola con la reflejada por el espejo de referencia. Con ello se genera una imagen final con una escala de colores donde las zonas de alta reflectividad, que corresponden a áreas de bloqueo parcial o total al paso de la luz (sangre, fibrosis…), se muestran en tonos rojo-blanco; mientras que las imágenes de zonas de baja reflectividad, que implican baja o nula resistencia al paso de la luz (quistes, edema…), se muestran en el espectro azul-negro.

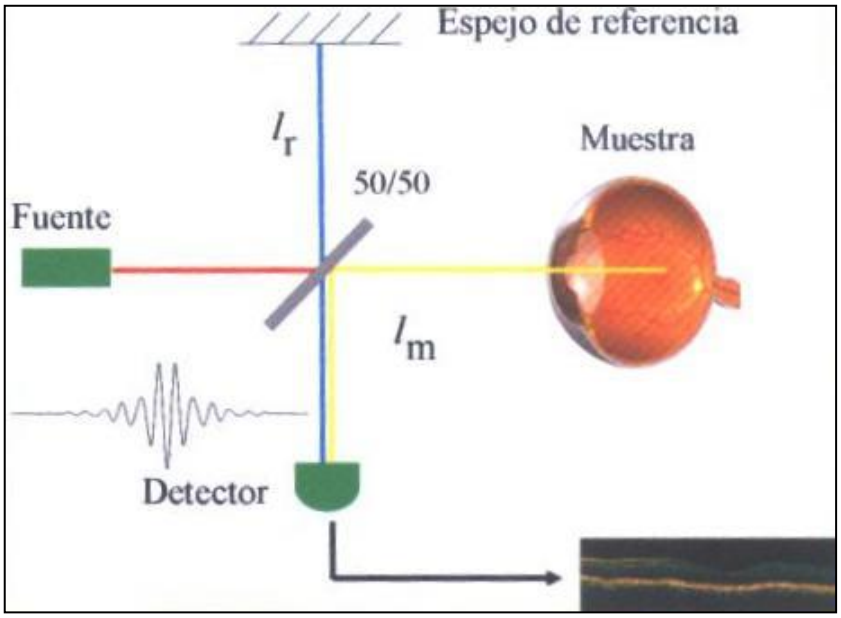

Figura 6. Bases físicas de la OCT.

La CFNR puede ser identificada y su espesor medido de forma objetiva gracias a las siguientes características: disposición de la fibras nerviosas de la retina perpendiculares al haz de luz, reflectividad de la interfase vítreo - membrana limitante interna y la alta reflectividad de la interfase epitelio pigmentario - fotoreceptores. Las

estrategias con haz de luz circular entorno a la cabeza del nervio permiten el cálculo de grosor en los cuatro cuadrantes y por sectores.

Desde un punto de vista operativo, la OCT establece y calcula el grosor retiniano como la distancia entre la interfase vitreorretiniana y la unión entre el segmento interior y exterior de los fotorreceptores, justo internamente al epitelio pigmentario retiniano. De esta manera, considera el grosor retiniano y de la CFNR, siendo éste último la distancia entre el límite posterior de la CFNR y la interfase vitreorretiniana. En la figura 7 se muestra una imagen transversal en la cual aparece el grosor retiniano y de la CFNR.

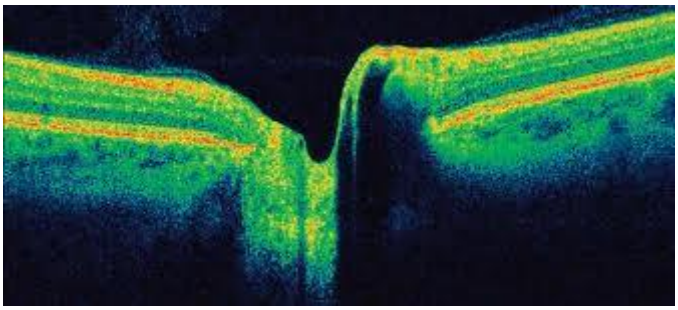

Figura 7. Imagen topográfica del grosor retiniano y de la CFNR.

Este proceso de análisis y determinación de puntos y líneas de referencia se realiza en cada uno de los barridos lineales incluidos en el protocolo de adquisición y, a continuación, integra la totalidad de los mismos para obtener los resultados de toda la cabeza del nervio y determinar los diferentes parámetros morfométricos papilares.

El dispositivo OCT posee una base de normalidad con la que compara automáticamente los resultados de cada sujeto evaluado en relación a su edad, raza y sexo y así determina la probabilidad de que la exploración de ese individuo pueda considerarse normal.

En nuestros estudios se utilizaron dos tipos de dispositivos OCT de última generación: OCT Cirrus y OCT Spectralis.

El dispositivo OCT Cirrus (Carl Zeiss Meditec Inc, Dublin, California, EEUU) es un tomógrafo de dominio espectral capaz de realizar mediciones con una resolución de 5/1.000 milímetros y más de 67 millones de puntos de información diferentes mediante el uso de la tecnología de infrarrojos con una velocidad máxima de 27.000 escáneres por segundo.

El protocolo de nervio óptico de la OCT Cirrus genera imágenes de un cubo de 200 por 200 micras alrededor del nervio óptico. Los parámetros analizados en nuestro estudio fueron el espesor medio de la CFNR, el espesor en cada uno de los cuadrantes de la CFNR (superior, inferior, temporal y nasal), y el espesor en los doce sectores horarios del nervio óptico. A los sectores horarios se les asignó un número de posición (C1 a C12) en el sentido horario para el ojo derecho y en el sentido anti horario para el izquierdo.

El protocolo macular incluyó un cubo macular de 512x128 micras que proporcionó los valores de los espesores como un mapa de colores para las nueve áreas descritas en el Early Treatment Diabetic Retinopathy Study (ETDRS). Éste estudio divide la mácula en 9 áreas definidas por tres círculos ubicados a 1, 3, y 6 mm, estos dos últimos a su vez están divididos en cuatro cuadrantes: superior, inferior, nasal y temporal. El área 1 representa la fóvea. Las áreas 2, 3, 4 y 5 forman el anillo interno y las áreas 6, 7, 8 y 9 forman el anillo externo. Los parámetros recogidos en nuestro estudio fueron el espesor medio y el volumen macular total calculado en el anillo de 6 mm de diámetro.

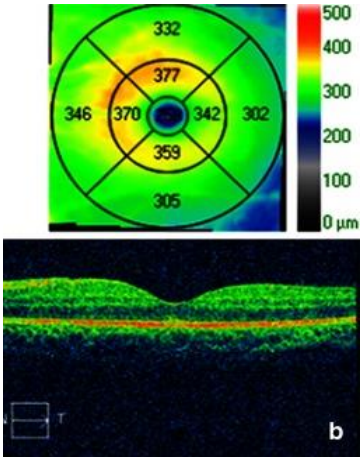

Figura 8. Imagen del mapa macular con los espesores de las 9 áreas descritas en el Early Treatment Diabetic Retinopathy Study (ETDRS) (arriba) y corte histológico del perfil macular (abajo).

La OCT Spectralis analiza de forma simultánea múltiples longitudes de onda del espectro del haz de luz reflejado, siendo 100 veces más rápido que la OCT previa de dominio tiempo, y adquiriendo unos 40.000 cortes por segundo. Incorpora un sistema de escaneo mediante óptica confocal (Confocal Scanning Laser Ophthalmoscope), que proporciona imágenes simultáneas con mejor contraste y detalle de la imagen, y analiza de forma exclusiva la información del punto de enfoque. Dispone de un sistema de seguimiento ocular que corrige los movimientos del ojo durante la adquisición de las imágenes, disminuyendo así los artefactos y logrando imágenes más reproducibles. Asimismo, establece unas referencias anatómicas que pueden emplearse en futuras exploraciones como marcadores para analizar la misma zona retiniana. La gran velocidad de adquisición de los tomógrafos de dominio espectral consigue valorar amplias áreas de la retina con una alta definición y de modo tridimensional. La posibilidad de realizar un estudio de seguimiento con imágenes previas hace que la valoración en el tiempo sea mucho más fácil e incluso se pueda conseguir en enfermos sin capacidad de fijación.

El protocolo RFNL (Retinal Nerve Fiber Layer) del Spectralis genera un mapa que contiene el espesor medio y el espesor de seis sectores (superonasal, nasal, inferonasal, inferotemporal, temporal, y superotemporal) en dirección a las agujas del

reloj para el ojo derecho y en contra de las agujas para el ojo izquierdo. Además generará una base de datos con todas las mediciones de los espesores de la CFNR para los 768 puntos registrados durante el escáner circular alrededor del nervio óptico. En nuestro estudio se registraron los espesores medio, por sectores y de los 768 puntos. El espesor de la CFNR se midió con un promedio de 16 B-scans consecutivos y circulares (diámetro 3,5 mm, 768 A-scans).

Para medir el espesor macular se utilizó el protocolo Fast macular. El mapa de espesores se representó en 9 subcampos de manera similar al OCT Cirrus. El parámetro evaluado en nuestro estudio fue el espesor macular medio.

Todas las imágenes fueron tomadas por el mismo operador con experiencia, en este caso, el doctorando. La calidad de las imágenes fue valorada previamente al análisis y aquellas con una calidad baja fueron descartadas.

La OCT Cirrus determina la calidad de las imágenes utilizando una medición de la señal que combina la relación señal-ruido con la uniformidad de la señal dentro de la imagen. Consta de una escala con un rango del 1 al 10, donde 1 es una calidad de imagen pobre y 10 es una calidad de imagen excelente. Solo las imágenes con una puntuación mayor de 7 fueron incluidas en nuestro estudio.

La OCT Spectralis utiliza una barra de calidad azul en la imagen para indicar la calidad de la señal. La puntuación de la calidad va desde un rango entre 0 (baja calidad) y 40 (excelente calidad). Solo las imágenes con una puntuación mayor de 25 fueron analizadas.

EXPLORACIÓN NEUROFISIOLÓGICA

Los potenciales evocados visuales (PEV) recogen la respuesta eléctrica cerebral obtenida por estimulación visual de la corteza occipital. Está originada fundamentalmente a nivel del área 17 (estriada) con participación de áreas de asociación 18 y 19. Explora la integridad de la vía visual desde la mácula hasta la

corteza occipital. El 80% de la respuesta es generada por los 8º centrales de la retina. Las áreas periféricas contribuyen menos, ya que la representación cortical es menor que la de las áreas centrales. En el 20% restante de la respuesta, la contribución del hemicampo inferior es mayor que la del superior.

La respuesta obtenida tiene una morfología en V. El complejo está formado por los componentes N75-P100-N135. El componente principal es P100, del que se valora la latencia y amplitud. El estímulo utilizado puede ser de dos tipos: pattern o flash. Este último solamente se aplica en niños con deficiente colaboración y en pacientes con opacidades de medios y no se ha utilizado en nuestro estudio. El estímulo pattern puede presentarse en forma de campo completo o por hemicampos. En el pattern los cuadros pueden ser de varios tamaños: los más pequeños evalúan el área foveal y los más grandes, la región perifoveal.

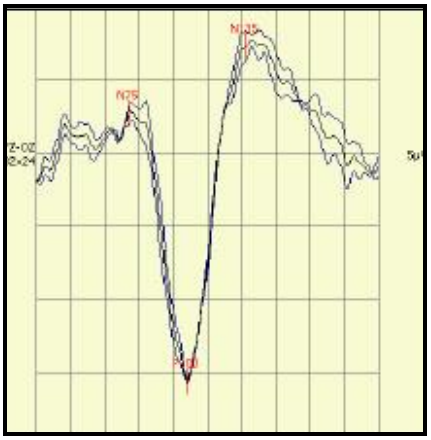

Figura 9. Potencial evocado visual.

Cualquier alteración de la vía visual puede producir un PEV patológico. En la neuropatía óptica secundaria a enfermedad desmielinizante se suele producir un retraso en la latencia de P100 y, con menor frecuencia, una reducción en la amplitud. Este aumento de la latencia no se correlaciona con la pérdida de agudeza visual y, de

hecho, persiste una vez que se recupera la visión. También es útil en el diagnóstico de neuritis subclínicas.

En nuestros estudios se empleó el equipo Neuronic sensewitness 4.0 (Neuronic Zaragoza, Spain) y unos electrodos de disco bañados en cloruro de plata colocados en el cuero cabelludo de la zona occipital (Oz, electrodo activo) y en el área frontal (Fz, electrodo de referencia). Como electrodo de tierra se colocó un electrodo de baja impedancia en la frente del paciente. Los estímulos se presentaron de forma monocular y la frecuencia de alternancia de los estímulos *pattern* fue de 2 Hz. Se empleó un monitor de vídeo de 26 x 20 centímetros colocado a un metro de distancia del sujeto (ángulo visual de 16º) y el tamaño de los cuadrados fue de 1º de arco. El promedio de luminancia fue de 93,5 candelas/m^2, con un contraste del 99%. Se analizaron la latencia y la amplitud del componente principal positivo, reconocido convencionalmente como una deflexión hacia abajo (onda P100).

3.3 Recogida y análisis de datos

Todas las variables mencionadas fueron registradas en una base de datos elaborada con el programa FileMaker Pro 8.5 (File Marker Inc., Santa Clara, CA).

Para una mejor compresión del análisis de los datos, a continuación se detalla la técnica estadística utilizada en cada uno de los trabajos de investigación.

1. *Herrero R, Garcia-Martin E, Almarcegui C, Ara JR, Rodriguez-Mena R, Martin J, Satue M, Dolz I, Fernandez J, Pablo LE. Progressive degeneration of the retinal nerve fiber layer in patients with multiple sclerosis. Invest Ophthalmol Vis Sci. 2012;53(13):8344-9. ISSN: 0146-0404. PMID: 23154461.*

Se realizó un estudio longitudinal prospectivo de 3 años de seguimiento. Se incluyeron un total de 94 pacientes con EM (188 ojos) y 50 sujetos sanos (100 ojos) que fueron evaluados en el momento basal, a los 12, 24 y 36 meses. Para el análisis estadístico se utilizó el SPSS IBM (version 19.0; SPSS Inc, Chicago, IL).

Previamente al análisis de los datos se comprobó el ajuste de las variables a la normalidad mediante el test de Kolmogorov-Smirnov. Los resultados de cada variable obtenidos en las sucesivas exploraciones fueron comparados entre ambos grupos (EM y controles sanos) mediante un test de análisis de la varianza ANOVA, con el objetivo de detectar diferencias en la estructura de la CFNR asociadas a la evolución de la enfermedad en este periodo de seguimiento.

Mediante un análisis de Pearson se llevó a cabo un estudio de correlación entre las variables estructurales (OCT) y las funcionales (agudeza visual, campimetría, visión cromática y PEV). Se determinó el coeficiente de correlación de Pearson (r) y la significación estadística de la asociación (P). El coeficiente de correlación de Pearson puede tomar un valor en un rango que va de -1 a 1. Un valor de 0 indica que no existe asociación entre las dos variables. Un valor mayor de 0 indica una asociación positiva, es decir, si el valor de una variable aumenta, también lo hace el de la otra variable. Y por último, un valor menor de 0 indica una asociación negativa: si el valor de una variable aumenta, el valor de la otra disminuye.

Finalmente, se dividió a los pacientes en dos grupos: los que habían recibido tratamiento para la EM y lo que no habían sido tratados. Se analizó si existían diferencias significativas en los cambios registrados en las variables durante los 3 años de seguimiento mediante el test estadístico T de Student, con el objetivo de estudiar si el tratamiento es un factor protector para la degeneración de la CFNR que tiene lugar en la EM.

Un nivel de $p<0,05$ fue considerado significativo para todos los análisis estadísticos.

2. Garcia-Martin E, Pablo LE, Herrero R, Satue M, Polo V, Larrosa JM, Martin J, Fernandez J. Diagnostic ability of a linear discriminant function for Spectral domain optical coherence tomography in multiple sclerosis patients. Ophthalmology 2012;119(8):1705-11. ISSN: 0161-6420. PMID: 22480742.

Se reclutaron dos muestras independientes de 115 sujetos sanos y 115 pacientes con EM. De la población total se seleccionó de forma randomizada una muestra para desarrollar la función lineal discriminante ("teaching set") y otra muestra para comprobar la actuación de la función lineal discriminante ("validating set").

En la muestra "teaching set" se realizó un análisis de regresión logística binaria, utilizado cuando la variable dependiente es dicotómica (sano o enfermo) y las variables independientes son de cualquier tipo. Las variables dependientes fueron el diagnóstico de EM (sí o no), y las variables predictivas los 768 espesores de la CFNR, el espesor medio y los espesores en los 6 sectores (superonasal, nasal, inferonasal, inferotemporal, temporal, and superotemporal) obtenidos en la OCT Spectralis.

La importancia relativa de cada variable independiente se evaluó mediante un análisis de regresión logística binaria utilizando el método de Foward Wald. El test Wald-w2 sirve para comprobar la contribución única de cada predictor en el contexto de los otros predictores (manteniendo constantes los demás predictores).

La función lineal discriminante fue una puntuación calculada tomando la suma ponderada de las variables predictivas. Los parámetros significativos de la OCT se combinaron para generar una nueva variable denominada función lineal discriminante, de tal manera que las diferencias encontradas entre ojos sanos y ojos con EM fueron maximizadas. La muestra "validación set" se utilizó para probar y comparar la precisión diagnóstica de dicha función lineal discriminante con otros parámetros de la CFNR del OCT Spectralis. Se trazaron curvas ROC (Receiver operating characteristic) para

todos los parámetros y se compararon con la curva ROC obtenida para la función lineal discriminante propuesta.

Por último, se analizaron las diferencias entre las curvas ROC para comparar los valores del área bajo la curva (AUC) utilizando el método Hanley-McNeil. Los puntos de corte se calcularon con el software MedCalc, como los puntos con el mejor balance de sensibilidad-especificidad. Se calcularon las sensibilidades de cada parámetro para valores fijos de especificidad del 85% y 95%, y se determinaron los valores predictivos positivo y negativo.

3. Garcia-Martin E, Calvo B, Malvè M, Herrero R, Fuertes I, Ferreras A, Larrosa JM, Polo V, Pablo LE. Three-dimensional geometries representing the retinal nerve fiber layer in multiple sclerosis, optic neuritis, and healthy eyes. Ophthalmic Research 2013 (en prensa). ISSN: 0030-3747.

Se incluyeron dos muestras independientes de 110 sujetos sanos y 130 pacientes con EM de tipo remitente recurrente. Un total de 230 ojos (108 sanos y 122 pacientes con EM) fueron analizados y se eligió de forma aleatoria un ojo de cada paciente. Todos ellos fueron evaluados mediante el OCT Spectralis con la versión de software 5.4b. Se creó un modelo geométrico del nervio óptico mediante las medidas de la CFNR utilizando el Autodesk Invertor (versión 11.0, Barcelona, España). Las variables independientes del estudio fueron el diagnóstico de EM (sí o no) y las variables predictivas fueron los 768 parámetros del espesor de la CFNR, el espesor medio y el espesor en cada uno de los seis sectores medidos mediante la OCT Spectralis. Los resultados estructurales proporcionados por la OCT se compararon entre ojos sanos, ojos de pacientes con EM y neuritis óptica previa y ojos de pacientes con EM sin neuritis previa, mediante el test de ANOVA para el análisis de la varianza.

Los espesores de la CFNR se mostraron en un modelo en tres dimensiones (3D) que representó una aproximación al ojo humano. Este modelo fue reconstruido usando el software Autodesk Invertor (SolidWorks Inc., Dassault, SolidWorks Corp., France) y se presentó como una perfecta esfera dividida en seis sectores (superonasal, nasal, inferonasal, inferotemporal, temporal, y superotemporal, respectivamente). De esta forma, fue posible obtener una modelo visual de la afectación de la CFNR en pacientes con EM con y sin previos episodios de neuritis óptica.

4. García-Martín E, Herrero R, Bambo MP, Ara JR, Martin J, Polo V, Larrosa JM, Garcia-Feijoo J, Pablo LE. Artificial neural network techniques to improve the ability of optical coherence tomography to detect optic neuritis. Seminars of Opthalmology 2013 (en prensa). ISSN: 0882-0538.

Se incluyeron dos muestras independientes de 108 sujetos sanos y 122 pacientes con EM de tipo remitente recurrente. 6 pacientes con EM no completaron todos los requisitos de las pruebas y fueron excluidos del análisis. 7 sujetos que presentaron artefactos, partes perdidas o or showing seemingly distorted anatomy fueron excluidos (4 pacientes y 3 sujetos sanos). Un total de 217 ojos (105 sanos y 112 pacientes con EM) fueron incluidos en el análisis estadístico. Un ojo de cada sujeto fue elegido de forma aleatoria para el estudio.

Se utilizó la OCT Spectralis con el software versión 5.4b. Los 768 A-scans proporcionados por la OCT Spectralis para medir el espesor medio de la CFNR y el espesor en los 6 sectores fue registrado e incluido en una base de datos diseñada para este estudio utilizando el programa FileMaker Pro 8.5 (File Marker Inc., Santa Clara, CA). Para el análisis estadístico se utilizó el SPSS IBM (version 18.0; SPSS Inc, Chicago, IL) y para realizar el análisis de redes neuronales artificiales se utilizó el Software Rapidminer 5.1.006 (Rapid I GmbH, Dortmund, Germany). Los ojos de

pacientes con EM fueron divididos en dos subgrupos: 41 ojos con antecedente de neuritis óptica y 71 ojos sin antecedente previo de neuritis óptica. Se evaluó el rendimiento de la técnica de análisis de redes neuronales artificiales para clasificar las mediciones de la CFNR proporcionadas por la OCT Spectralis como pacientes con EM o sujetos sanos.

Las redes neuronales artificiales son herramientas de extracción de datos utilizadas fundamentalmente para buscar patrones de comportamiento en un conjunto de datos, aprender estos patrones y desarrollar la habilidad de clasificar nuevos patrones correctamente. La red neuronal parte de un conjunto de datos de entrada suficientemente significativo y el objetivo es conseguir que aprenda automáticamente las propiedades deseadas. Las redes neuronales artificiales pueden clasificarse en función del patrón de conexiones que presenta, definiéndose así dos tipos básicos de redes:

- Redes de propagación hacia delante o acíclicas: en las que todas las señales van desde la capa de entrada hacia la salida sin existir ciclos ni conexiones entre neuronas de la misma capa de red neuronal. A su vez se clasifican en monocapa o multicapa.
- Redes recurrentes: presentan al menos un ciclo cerrado de activación neuronal.

En este estudio, se utilizó un patrón de red neuronal entrenado por un algoritmo de propagación hacia delante conocido como perceptrón multicapa. Este método es uno de los más utilizados, utiliza una arquitectura de avance y como mejora del perceptron simple, puede emular cualquier función continua. El perceptrón multicapa está formado por múltiples capas (siempre más de tres), las cuales se dividen en:

- Capa de entrada: donde entra la información. En nuestro caso las mediciones de espesores de la OCT.

- Capa oculta: puede ser una o más capas, y realizan parte del proceso para enviarlo a la salida.
- Capa de salida: última capa del perceptrón multicapa, donde se devuelve el resultado. En nuestro caso EM o controles, y ojos con neuritis óptica o sin neuritis óptica.

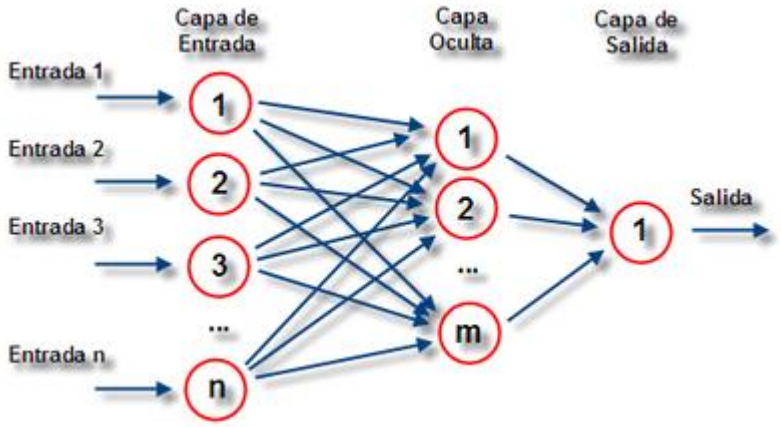

Figura 10. Esquema de una Red Neuronal Artificial de tipo Perceptrón simple con *n* neuronas de entrada, *m* neuronas en su capa oculta y una neurona de salida.

El entrenamiento de los clasificadores de aprendizaje automático se realizó con cada espesor de la CFNR por separado, así como con todos los 768 espesores de la CFNR utilizados conjuntamente.

Se realizó un análisis de regresión lineal para normalizar la edad, la refracción y el espesor de la CFNR a nuestra base de datos, y los coeficientes de derivación para calcular los valores corregidos del espesor de la CFNR.

4. CONCLUSIONES

I. El análisis de la capa de fibras nerviosas de la retina es un buen biomarcador de la degeneración axonal progresiva que se produce en la esclerosis múltiple y es útil para evaluar la progresión de la enfermedad y la eficacia de los tratamientos en la protección de la degeneración axonal.

II. Las técnicas de análisis funcional y estructural del nervio óptico son útiles para la detección de daño secundario a esclerosis múltiple y existe correlación entre las variables estructurales obtenidas mediante la tomografía de coherencia óptica y las variables funcionales proporcionadas por el campo visual, la medición de la agudeza visual y los potenciales evocados visuales.

III. La técnica estadística de redes neuronales artificiales pueden identificar correctamente un alto porcentaje de sujetos con esclerosis múltiples y permite clasificar aquellos ojos que han presentado antecedente de neuritis ópticas, con mayor precisión diagnóstica que cualquier parámetro aislado de la capa de fibras nerviosas de la retina obtenido a partir de la tomografía de coherencia óptica.

IV. La representación del espesor de la capa de fibras nerviosas de la retina utilizando el modelo de geometría en tres dimensiones nos permite observar la distribución del daño axonal en pacientes con esclerosis múltiple con una mayor afectación del sector temporal, especialmente en aquellos pacientes con neuritis óptica previa.

V. La función lineal discriminante que combina varios espesores de la capa de fibras nerviosas de la retina mejora la capacidad de la tomografía de coherencia óptica Spectralis para detectar esclerosis múltiple y distinguir entre ojos con antecedente y sin antecedente de neuritis óptica.

BIBLIOGRAFÍA DE LA INTRODUCCIÓN Y METODOLOGÍA

1. Palace J. Inflammation versus neurodegeneration: consequences for treatment. J Neurol Sci 2007; 259: 46-49.
2. Hauser SL, Oksenberg JR. The neurobiology of multiple sclerosis: genes, inflammation, and neurodegeneration. Neuron 2006; 52: 61-76.
3. Khanifar AA, Parlitsis GJ, Ehrlich JR, Aaker GD, D'Amico DJ, Gauthier SA, et al. Retinal nerve fiber layer evaluation in multiple sclerosis with spectral domain optical coherence tomography. Clin Ophthalmol 2010; 4: 1007-1013.
4. Sergott RC. Optical coherence tomography: measuring in-vivo axonal survival and neuroprotection in multiple sclerosis and optic neuritis. Curr Opin Ophthalmol 2005; 16: 346-350.
5. Zaveri MS, Conger A, Salter A, Frohman TC, Galetta SL, Markowitz CE, et al. Retinal imaging by laser polarimetry and optical coherence tomography evidence of axonal degeneration in multiple sclerosis. Arch Neurol 2008; 65: 924-928.
6. Gundogan FC, Demirkaya S, Sobaci G. Is optical coherence tomography really a new biomarker candidate in multiple sclerosis? A structural and functional evaluation. Invest Ophthalmol Vis Sci 2007; 48: 5773-5781.
7. Garcia-Martin E, Pueyo V, Martin J, Almarcegui C, Ara JR, Dolz I, et al. Progressive changes in the retinal nerve fiber layer in patients with multiple sclerosis. Eur J Ophthalmol 2010; 20(1): 167-73.
8. Garcia-Martin E, Pueyo V, Pinilla I, Ara JR, Martin J, Fernandez J. Fourier-Domain OCT in multiple sclerosis patients: Reproducibility and ability to detect retinal nerve fiber layer atrophy. Invest Ophthalmol Vis Sci 2011; 52:4124-4131.

9. Frohman EM, Dwyer MG, Frohman T, Cox JL, Salter A, Greenberg BM, et al. Relationship of optic nerve and brain conventional and non-conventional MRI measures and retinal nerve fiber layer thickness, as assessed by OCT and GDx: a pilot study. J Neurol Sci 2009; 282(1-2): 96-105.
10. Lamirel C, Newman NJ, Biousse V. Optical coherence tomography (OCT) in optic neuritis and multiple sclerosis. Rev Neurol (Paris) 2010; 166(12): 978-986.
11. Talman LS, Bisker ER, Sackel DJ, Long DA Jr, Galetta KM, Ratchford JN, et al. Longitudinal study of vision and retinal nerve fiber layer thickness in multiple sclerosis. Ann Neurol 2010; 67: 749-760.
12. Henderson AP, Trip SA, Schlottmann PG, Altmann DR, Garway-Heath DF, Plant GT, et al. A preliminary longitudinal study of the retinal nerve fiber layer in progressive multiple sclerosis. J Neurol 2010; 257(7): 1083-1091.
13. Ratchford JN, Quigg ME, Conger A, Frohman T, Frohman E, Balcer LJ, et al. Optical coherence tomography helps differentiate neuromyelitis optica and MS optic neuropathies. Neurology 2009; 73: 302-308.
14. Syc SB, Warner CV, Hiremath GS, Farrell SK, Ratchford JN, Conger A, et al. Reproducibility of high-resolution optical coherence tomography in multiple sclerosis. Mult Scler 2010; 16(7): 829-839.
15. Pueyo V, Martin J, Fernandez J, Almarcegui C, Ara J, Egea C, et al. Axonal loss in the retinal nerve fiber layer in patients with multiple sclerosis. Mult Scler 2008; 14: 609-614.
16. Pueyo V, Polo V, Larrosa JM, Mayoral F, Ferreras A, Honrubia FM. Reproducibility of optic nerve head and retinal nerve fiber layer thickness measurements using optical coherence tomography. Arch Soc Esp Oftalmol 2006; 81(4): 205-211.

17. Garcia-Martin E, Pueyo V, Ara J, Almarcegui C, Martin J, Pablo L. Effect of optic neuritis on progressive axonal damage in multiple sclerosis patients. Mult Scler. 2011;17: 830-837.
18. Wojtkowski M, Srinivasan V, Fujimoto JG, Ko T, Schuman JS, Kowalczyk A, et al. Three dimensional retinal imaging with high-speed ultrahigh-resolution optical coherence tomography. Ophthalmology 2005; 112: 1734-1746.
19. Garcia-Martin E, Pueyo V, Almarcegui C, Martin J, Ara JR, Sancho E, et al. Risk factors for progressive axonal degeneration of the retinal nerve fibre layer in multiple sclerosis patients. Br J Ophthalmol 2011; 95: 1577-1582.
20. Garcia-Martin E, Pinilla I, Sancho E, Almarcegui C, Dolz I, Rodriguez-Mena D, et al. Optical coherence tomography in retinitis pigmentosa: Reproducibility and capacity to detect macular and retinal nerve fiber layer thickness alterations. Retina 2012; 32(8):1581-1591.
21. Kallenbach K, Sander B, Tsakiri A, Wanscher B, Fuglø D, Larsen M, et al. Neither retinal nor brain atrophy can be shown in patients with isolated unilateral optic neuritis at the time of presentation. Mult Scler 2011; 17(1): 89-95.
22. Burgansky-Eliash Z, Wollstein G, Chu T, Ramsey JD, Glymour C, Noecker RJ, et al. Optical coherence tomography machine learning classifiers for glaucoma detection: a preliminary study. Invest Ophthalmol Vis Sci 2005; 46: 4147-4152.
23. Garcia-Martin E, Pablo LE, Herrero R, Satue M, Polo V, Larrosa JM, et al. Diagnostic ability of a linear discriminant function for Spectral domain optical coherence tomography in multiple sclerosis patients. Ophthalmology 2012; 119(8): 1705-1711.
24. Slater JD, Wu FY, Honig LS, Ramsay RE, Morgan R. Neural network analysis of the P300 event-related potential in multiple sclerosis. Electroencephalogr Clin Neurophysiol 1994; 90(2): 114-122.

25. Wu FY, Slater JD, Honig LS, Ramsay RE. A neural network design for event-related potential diagnosis. Comput Biol Med 1993; 23(3): 251-264.
26. Wu FY, Slater JD, Ramsay RE. Neural network approach in multichannel auditory eventrelated potential analysis. Int J Biomed Comput 1994; 35(3): 157-168.
27. Pablo LE, Ferreras A, Pajarín AB, Fogagnolo P. Diagnostic ability of a linear discriminant function for optic nerve head parameters measured with optical coherence tomography for perimetric glaucoma. Eye (Lond) 2010; 24: 1051-1057.
28. Parikh RS, Parikh SR, Sekhar GC, Prabakaran S, Babu JG, Thomas R. Normal age-related decay of retinal nerve fiber layer thickness. Ophthalmology 2007;114:921-926.
29. Gordon-Lipkin E, Chodkowski B, Reich DS, Smith SA, Pulicken M, Balcer LJ, et al. Retinal nerve fiber layer is associated with brain atrophy in multiple sclerosis. Neurology 2007;69:1603-1609.
30. Dörr J, Wernecke KD, Bock M, Gaede G, Wuerfel JT, Pfueller CF, et al. Association of retinal and macular damage with brain atrophy in multiple sclerosis. PLoS One 2011;6:e18132.
31. Garcia-Martin E, Pueyo V, Fernandez J, Martín J, Ara JR, Almarcegui C, et al. Effect of treatment in loss of retinal nerve fibre layer in multiple sclerosis patients. Arch Soc Esp Oftalmol 2010;85:209-214.
32. Zimmermann H, Freing A, Kaufhold F, Gaede G, Bohn E, Bock M, Oberwahrenbrock T, Young KL, Dörr J, Wuerfel JT, Schippling S, Paul F, Brandt AU. Optic neuritis interferes with optical coherence tomography and magnetic resonance imaging correlations. Mult Scler 2013;19(4):443-450.
33. Siger M, Dziegielewski K, Jasek L, Bieniek M, Nicpan A, Nawrocki J, Selmaj K. Optical coherence tomography in multiple sclerosis: thickness of the

retinal nerve fiber layer as a potential measure of axonal loss and brain atrophy. J Neurol 2008; 255(10): 1555-1560.

34. Bain AC, Meaney DF. Tissue-level thresholds for axonal damage in an experimental model of central nervous system white matter injury. J Biomech Eng 2000; 122(6): 615-622.
35. LaPlaca MC, Cullen DK, McLoughlin JJ, Cargill RS. High rate shear strain of three-dimensional neural cell cultures: a new in vitro traumatic brain injury model. J Biomech 2005; 38(5): 1093-1105.
36. Wang JH, Thampatty BP. An introductory review of cell mechanobiology. Biomech Model Mechanobiol 2006; 5(1): 1-16.
37. Polman CH, Reingold SC, Banwell B, Clanet M, Cohen JA, Filippi M, et al. Diagnostic criteria for multiple sclerosis: 2010 revisions to the McDonald criteria. Ann Neurol 2011;69(2):292-302.
38. Katz J, Tielsch JM, Quigley HA, Sommer A. Automated perimetry detects visual field loss before manual Goldmann perimetry. Ophthalmology 1995; 102:21-26.
39. Beck RW, Bergstrom TJ, Lichter PR. A clinical comparison of visual field testing with a new automated perimeter; the Humphrey Field Analyzer, and the Goldmann perimeter. Ophthalmology 1985; 92:77-82.

APÉNDICE I. CARTAS DE ACEPTACIÓN DE LOS TRABAJOS PENDIENTES DE PUBLICACIÓN

Ms No.: 201209019

Title: Three-dimensional geometries representing the retinal nerve fiber layer in multiple sclerosis, optic neuritis, and healthy eyes

Dear Dr. Garcia-Martin,

Thank you for submitting your manuscript to "Ophthalmic Research".

We would like to inform you that your paper has now been accepted for publication and passed on to Mr. Christoph REBER from the Production Dept., from whom you will hear in due time.

We hope you will continue to submit work from your group to "Ophthalmic Research" in the future.

With kind regards,

Sandrine Maguire

Editorial Office 'Ophthalmic Research'

17-Jan-2013

Dear Dr Garcia-Martin:

Your manuscript entitled "Artificial neural network techniques to improve the ability of optical coherence tomography to detect optic neuritis.", which you submitted to Seminars In Ophthalmology, has been reviewed. The reviewer comments are included at the bottom of this letter.

The reviews are in general favourable and suggest that, subject to minor revisions, your paper could be suitable for publication. Please consider these suggestions, and I look forward to receiving your revision.

When you revise your manuscript please highlight the changes you make in the manuscript by using the track changes mode in MS Word or by using bold or colored text.

To submit the revision, log into http://mc.manuscriptcentral.com/nsio and enter your Author Center, where you will find your manuscript title listed under "Manuscripts with Decisions." Under "Actions," click on "Create a Revision." Your manuscript number has been appended to denote a revision. Please enter your responses to the comments made by the reviewer(s) in the space provided. You can use this space to document any changes you made to the original manuscript. Please be as specific as possible in your response to the reviewer(s).

IMPORTANT: Your original files are available to you when you upload your revised manuscript. Please delete any redundant files before completing the submission.

Because we are trying to facilitate timely publication of manuscripts submitted to Seminars In Ophthalmology, your revised manuscript should be uploaded as soon as possible. If it is not possible for you to submit your revision in a reasonable amount of time, we may have to consider your paper as a new submission.

Once again, thank you for submitting your manuscript to Seminars In Ophthalmology and I look forward to receiving your revision.

Sincerely,

Dr Thomas Friberg

Seminars In Ophthalmology

APÉNDICE II. FACTOR DE IMPACTO DE LAS REVISTAS Y ÁREAS TEMÁTICAS

1. Autores: Herrero R, Garcia-Martin E, Almarcegui C, Ara JR, Rodriguez-Mena R, Martin J, Satue M, Dolz I, Fernandez J, Pablo LE.

   Título: Progressive degeneration of the retinal nerve fiber layer in patients with multiple sclerosis.

   Revista: Invest Ophthalmol Vis Sci. 2012; 53(13):8344-9.

   ISSN: 0146-0404

   PMID: 23154461

   Índice de Impacto (JCR 2011): 3,862

   Posición entre las revistas de oftalmología en el JCR: 6/56.

   Área temática de la revista: Oftalmología

2. Autores: Garcia-Martin E, Pablo LE, Herrero R, Satue M, Polo V, Larrosa JM, Martin J, Fernandez J.

   Título: Diagnostic ability of a linear discriminant function for Spectral domain optical coherence tomography in multiple sclerosis patients

   Revista: Ophthalmology 2012; 119(8):1705-11.

   ISSN: 0161-6420

   PMID: 22480742

   Índice de Impacto (JCR 2011): 5,567.

   Posición entre las revistas de oftalmología en el JCR 2011: 2/56.

   Área temática de la revista: Oftalmología

3. Autores: Garcia-Martin E, Calvo B, Malvè M, Herrero R, Fuertes I, Ferreras A, Larrosa JM, Polo V, Pablo LE.

   Título: Three-dimensional geometries representing the retinal nerve fiber layer in multiple sclerosis, optic neuritis, and healthy eyes.

   Revista: Ophthalmic Research 2013 (en prensa)

ISSN: 0030-3747

Índice de Impacto (JCR 2011): 1,561

Posición entre las revistas de oftalmología en el JCR 2011: 27/56.

Área temática de la revista: Oftalmología

4. Autores: Garcia-Martin E, Herrero R, Bambo MP, Ara JR, Martin J, Polo V, Larrosa JM, Garcia-Feijoo J, Pablo LE.

   Título: Artificial neural network techniques to improve the ability of optical coherence tomography to detect optic neuritis.

   Revista: Seminars of Ophthalmology 2013 (en prensa)

   ISSN: 0882-0538

   Índice de Impacto (JCR 2010): 0,901

   Posición entre las revistas de oftalmología en el JCR 2011: 44/56

   Área temática de la revista: Oftalmología

APÉNDICE III. JUSTIFICACIÓN DE LA CONTRIBUCIÓN DEL DOCTORANDO EN CADA PUBLICACIÓN

1. *Herrero R, Garcia-Martin E, Almarcegui C, Ara JR, Rodriguez-Mena R, Martin J, Satue M, Dolz I, Fernandez J, Pablo LE. Progressive degeneration of the retinal nerve fiber layer in patients with multiple sclerosis. Invest Ophthalmol Vis Sci. 2012;53(13):8344-9. ISSN: 0146-0404. PMID: 23154461.*

El doctorando realizó todo el trabajo de campo con los pacientes y las pruebas oftalmológicas, coordinó el resto de pruebas, realizó la recogida de datos, la redacción del artículo y participó en la realización de los diversos análisis estadísticos, en la revisión y en la corrección del artículo científico.

2. *Garcia-Martin E, Pablo LE, Herrero R, Satue M, Polo V, Larrosa JM, Martin J, Fernandez J. Diagnostic ability of a linear discriminant function for Spectral domain optical coherence tomography in multiple sclerosis patients. Ophthalmology 2012;119(8):1705-11. ISSN: 0161-6420. PMID: 22480742.*

El doctorando realizó todo el trabajo de campo con los pacientes y las pruebas oftalmológicas, coordinó el resto de pruebas, realizó la recogida de datos, participó en los diversos análisis estadísticos y en la redacción, revisión y corrección del artículo científico.

3. *Garcia-Martin E, Calvo B, Malvè M, Herrero R, Fuertes I, Ferreras A, Larrosa JM, Polo V, Pablo LE. Three-dimensional geometries representing the retinal nerve fiber layer in multiple sclerosis, optic neuritis, and healthy eyes. Ophthalmic Research 2013 (en prensa). ISSN: 0030-3747.*

El doctorando realizó todo el trabajo de campo con los pacientes y las pruebas oftalmológicas, coordinó el resto de pruebas, realizó la recogida de datos, participó en los diversos análisis estadísticos y en la redacción, revisión y corrección del artículo científico.

4. *García-Martín E, Herrero R, Bambo MP, Ara JR, Martin J, Polo V, Larrosa JM, Garcia-Feijoo J, Pablo LE. Artificial neural network techniques to improve the ability of optical coherence tomography to detect optic neuritis. Seminars of Opthalmology 2013 (en prensa). ISSN: 0882-0538.*

El doctorando realizó todo el trabajo de campo con los pacientes y las pruebas oftalmológicas, coordinó el resto de pruebas, realizó la recogida de datos, participó en los diversos análisis estadísticos y en la redacción, revisión y corrección del artículo científico.

APÉNDICE IV. RENUNCIA DE LOS COAUTORES NO DOCTORES A USAR EL ARTÍCULO EN SU PROPIA TESIS DOCTORAL

Yo, María Satué Palacián, que figuro como coautora de los artículos:

- "Garcia-Martin E, Pablo LE, Herrero R, Satue M, Polo V, Larrosa JM, Martin J, Fernandez J. **Diagnostic ability of a linear discriminant function for Spectral domain optical coherence tomography in multiple sclerosis patients**. Ophthalmology 2012; 119(8):1705-1711. ISSN: 0161-6420. PMID: 23154461".
- "Herrero R, Garcia-Martin E, Almarcegui C, Ara JR, Rodriguez-Mena R, Martin J, Satue M, Dolz I, Fernandez J, Pablo LE. **Progressive degeneration of the retinal nerve fiber layer in patients with multiple sclerosis**. Invest Ophthalmol Vis Sci. 2012;53(13):8344-9. ISSN: 0146-0404. PMID: 23154461".

Renuncio a presentar dichos trabajos como parte de mi tesis doctoral.

En Zaragoza, a fecha 14 de Marzo de 2013

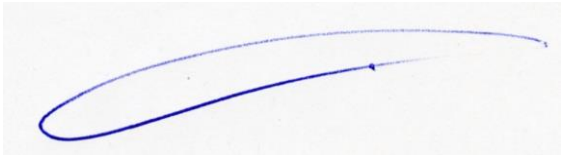

Fdo: María Satué Palacián.

Yo, Maria Pilar Bambó Rubio, que figuro como coautora del artículo: “García-Martín E, Herrero R, Bambo MP, Ara JR, Martin J, Polo V, Larrosa JM, Garcia-Feijoo J, Pablo LE. **Artificial neural network techniques to improve the ability of optical coherence tomography to detect optic neuritis**. Seminars of Opthalmology 2013 (en prensa). ISSN: 0882-0538” renuncio a presentar dicho trabajo como parte de mi tesis doctoral.

En Zaragoza, a fecha 14 de Marzo de 2013.

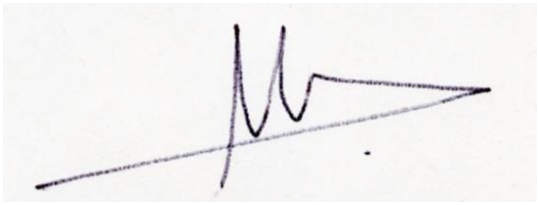

Fdo: Maria Pilar Bambó Rubio.

Yo, Diego Rodriguez Mena, que figuro como coautor del artículo: “Herrero R, Garcia-Martin E, Almarcegui C, Ara JR, Rodriguez-Mena R, Martin J, Satue M, Dolz I, Fernandez J, Pablo LE. **Progressive degeneration of the retinal nerve fiber layer in patients with multiple sclerosis**. Invest Ophthalmol Vis Sci. 2012;53(13):8344-9. ISSN: 0146-0404. PMID: 23154461” renuncio a presentar dicho trabajo como parte de mi tesis doctoral.

En Zaragoza, a fecha 14 de Marzo de 2013

Fdo: Diego Rodriguez Mena.

Yo, Isabel Dolz Zaera, que figuro como coautora del artículo: “Herrero R, Garcia-Martin E, Almarcegui C, Ara JR, Rodriguez-Mena R, Martin J, Satue M, Dolz I, Fernandez J, Pablo LE. **Progressive degeneration of the retinal nerve fiber layer in patients with multiple sclerosis**. Invest Ophthalmol Vis Sci. 2012;53(13):8344-9. ISSN: 0146-0404. PMID: 23154461” renuncio a presentar dicho trabajo como parte de mi tesis doctoral.

En Zaragoza, a fecha 14 de Marzo de 2013

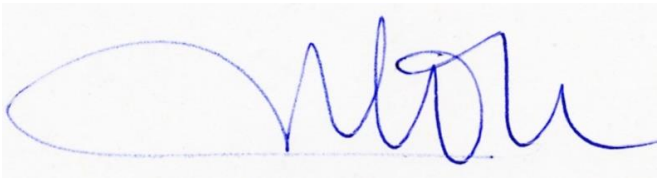

Fdo: Isabel Dolz Zaera